CRANFIELD UNIVERSITY

NNABUIFE GODFREY SOMTOCHUKWU

NEW MULTIPHASE FLOW MEASUREMENTS FOR SLUG CONTROL

SCHOOL OF WATER, ENERGY, AND ENVIRONMENT
Oil and Gas Centre

PhD
Academic Year: 2016 - 2019

Supervisor: Dr James Whidborne
Associate Supervisor: Dr Liyun Lao
January 2019

CRANFIELD UNIVERSITY

SCHOOL OF WATER, ENERGY, AND ENVIRONMENT
Oil and Gas Centre

PhD

Academic Year 2016 - 2019

NNABUIFE GODFREY SOMTOCHUKWU

New Multiphase Flow Measurements for Slug Control

Supervisor: Dr James Whidborne
Associate Supervisor: Dr Liyun Lao
January 2019

This thesis is submitted in partial fulfilment of the requirements for the degree of Doctor of Philosophy

ABSTRACT

Severe slug flow is undesirable in offshore oil production systems, particularly for late-life fields. Active control through choking is one of the effective approaches to mitigating/controlling severe slug flow in oil production pipeline-riser systems. However, existing active slug control systems may limit oil production due to overchoking. Another problem in most active control systems is their dependency on information obtained from subsea measurements such as riser base pressure for active slug flow control.

Both of these control challenges have been satisfactorily solved through the introduction of new multiphase flow topside measurements that are reliable and efficient in providing flow information for active slug control systems. By using Venturi multiphase flow topside measurements and Doppler ultrasonic measurements, an active slug flow control system is proposed to suppress severe slug flows without limiting oil production. Experimental and simulated results demonstrate that under active slug control, the proposed system is able not only to suppress slug flow but also to increase oil production compared to manual choking.

Another objective of this research was to assess the applicability of continuous-wave Doppler ultrasonic (CWDU) techniques for accurate identification of gas-liquid flow regimes in pipeline-riser systems.

Firstly, flow regime classification using the kernel multi-class support-vector machine (SVM) approach from machine learning (ML) was investigated. For a successful industrial application of this approach, the feasibility of conducting principal component analysis (PCA) for visualising the information from intrinsic flow regime features in two-dimensional space was also investigated. The classifier attained 84.6% accuracy on test samples and 85.7% accuracy on training samples. This approach showed the success of the CWDU, PCA-SVM, and virtual flow regime maps for objective two-phase flow regime classification on pipeline-riser systems, which would be possible for industrial application.

Secondly, an approach that classifies the flow regime by means of a neural network operating on extracted features from the flow’s ultrasonic signals using

either discrete wavelet transform (DWT) or power spectral density (PSD) was proposed. Using the PSD features, the neural network classifier misclassified 3 out of 31 test datasets and gave 90.3% accuracy, while only one dataset was misclassified with the DWT features, yielding an accuracy of 95.8%, thereby showing the superiority of the DWT in feature extraction of flow regime classification. This approach demonstrates the employment of a neural network and DWT for flow regime identification in industrial applications, using CWDU. The scheme has significant advantages over other techniques in that it uses a non-radioactive and non-intrusive sensor.

The two investigated methods for gas-liquid two-phase flow regime identification appear to be the first known successful attempts to objectively identify gas-liquid flow regimes in an S-shape riser using CWDU. The CWDU approaches for flow regime classification on pipeline-riser systems were successful and proved possible in industrial applications.

Keywords: multiphase flow; clamped-on, non-radioactive, non-intrusive measurements; riser slug flow; pipeline-riser system; differential pressure, Venturi flow meter; choking; active slug control.

ACKNOWLEDGEMENTS

After an intensive period of three years, today is the day: writing this note of thanks is the final addition to my Ph.D. work. It has been a period of intense learning for me, not only in the scientific areas but also on a personal level. Writing this thesis has had a big impact on me. I would like to reflect on the people who have supported and helped me so much throughout this period.

Firstly, I would like to thank the King of kings, the God of gods for giving me the opportunity, strength, ability, and knowledge to undertake this research and to persevere and complete it satisfactorily. Without Almighty God's blessings, this achievement would not have been possible. In my journey towards this Ph.D. degree, God has helped me greatly.

I am extremely grateful to my first primary supervisor, Prof Yi Cao, who started this research work with me from topic selection to finding the results. His immense knowledge, motivation, useful discussions, brainstorming sessions, and patience have given me more power and spirit to excel in research writing. Conducting an academic study regarding such a complex topic should not have been as simple as he made this for me. Although due to circumstances beyond his control, he was not able to continue as my supervisor to the end of my Ph.D. work.

I would like to express my sincere gratitude to my second primary supervisor Prof Falcone Gioia for her support, motivation, and immense knowledge. Her guidance and suggestions helped me through the entirety of the research and writing this thesis. Again, due to constraints, she did not continue to supervise me until the end of my Ph.D. work.

I am also pleased to say a very big thank you to my third and final primary supervisor in the person of Dr James Whidborne. In him, I have found a friend, a teacher, a role model, an inspiration, and a pillar of support. He has been there providing his heartfelt support and guidance at all times and has given me

invaluable inspiration, guidance, and suggestions in my quest for knowledge. He has given me the freedom to pursue my Ph.D. research, while silently and unobtrusively ensuring that I stay on course and do not deviate from the core of my research. Without his able guidance, this thesis would not have been possible, and I shall eternally be grateful to him for his assistance. I remain amazed that despite his busy schedule, he was able to go through the final draft of my thesis and meet me in less than a week with comments and suggestions on almost every page. He is an inspiration.

I take pride in acknowledging the insightful guidance of my Ph.D. co-supervisor Dr Lao Liyun, for sparing his valuable time whenever I approached him and for showing me the way ahead. He started as my Ph.D. subject advisor then became one of the members of my review committee, and he finally ended up as my second supervisor. For your brilliant suggestions, criticisms, good judgment and comments, thanks to you.

Apart from my supervisors, I would like to thank the rest of my Ph.D. review committee: Prof Peter Jarvis, Dr Verdin Patrick, and Dr Sophie Rock not only for their encouragement and insightful comments but also for the hard questions which inspired me to widen my research from various perspectives.

I would like to thank my Ph.D. Viva panel: Dr Jie Zhang from Newcastle University who was the external examiner, Dr Auger Daniel, the internal examiner and chair of Viva, Dr Robert Grabowski for their tough and insightful questions and comments, which has helped me to restructure my thesis appropriately. They sat me down for five hours and grilled me with questions. A massive thank you to you all for being a part of my success story.

I am also grateful to the following university staff: Sam Skears, Stan Collins, and Rockall Abbi for their unfailing support and assistance.

I have great pleasure in acknowledging my gratitude to my colleagues and fellow research scholars at Cranfield University, Dr Prafull Sharma, Dr Baba Musa

Abbagoni, and Mr Pilario Karl Ezra in ensuring that the fire keeps burning, being there at times when I required motivation, and propelling me on the course of this thesis. Their support, encouragement, and credible ideas have been great contributors to the completion of the thesis.

Finally, I am grateful to my parents, siblings, and friends who remembered me in their prayers for ultimate success. I consider myself nothing without them. They gave me enough moral support, encouragement, and motivation to accomplish my personal goals.

TABLE OF CONTENTS

THE LIST OF FIGURES

LIST OF TABLES

LIST OF ABBREVIATIONS

ANNs	Artificial Neural Networks
CAPEX	Capital Expenditure
CMAS	Compositional Multiphase Advanced Simulator
CWDU	Continuous Wave Doppler Ultrasound
DPV	Differential Pressure from Venturi (inlet-throat)
DWTs	Discrete Wavelet Transforms
FAD	Free Air Delivery
ISC	Inferential Slug Controller
MSEs	Mean Square Errors
MFMs	Multiphase Flow Metres
OPEX	Operational Expenditure
OPCs	Open Platform Communications
OLGA	Oil and Gas simulator software
PCA	Principal Component Analysis
PDF	Probability Density Function
PT	Pressure at the Top riser
PSD	Power Spectral Density
Q	Flowrate
ROL	Liquid Density
SCADA	Supervisory, Control and Data Acquisition
SVM	Support Vector Machine
TACITE	Transient Analysis Code by IFP Total and ELF
U	Velocity

CHAPTER ONE

1 Introduction

1.1 Background and motivation

In offshore platforms, hydrocarbon fluids produced are conveyed through pipelines typically as a mixture of sand, gas, water, and oil. One of the common flow regimes encountered during the produced fluid transportation is called slug flow (Issa and Kempf, 2003).

Slug flow is a flow regime in the multiphase pipeline that is characterised by varying, intermittent or irregular flows and surges of gas and liquid through any cross-section of a pipeline (Godhavn, Fard and Fuchs, 2005). Slug flow, in general, is the most challenging gas-liquid flow regime. Understanding slug flow is complex due to its multi-dimensional fluid processes and its transient nature that characterises it. Because slug flow is unstable and complex, it is difficult to predict the mass transfer, pressure drop and heat. The flow nature varies relying upon whether the pipeline is inclined, vertical or horizontal (Havre, Stornes and Stray, 2000).

Despite the number of multiphase flow slug flow mitigation and control strategies in use in the industry today, there has not been a one-stop solution for its management due to its complex nature.

An enormous amount of work has been carried out investigating the applicability of upstream measurements for slug control (Courbot, 1996; Schmidt, Brill and Beggs, 1980; Henriot et al., 1999; Molyneux, P. D., Kinvig, 2000; Pedersen, Durdevic and Yang, 2017). However, only limited studies have investigated the use of topside measurements for slug control (Godhavn, Fard and Fuchs, 2005; Sivertsen and Skogestad, 2005a; Storkaas and Skogestad, 2007; Fard, Godhavn and Sagatun, 2006; Arrieta, Vilanova and Balaguer, 2008; Sivertsen, Alstad and Skogestad, 2009a; Ehinmowo and Cao, 2016; Tandoh, Cao and Avila, 2016). To

date, there is limited knowledge on the applicability of topside only measurements for slug control.

Upstream measurement, which is multiphase flow measurement that is used in the seabed, riser base pressure, for example, is good for slug control but requires a subsea instrument. The main disadvantages of subsea measurements are high Operational Expenditure (OPEX) and Capital Expenditure (CAPEX) cost. Subsea instruments are expensive and may not be feasible for brownfields (aging fields). Subsea instruments are expensive to install, maintain and sometimes unavailable and when they are available, their reliability is always a concern. Moreso, other challenges are associated with subsea pressure and down-hole measurements as any instrument to be deployed should be able to withstand the higher temperature and pressure conditions. The operations of these instruments in the harsh environment require constant calibration and maintenance. This lack of reliability, alongside with the cost associated with the constant calibration and down-hole gauges replacement makes it less attractive (Awadalla et al., 2016). The advantages of using topside only measurements for slug control are enormous; these include low CAPEX and OPEX cost, less maintenance and higher reliability than subsea measurements. Hence, there is a need to develop methods for slugging control that uses topside only measurements.

Doppler ultrasound technique use for slug flow control will be accessed which will aid in minimising both OPEX and CAPEX involved in running the oil fields. The choice of the Doppler ultrasound technique used in this work is due to its non-radioactive and non-intrusive nature over multiphase flow metre techniques associated with intrusive and radioactive sensors. Non-intrusive and non-radioactive Multiphase Flow Metres (MPFMs) are less expensive to construct because they do not use radioactive materials. Furthermore, the operating expenditure of Doppler ultrasound is less than that of radioactive equipment due to enormous expenses associated with the various environmental, safety and health requirements.

1.2 Why is slug flow a problem

Considerable equipment damages and operating problems caused by slug flow have been reported (Shotbolt, 1986). Some of the slug flow problems encountered at different platforms include the following:

- Large pressure variations, which reduces wells lifting capacity (Tandoh, Cao and Avila, 2016).
- Long-term damage to the reservoir due to resulting bottom hole pressure fluctuations, causing a permanent decrease in the production of gas and oil from the reservoir (Mokhatab, Towler and Purewal, 2007).
- The presence of slug flow in gas and oil pipelines can increase corrosion rates and may decrease the efficiency of a corrosion inhibitor (Ehinmowo and Cao, 2015).
- Severe slug flow can even cause platform trips and plant shutdown leading to plant abandonment (Godhavn, Fard and Fuchs, 2005).
- More frequently, the large and rapid variation in flow causes unwanted flaring and reduces the operating capacity of the separation and compression unit (Godhavn, Fard and Fuchs, 2005).
- The oscillating pressure may cause wear and tear on processing equipment and will reduce the lifetime and increase the maintenance costs compared to production with a steady flow (Mokhatab and Towler, 2007).
- Slug flow causes a decrease in the average flow output, which can easily be as large as 50%. This inefficiency results in significant profit losses (Di Meglio et al., 2010).
- Large disturbances in the separator train cause poor phase separation and varying water quality at the separator water outlet (Fard, Godhavn and Sagatun, 2006).

1.3 Reasons for slug flow control

Successful mitigation/control of slug flow will help to prevent unwanted gas flaring, oil spillage, the unwanted shutdown of plants, and reduce expenditures for unplanned maintenance thereby maximising the following:

- Economic benefits: Slug flow mitigation/control has substantial economic benefits; this is one of the main reason why a lot of effort and money has been invested in search of robust solutions to the problems caused by slug flow (Mohmmed et al., 2019).
- Increase in production: Slug flow mitigation/control can increase hydrocarbon throughput (Ogazi et al., 2009).
- Well testing: The process of well testing could be very rigorous. Elimination or drastic reduction in slug flow would allow the operator to test more wells, more frequently, with more consistent accuracy without experiencing intermittent flow that could lead to the unwanted shutdown of plants. The overall well test time and the cost will also be significantly reduced (Falcone et al., 2002).
- Reservoir management: The depletion of conventional oil wells has made reservoir management vital. Elimination or prevention of the slug flow regime will help in enhancing the developments in reservoir management and production techniques geared towards maximising the production capabilities of these wells (Falcone et al., 2002).
- Custody transfer: This is an essential process for operators in the oil and gas industries. Precise and continuous custody transfer measurement for hydrocarbon products sales and distribution is critical for the industry. Slug flow regime elimination would enhance the smooth and continuous flow of hydrocarbons which is desirable for custody transfer (Thorn, Johansen and Hjertaker, 2013).
- Production Allocation: This arises when different wells and fields owned by different operators are commingled in the same pipeline for export to a common processing facility. For this process to be successful, intermittent or irregular flow needs to be avoided (Falcone et al., 2002).

- Production Monitoring: There is a preference for multiphase metering flow meters over conventional ones by the oil and gas industry operators. Multiphase Flow Meters (MFM) are known for their ability to give continuous online measurements. However, the elimination of slug flow would prevent any interruption to these processes (Falcone et al., 2002).
- Flow Assurance: Flow assurance technology has played a vital role in the development of the oil and gas industry over the past three decades. The term ‘’flow assurance’’ covers the entire spectrum of design tools, knowledge, equipment, methods and professional skills needed to ensure the safe, uninterrupted and simultaneous transport of gas, oil and water from reservoirs to the processing facilities (Gao et al., 2020). Slug flow regime mitigation would help in enhancing these processes and ensuring of uninterrupted extraction and transportation of gas, oil, and water from reservoirs to the processing facilities (Enilari and Kara, 2015).

1.4 The phenomenon of riser-induced slug flow

Subsea gas/oil production and exploration facilities production optimisation have been rigorously examined, as any promising enhanced hydrocarbon recovery can result in substantial economic benefits (Havre, Stornes and Stray, 2000). Hence, in offshore oil and gas industries, multiphase flow behaviour in pipelines-flow-lines is a big challenge. A lot of effort and investment have been made investigating this slug flow phenomenon. One of the purposes of investigating the slug flow phenomenon is because any change in the plant operating conditions will affect the pipeline flow behaviour. Thus, this has a significant impact on prominent factors such as safety, maintenance, and productivity. A sketch of riser-induced slugging is illustrated in Figure 1-1.

Slug flow has an adverse effect on the topside processing facilities during the production of oil and gas offshore due to significant variations in pressure and flow rates (Taitel et al., 1990). Some of the common problems caused by slugging are operating capacity reduction and unwanted flaring. The pressure variations

also cause strains on some parts of the system such as bends and valves. In most cases, the burden in the compressors and separators at the top side becomes so large that it causes enough damage to cause a shutdown of the plant; this is a massive disadvantage to oil-producing companies.

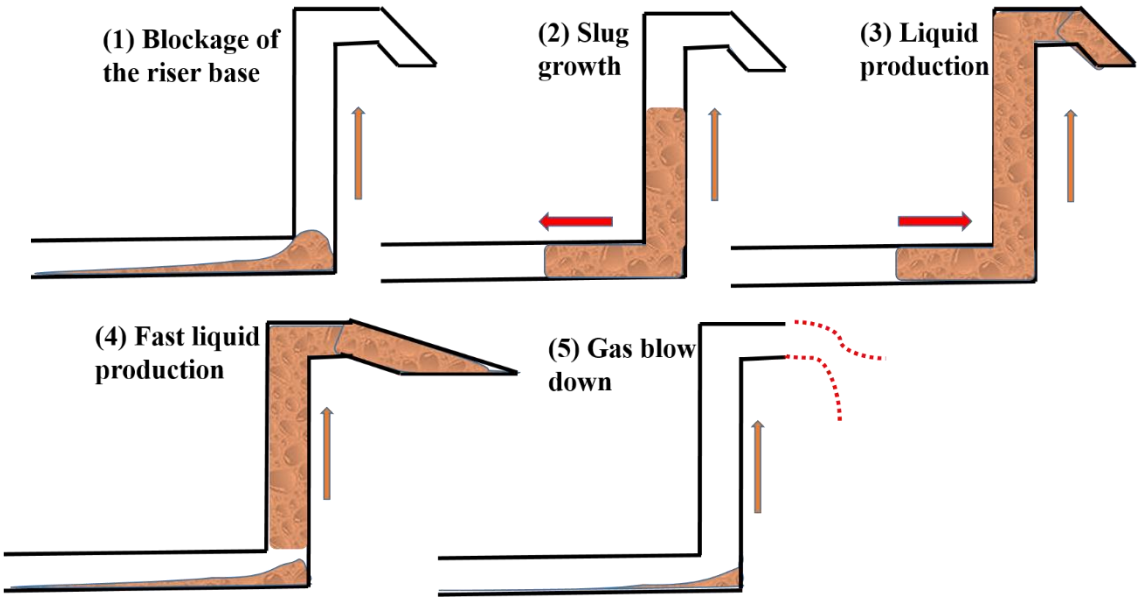

Figure 1-1: The five stages of the riser-induced slug flow cycle (Malekzadeh, Henkes and Mudde, 2012).

There are several possible ways of preventing/reducing slug flow. Design changes are one, for instance, increasing the separators size, gas lift or slug catcher installation, changing the topology of the pipeline. However, the installation and maintenance of this new equipment are expensive. Another method is to vary the system operating conditions; this is done by choking the valve at the topside. The significant disadvantage of this method is a production rate reduction due to the pressure increase in the pipeline.

The benefits of applying active feedback control of the throttle valve are enormous. It is economically efficient and effective than the deployment of new equipment, and it can eliminate slugging flow in the system effectively, thereby relieving the system from the strain. Hence, the system maintenance issues will

be reduced and much money saved (Ehinmowo and Cao, 2015b). In addition, a high production rate is more feasible with active control than the common choking of the topside valve.

Subsea multiphase measurements are typically included during control system design, pressure measurements at the riser base or further upstream, are some of the measurements. In slug flow mitigation/control, subsea measurements have been proven to be useful in slug flow mitigate/control (Taitel et al., 1990). Hence, in the absence of these measurements, slug mitigation/control gets more difficult.

However, subsea measurements are often not readily available, are expensive to implement and are less reliable than the topside measurements. Hence, there is a need to control slug using only the topside measurements. This raises some questions such as the possibility of improving the system performance by using a single topside measurement or a combination of topside measurements. Are these results the same or comparable to the ones gotten when controllers based on subsea measurements were deployed?

Continuous-wave Doppler ultrasound (CWDU) uses Doppler-shift frequency representing flow velocities to develop techniques for accurate prediction of flow regimes (Übeyli and Güler, 2005). CWDU is the clamp-on, simple, non-radioactive, non-intrusive and non-invasive measurement. Hence, the installation is relatively inexpensive. CWDU provides reliable online information about slug events from which reliable statistical description can be derived for slug flow control. CWDU field of application extends far beyond what is obtainable with radioactive or intrusive local instruments. The gamma-ray densitometer is a non-intrusive technique that does not disturb the flow under investigation. The technique has been used widely in a variety of multiphase flow in nuclear energy and energy power (Chan and Banerjee, 1981), but it is radioactive. CWDU can fill in the gap of gamma-ray densitometer in the industry.

1.5 Flow Regimes

When liquid and gas flows together in a pipeline, there are different flow regimes, or geometrical configurations, that are observed to occur. The flow regime depends on the flow rates of each of the phases, fluid properties and the size of the pipe (Wu et al., 2017).

Avoiding slug flow in the pipeline brings substantial economic benefits. Hence, it is imperative to predict or detect the flow regime before starting production to tackle the problems as soon as possible. Conventionally, a flow regime map is developed to predict the flow regime that will occur in the pipeline (Liu et al., 2018). The flow regime is estimated by quantities such as gas/liquid densities, pipe diameter, gas/liquid viscosities, gas/liquid surface tension pipe inclination, and gas/liquid superficial velocities. As these quantities may vary along the pipeline, the flow regime can also vary along the pipeline (Hewitt and Roberts, 1969). The reliance of the flow regime on the parameters above describes the so-called flow regime map.

1.6 The aim and objectives

It is proposed that CWDU-based measurements have this potential as discussed above. Hence, the thesis aims to develop a CWDU system for slug flow control and to seek new multiphase flow measurements that are more sensitive to slug flow to improve slug control performance.

The individual objectives of this research are as follows:

1) Develop a continuous wave Doppler ultrasound (CWDU) system for multiphase flow slug control.
2) Determine the applicability of CWDU for flow regime identification: Effectiveness of CWDU to distinguish between different flow patterns will be determined.
3) Determine the applicability of CWDU for riser slug control
4) Control slug using differential pressure (DPv) and throat pressure (pt) measurement from venturi metre.

1.7 Methodology

The project adopts a combination of model-based and experimental analysis methodology. Model-based analysis often uses extensive simulation experimentation. The reasons for adopting these research methodologies are explained in subsections below.

1.7.1 Simulation

The OLGA (OiL and GAs) Dynamic Multiphase Flow Simulator 2015.2.1 (https://www.software.slb.com/products/olga) was adopted for this research work to model different types of pipeline-riser for the mitigation and control of slug flow. OLGA was originally developed as a dynamic one-dimensional modified two-fluid model for two-phase hydrocarbon flow in pipelines and pipeline networks, with processing equipment included. Later, a water option was included which treats water as a separate liquid phase (Masella et al., 1998).

OLGA is a modified two-fluid model, that is separate continuity equations for the gas, liquid bulk and liquid droplets are applied; these may be coupled through interfacial mass transfer. The OLGA simulator models transient flow or time-dependent behaviours to maximise production. In deep-water, OLGA dynamic simulation is vital and is used widely in both onshore and offshore developments to examine wellbores and pipeline transient behaviour. From the dynamics of the wellbore of any well completion to pipeline systems with all kinds of process instruments, OLGA provides a reliable prognosis of the operating conditions involving transient flow. OLGA transient simulation provides an added dimension to steady-state analyses by predicting the dynamics of the system such as fluid compositions, operational changes, time-varying changes in flow-rates, solids deposition and temperature hence, the choice of OLGA simulator usage in this work (https://www.software.slb.com).

From OLGA simulator version 7 onward, separate momentum equations are solved for each of the three phases (water, oil, gas). A slip relation gives the velocity of any entrained liquid droplets in the gas phase. One mixture energy

equation is applied; both phases are at the same temperature. This yields seven conservation equations to be solved; three continuity equations for liquid droplets in gas, bulk liquid and gas, two momentum equations with one for combined liquid droplets in gas and gas, and one for liquid, finally one for energy (Bendiksen et al., 2007). The OLGA equations are presented below:

Continuity equations for gas phase and bulk liquid phase are given in equation (1-1) and (1-2) respectively while the liquid droplet within the gas phase is given in equation (1-3).

$$\frac{\delta(V_g\rho_g)}{\delta t} = -\frac{1}{A}\frac{\delta}{\delta z}\left(AV_g\rho_g v_g\right) + \psi_g + G_g \quad 1\text{-}1$$

$$\frac{\delta(V_l\rho_l)}{\delta t} = -\frac{1}{A}\frac{\delta}{\delta z}(AV_l\rho_l v_l) - \psi_g\frac{V_l}{V_l+V_g} - \psi_e + \psi_d + G_l \quad 1\text{-}2$$

$$\frac{\delta(V_l\rho_l)}{\delta t} = -\frac{1}{A}\frac{\delta}{\delta z}(AV_D\rho_l v_D) - \psi_g\frac{V_D}{V_l+V_D} + \psi_e - \psi_D + G_{D.} \quad 1\text{-}3$$

where V_l, V_D and V_g are volume fraction of liquid, liquid droplets and gas respectively. The mass transfer between the phases is given as ψ_g. The deposition and entrainment rates are ψ_D and ψ_e respectively. The pipe cross-sectional area is represented as A and G is the mass source.

Momentum equations for gas phase, liquid droplets, and liquid at the wall are presented in equation (1-4), (1-5) and (1-6) respectively.

$$\frac{\delta(V_g\rho_g v_g)}{\delta t} = -V_g\left(\frac{\delta P}{\delta z}\right) - \frac{1}{A}\frac{\delta}{\delta z}\left(AV_g\rho_g {v_g}^2\right) - \lambda_g\frac{1}{2}\rho_g|v_g|v_g \times \frac{S_g}{4A} - \lambda_i\frac{1}{2}\rho_r|v_r|v_r\frac{S_i}{4A} + V_g\rho_g g\cos\theta + \psi_g v_a - F_D. \quad 1\text{-}4$$

$$\frac{\delta(V_D\rho_l v_D)}{\delta t} = -V_D\left(\frac{\delta P}{\delta z}\right) - \frac{1}{A}\frac{\delta}{\delta z}(AV_D\rho_l {v_D}^2) + V_D\rho_l g\cos\theta - \psi_g\frac{V_D}{V_l+V_D}v_a + \psi_e v_i - \psi_D v_D + F_{D.} \quad 1\text{-}5$$

Combining equation (1-4) and (1-5) gives

$$\frac{\delta(V_g\rho_g v_g + V_D\rho_l v_D)}{\delta t} = -(V_g + V_D)\left(\frac{\delta P}{\delta z}\right) - \frac{1}{A}\frac{\delta}{\delta z}\left(AV_g\rho_g {v_g}^2 + AV_D\rho_l {v_D}^2\right) - \lambda_g \frac{1}{2}\rho_g |v_g| v_g \frac{S_g}{4A} - \lambda_i \frac{1}{2}\rho_r |v_r| v_r \frac{S_i}{4A} + (V_g\rho_g + V_D\rho_l) g\cos\theta + \psi_g \frac{V_l}{V_l + V_D} v_a + \psi_e v_i - \psi_D v_D. \quad 1\text{-}6$$

$$\frac{\delta(V_l\rho_l v_l)}{\delta t} = -V_l\left(\frac{\delta P}{\delta z}\right) - \frac{1}{A}\frac{\delta}{\delta z}(AV_l\rho_l {v_l}^2) - \lambda_l \frac{1}{2}\rho_l |v_l| v_l \frac{S_l}{4A} + \lambda_i \frac{1}{2}\rho_r |v_r| v_r \frac{S_i}{4A} + V_l\rho_l g\cos\theta + \psi_g \frac{V_l}{V_l + V_D} v_a - \psi_e v_i + \psi_D v_D - V_D d(\rho_l - \rho_g) g \frac{\delta V_l}{\delta z}\sin\theta \quad 1\text{-}7$$

where P is the pressure, S is the wetted perimeter, v_r is the relative velocity, θ is the angle of the inclination, and F_D droplet/gas drag term. The friction coefficients for interface, liquid, and gas are λ_i, λ_l and λ_g respectively.

Equation (1-8) is the mixture energy conservation equation. E is the internal energy per unit mass, U is the heat transfer, H_s is the mass source enthalpy

$$\frac{\delta}{\delta t}\left[m_g\left(E_g + \frac{1}{2}{v_g}^2 + gh\right) + m_l\left(E_l + \frac{1}{2}{v_l}^2 + gh\right) + m_D\left(E_D + \frac{1}{2}{v_D}^2 + gh\right)\right] = - \frac{\delta}{\delta z}\left[m_g V_g\left(H_g + \frac{1}{2}{v_g}^2 + gh\right) + m_l V_l\left(H_l + \frac{1}{2}{v_l}^2 + gh\right) + m_D V_D\left(H_D + \frac{1}{2}{v_D}^2 + gh\right)\right] + H_s + U. \quad 1\text{-}8$$

The strengths of OLGA are:

1. OLGA is the most widely used transient multiphase flow pipeline tool in the oil and gas industry (Faluomi et al., 2017).
2. It is robust (https://www.software.slb.com).
3. It contains advanced slug-tracking and heat transfer models (Kjeldby, Henkes and Nydal, 2013).
4. It is also available on-line (https://www.software.slb.com/products/olga).

The main weakness of OLGA is:

Little or no capabilities to link user-defined sub-models. For example, Shell Flow Correlations are not available in OLGA.

Why OLGA simulator

There are many other dynamic pipeline simulators for the control and design of gas and oil pipelines such as TACITE (Transient Analysis Code by IFP Total and ELF), COMPAS (Compositional MultiPhase Advanced Simulator) and LedaFlow (http://www.ledaflow.com); (Choi et al., 2013). However, for the benefit of this work, OLGA was chosen because it is the most recognised and widely used software in the oil and gas industries for multiphase flow transient analysis. The slug tracking option is available in OLGA, but not in COMPAS. The slug tracking option makes it easier to simulate the terrain-induced slug flow phenomenon, which is likely to occur on a hilly terrain pipeline with low flow rates. COMPAS is not available as a stand-alone simulator (Stand-alone means that the interest is solely in the pipeline dynamics) and it always applies component tracking, the required computer time with COMPAS is often longer than OLGA stand-alone simulator without component tracking. This makes it difficult to use COMPAS as a design tool if a large number of simulations are required (Okereke and Omotara, 2018).

1.7.2 Experimental Facility

The Oil and Gas centre at Cranfield University has one of the best multiphase test facilities in the UK, which is near the industrial scale and it is fully automated with a state-of-art industrial standard distributed control system (Ogazi et al., 2010). By accessing this unique facility, real slug flow control challenges directly related to the industry and research activities will be accessed using different pipeline-riser system (See chapter three for more details).

1.8 Contributions

This research addresses the applicability of ultrasonic techniques for slug control and seeks for other multiphase flow measurements for slug control such as differential pressure from venturi inlet to the venturi throat and pressure at the venturi throat.

The main contributions of this study are:

1) Ultrasound is proved a suitable technique for slug control, which could replace the use of gamma densitometers, which are radioactive.
2) This is the first known attempt to investigate the sensitivity of Doppler ultrasonic parameters for slug control. Hence, a patent has been applied for. It is a clamp-on, simple, non-radioactive, non-intrusive, non-invasive measurement, and the installation is relatively inexpensive.
3) Two-phase gas-liquid flow regime identification on S-shaped riser system using CWDU. This is the first successful attempt to classify various flow patterns on an S-shaped riser using CWDU.
4) The deployment of the differential pressure from the venturi meter (inlet to venturi throat) in combination with all available topside measurements for slug control.

1.9 Thesis Outline

The thesis structure is arranged in three main parts. The first part is an introduction to the research work, the literature review and the methodology used. The second part is the execution of the research work, and the third part draws the research work to a conclusion and suggests possible further work. The thesis structure is as presented in Figure 1-2. The structure of the thesis is as follows:

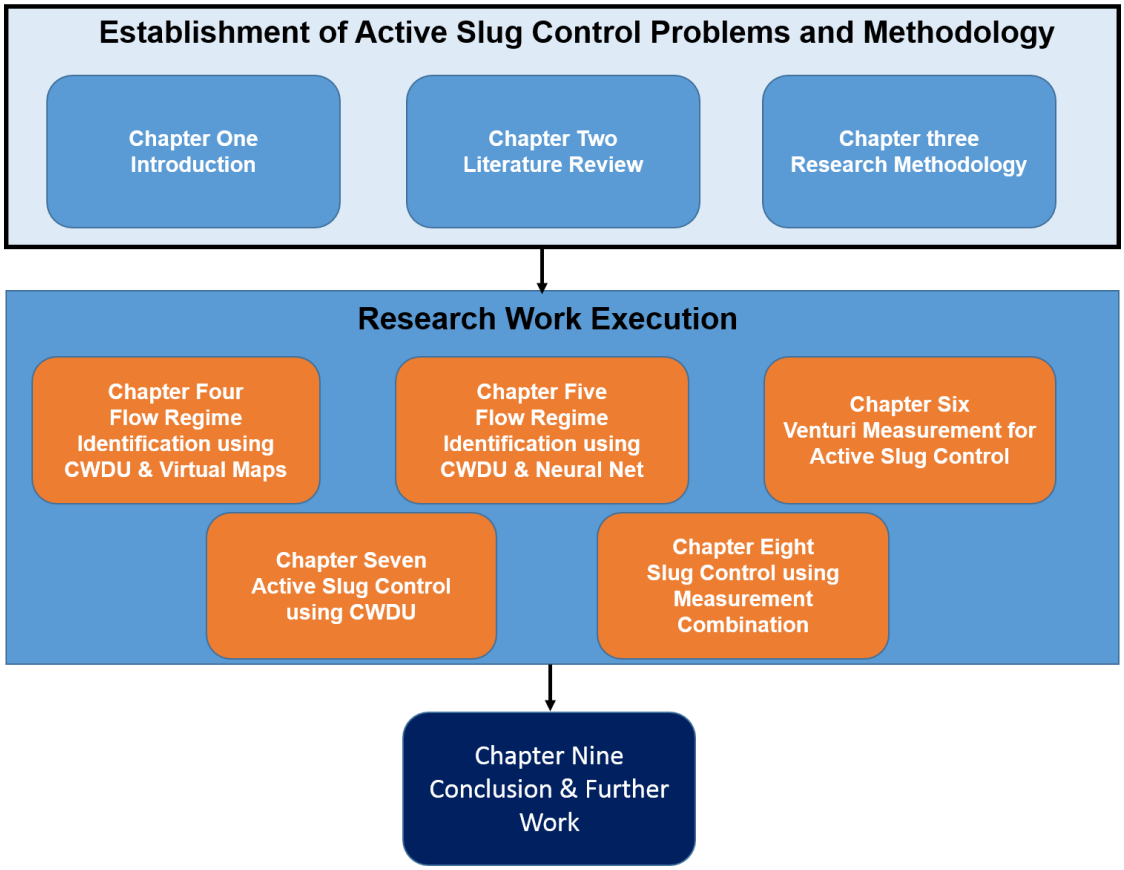

Figure 1-2: Thesis structure

Chapter one introduces the research work discussing the background of slug flow, its cyclic process, problems, and the benefits of its mitigation/control.

In chapter two, a comprehensive review of slug flow, the previous work done on slug control, its applications, benefits, and limitations are presented. First, the description of multiphase flow and slug flow is presented followed by the operation principles of slug flow control technologies.

In chapter three, the research experimental setup and procedures and data acquisition method are discussed. Pipeline dimensions and relevant operating conditions are also discussed.

In chapter four, a new non-intrusive and non-radioactive method for the identification of two-phase gas-liquid flow regimes using CWDU is proposed. Flow regimes are classified using the kernel multi-class Support Vector Machine

(SVM) approach from Machine Learning (ML). To better facilitate the applicability of the method to industrial practice, the feasibility of Principal Component Analysis (PCA) for visualising the information from intrinsic flow regime features in 2-dimensional space is investigated. To this end, a mapping is created so that in 2-dimensions, the mapped samples can be found clustered according to their associated flow regimes. The extracted features are categorised into one of the four flow regime classes: annular, churn, slug and bubbly flow regimes. Support Vector Machine is applied to the samples in the 2-dimensional space to create boundaries between the clusters. This results in a virtual flow regime map that serves as a visual aid for objective flow regime identification in the pipeline.

In chapter five, an approach that classifies the flow regime by means of a neural net operating on extracted features from Doppler ultrasonic signals of the flow using either Power Spectral Density (PSD) or Discrete Wavelet Transform (DWT) is proposed. The extracted features are categorised into one of the four flow regime classes as mentioned in chapter four. The scheme is tested on signals from an experimental facility. The neural network used in this work is a feedforward network with 20 hidden neurons. The network has four output neurons that correspond to the element number in the target vector. When PSD features are applied, the network has 13 inputs. However, when features from DWT are applied, the network has 40 inputs. In this chapter, the application of a neural network and DWT for flow regime classification in industrial applications, using a clamp-on Doppler ultrasonic sensor is demonstrated. The scheme has significant advantages over other techniques in that it uses a non-radioactive and non-intrusive sensor. This appears to be the first known successful attempt to objectively identify gas-liquid flow regimes in an S-shape riser using CWDU and a neural network.

In chapter six, the feasibility of the riser slug flow control by taking the differential pressure measurement from the venturi inlet to the throat is assessed. The controller was able to stabilise the flow with acceptable control performance. The experiment was successful; it was possible to control the flow satisfactorily far into the slug flow unstable region. Hence, a new multiphase flow topside

measurement for active slug flow control is introduced which not only aids in eliminating slug flow but also maximises oil production.

The gamma densitometer has also been demonstrated as a good candidate for slug control. It is a clamp-on, reliable, simple, non-intrusive, and non-invasive measurement, hence the installation is relatively inexpensive. Nevertheless, due to its radioactive nature, it is not well suited for offshore systems.

In chapter seven, another clamp-on, non-intrusive and non-invasive instrument, Doppler ultrasonic sensor, is studied for active slug control. Ultrasonic is proven to be a suitable technique for slug control which could replace the use of the gamma densitometer, which is radioactive in nature. Further cost reduction can be achieved through this novel and innovative ultrasonic technical operational alternatives, which can result in the reduction of CAPEX and OPEX. Ultrasonic techniques will also improve the feasibility of oil recovery costs for the marginally profitable field. Since the ultrasonic techniques as developed here are non-intrusive and non-invasive, the fields of application extend far beyond what is possible with local intrusive instruments.

In chapter eight, slug control using measurement combinations is investigated. The study indicates a way to achieve successful slug flow control performance. Finding a reliable variable for control (the controlled variable selection) using the topside measurements which is sensitive to slug flow. From multivariate statistics theory, it is known that varying directions of signals can be represented by several linear combinations (principal components) of the given signals through Principal Component Analysis (PCA). The one that corresponds to the maximum fluctuation is the first Principal Component (PC1). Using OLGA simulation, it has been found that velocity and venturi differential pressure flow is a reliable measurement for slug control, at least as successful as using the riser base pressure.

Finally, the research findings from the thesis are summarised, and the conclusions drawn in this thesis are presented in chapter nine. Possible future work is also highlighted.

1.10 Publications and Patents

The following publications have resulted from this research work.

Conference paper

Chapter Six

Somtochukwu Godfrey Nnabuife, Liyun Lao, James Whidborne, Yi Cao
Venturi Multiphase Flow Measurement for Active Slug Control
Published in International Journal of Automation and Computing.

Journal papers

Somtochukwu Godfrey Nnabuife, Prafull Sharma, Liyun Lao, James Whidborne
Optimal Filtering of Continuous-Wave Doppler Ultrasound Signals for Detection and Characterisation of Slug Events in a Multiphase Flow.
Drafted paper to be submitted to the Journal of Mechanical Systems and Signal Processing.

Chapter Four

Somtochukwu Godfrey Nnabuife, Karl Ezra S. Pilario, Liyun Lao, Yi Cao, Mahmood Shafiee
Identification of Gas-Liquid Flow Regimes Using a Non-intrusive Doppler Ultrasonic Sensor and Virtual Flow Regime Maps.
Published in Journal of Flow Measurement and Instrumentation.
Co-authors contributions:
The experiments were carried out under the supervision of Prof. Yi Cao and Dr. Liyun Lao. Prof. Yi and Dr. Liyun also helped in the proofreading of the manuscript while making sure that the objectives of the project are achieved. Dr. Mahmood

Shafiee took part in proofreading the manuscript. Mr. Karl Ezra Matlab code which can be accessed on ‘’https://uk.mathworks.com/matlabcentral/fileexchange/65232-binary-and multiclass-svm’’ was combined with my Matlab codes for the analysis of the ultrasonic signals.

Chapter Five

Somtochukwu Godfrey Nnabuife, Liyun Lao, James Whidborne
Objective Identification of Gas-Liquid Flow Regimes Using a Non-Invasive Ultrasonic Sensor and Neural Network
Submitted to Journal Measurement Science and Technology.

Chapter Seven

Yi Cao, Somtochukwu Nnabuife
Active Slug Control using Ultrasonic Sensor

Other papers

- Non-Intrusive Classification of Gas-Liquid Flow Regimes in an S-shape Pipeline-Riser Using Doppler Ultrasonic Sensor and Deep Neural Networks
  Submitted to Chemical Engineering Journal.
- Identification of Gas-Liquid Flow Regimes Using a Non-Invasive Ultrasonic Sensor and Convolutional Neural Network in an S-shape Riser

What differentiates this project from other methods used for flow regime identification and slug control

One of the main objectives of multiphase flow metering technology is to find a better and reliable metering technology that would replace the measurement function of the expensive, intrusive, invasive, radioactive, bulky, and

maintenance-intensive equipment such as test separator, gamma densitometer, and pitot tube. Some researchers adopted gamma densitometers for flow regime identification without considering the hazardous effects of these meters (Hanus et al., 2018). In some cases, the pitot tube which is intrusive was combined with gamma for flow regime classifications (Chan and Bzovey, 1990). However, in this research work, we proposed the use of CWDU which is non-intrusive, non-radioactive, and a clamp-on flow technology for flow regime identification. The clamp-on CWDU also allows retrofitting to existing pipelines which is still a huge challenge to most of the other techniques. The CWDU system developed is CAPEX and OPEX friendly when compared to other techniques that increase CAPEX and OPEX due to expensive installation cost, and maintenance cost.

Currently, flow instabilities in flexible pipeline-riser systems have attracted more attention. The first results reported on severe slug flow in flexible risers was by Tin, (1991). The experiments were carried out using air-water on three flexible riser systems namely, steep S riser, free-hanging catenary, and lazy S. It was observed that the behaviour of slug flow in flexible risers is different when compared to that of vertical risers (Zhu, Gao and Zhao, 2018).

Although a lot of effort has been made towards slug flow investigation in an S-shaped pipeline-riser (Li, Guo and Xie, 2017), limited efforts have been made towards its mitigation/control in an S-shape riser configuration system using top side only measurements. Hence, this is one of the things that differentiate this work on venturi and clamp-on CWDU measurements for slug flow control in an S-shaped riser system from that of others.

CHAPTER TWO

2 Review of Slug Flow

2.1 Introduction

This chapter reviews relevant literature on slug flow control technologies. Flow maps and the slug flow are discussed. Recent slug flow control techniques and their relevant applications are also presented. This starts with the categorisation of pipeline slug flow and an elaborate depiction of all the relevant slug flow control technologies. This chapter is structured as follows: Section 2.2 describes the multiphase flow and different types of flow regimes. In Section 2.3, slug flow and different types of slug flow were discussed. In Section 2.4, previous work on slug flow control are discussed; the merits and demerits of the various approaches are also discussed. Section 2.5 discussed slug control using a combination of topsides measurements. Section 2.6 described the machine learning, after which a summary of the chapter is presented in Section 2.7.

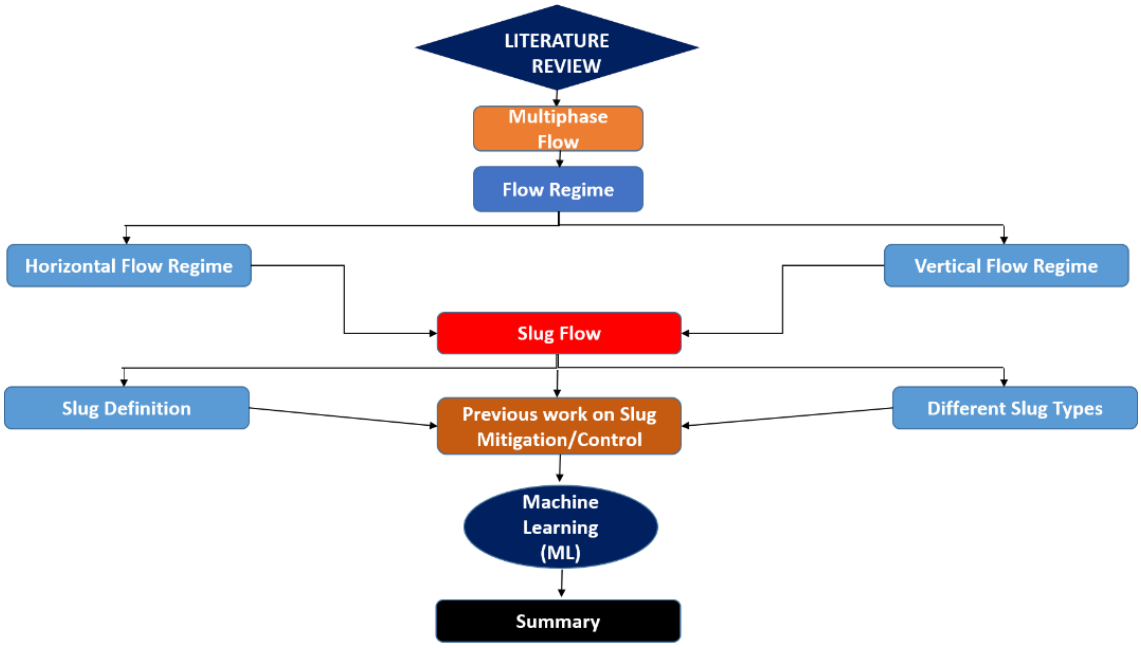

Figure 2-1: Literature review structure

2.2 Multiphase flow regime

2.2.1 Flow regime map

A flow regime map is an important tool used in obtaining an overview of the expected flow regimes in the pipeline system. It presents a description of the multiphase flow geometrical distribution in the pipeline. In the vertical pipes, the common gas-liquid flow regimes are slug flow, churn flow, annular and bubble flow while in horizontal pipelines, wavy stratified flow or stratified may occur in addition to other obtainable flow regimes observed in the vertical pipelines (Xiao and Hrnjak, 2019). Figure 2-2 shows the schematic diagram of the gas-liquid two-phase flow regime map for horizontal and vertical pipe

The flow pattern is driven by variables such as gas-liquid densities, gas-liquid surface tension, pipe incline, pipe diameter, gas-liquid viscosities, and gas-liquid superficial velocities. As these variables vary across the pipeline, the flow pattern also varies (Troniewski and Ulbrich, 1984). The flow regime's dependence on these variables defines the flow regime map.

The multiphase flow pattern is very challenging to predict. The flow can be steady or unsteady, turbulent or laminar, liquid and gas can be segregated, gas can flow as bubbles within the liquid, or liquid can flow as droplets within the gas. Various analyses are conducted when generating the flow pattern/regime map to establish the dependency of the flow regime/pattern on the volume fraction of the multiphase flow components. Hence, there are various flow regimes that can be studied such as two-phase air-water flows and three-phase air-water-oil flows (Cheng, Ribatski and Thome, 2008).

The flow regime/pattern commonly occurring in a vertical pipeline/riser is often different from that observed in a horizontal flow pipeline. For instance, a churn flow observed in a vertical flow pipeline is not the same in a horizontal flow pipeline; the stratified flow regime/pattern in a horizontal flow pipeline is not observed in a vertical flow pipeline.

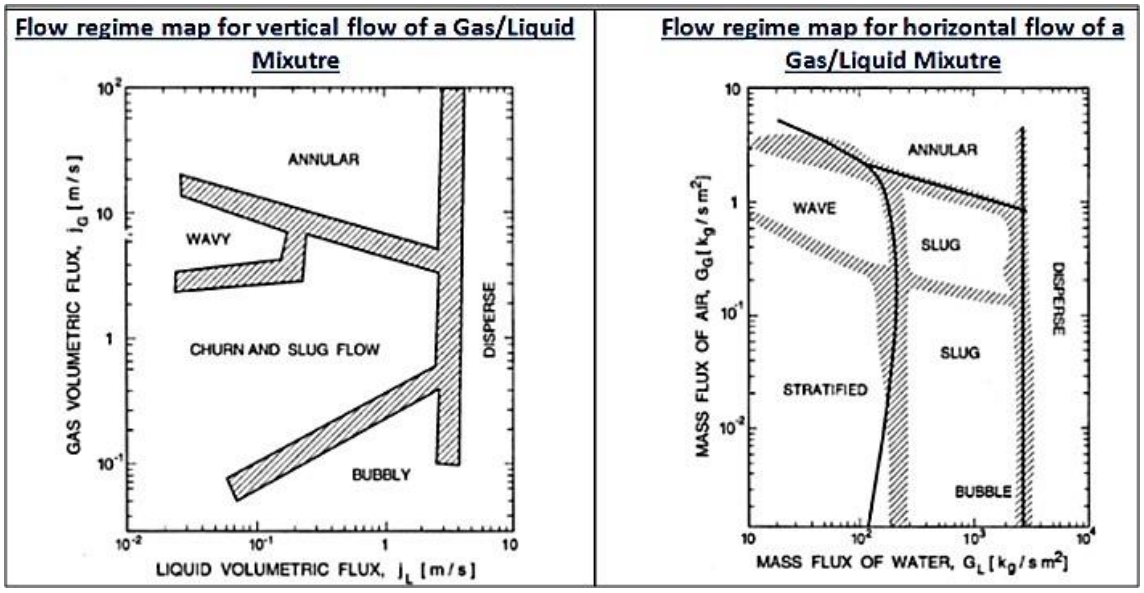

Figure 2-2: Flow regime map for horizontal and vertical flow map (Baghernejad et al., 2019)

2.2.2 **Flow Regime/pattern in a horizontal pipeline**

During high gas production, the gas forms a continuous phase. The liquid is then transported with the gas as droplets. This is known as an annular mist flow. If liquid films form on the wall, the flow regime is known as annular dispersed or core annular flow. If the configuration is mildly inclined or horizontal, the liquid film across the bottom of the pipe will be thicker than the liquid film across the topside (Rossi, De Fayard and Kassab, 2018).

At reduced gas production, liquid entrainment with the gas will become less, and the droplet of the liquid will no longer reach the top of the pipe. An automatic transition of the annular flow to stratified flow results. Both liquid and gas flow as dissociated (separated) films, with the liquid (heavier) below the gas (lighter). However, there may be some amount of liquid droplet entrainment in the gas film.

At the subside (moderate) gas flow rate, there will be an increase in the liquid flow rate. The liquid/gas interface will become uneven, providing room for a stratified flow transition to hydrodynamic slugging (also known as intermittent flow). In this type of flow regime, uneven liquid waves reach the top of the pipe

wall to form a liquid slug. Some amount of gas will form bubbles in the liquid slug body. The gas bubbles also occur behind the liquid slug.

The further increase of the liquid flow rate, at moderate to the low flow rate of gas, the gas bubble behind the liquid slug body will become uneven, and it will split up into smaller bubbles of gas. Now, the liquid will form a continuous phase, with a dispersion of small bubbles of gas. This flow regime is known as bubble flow (or dispersed bubble flow). Figure 2-3 illustrates these four flow regimes.

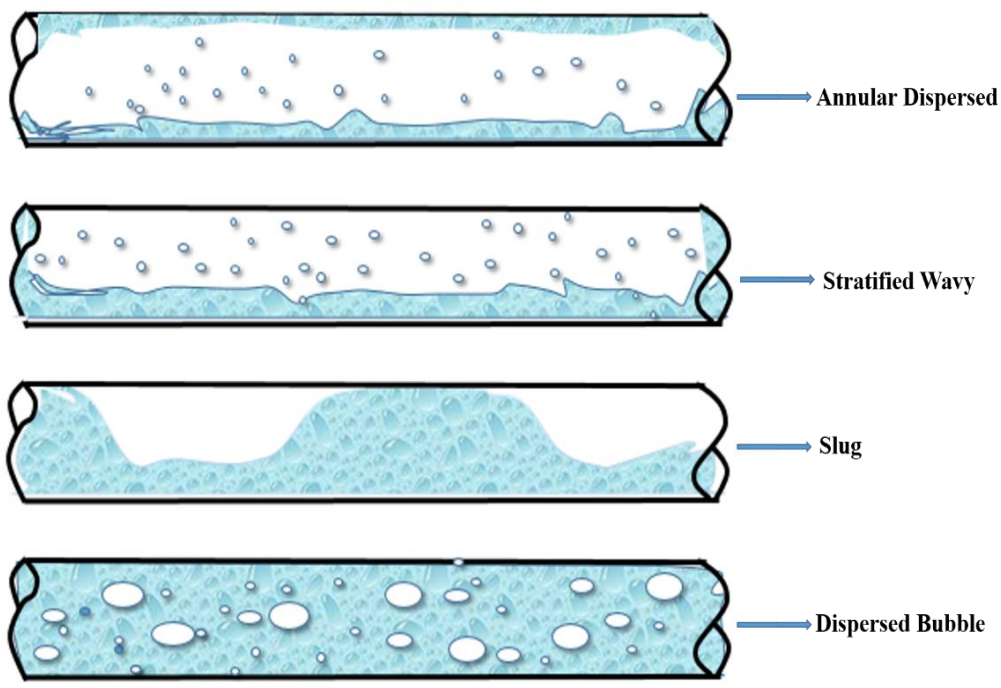

Figure 2-3: Horizontal pipeline flow pattern (Taitel, 1986)

2.2.3 **Flow regime/pattern in a vertical pipeline**

In the vertical section of the pipeline or the riser, different flow regime configurations emerge depending on the thermodynamics and transport properties of the fluid.

At a high liquid flow rate and the low gas flow rate, the liquid will create a continuous phase. The gas moves as a small bubble within the liquid. This is known as the bubble flow regime.

With a reduction of the liquid flow rate, and still at a relatively low gas flow rate, the small gas bubbles will disintegrate to form large gas bubbles. Hence, the liquid forms a slug body with small gas bubble entrainment, accompanied by a single large bubble of gas. This is known as a slug flow regime (intermittent flow).

If the liquid production remains low and gas flow rate increases, the large gas bubbles will become uneven, giving rise to a disordered, chaotic gas bubble transportation of different sizes and shapes. This is known as the churn flow regime (Wu et al., 2017).

If the gas flow rate is further increased to a high flow rate, and the liquid production is still low, it will create room for the transition to annular flow. Figure 2-4 illustrates the four flow regimes in a vertical pipe.

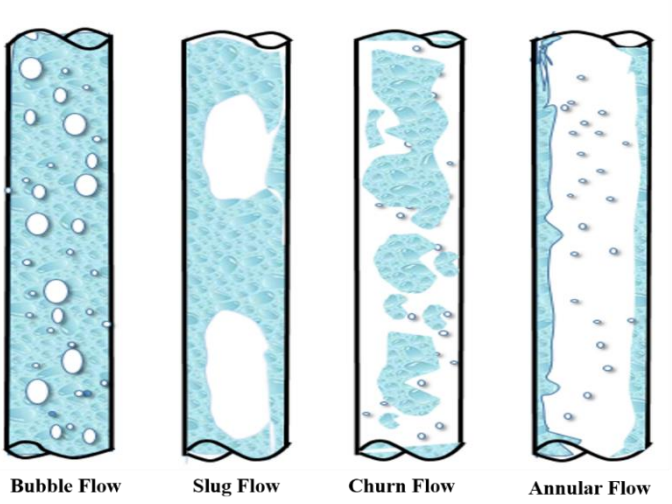

Figure 2-4: **Vertical pipeline flow pattern** (Kelessidis and Dukler, 1989; Wu et al., 2017).

2.3 **Slug flow**

Slug flow is a flow pattern/regime in multiphase flow pipelines that is characterised by varying, intermittent or irregular flows and surges of gas and liquid through any cross-section of a pipeline (Ehinmowo and Cao, 2016). Slug flow is, in general, the most common gas-liquid flow pattern. The existence of slug flow in oil and gas pipelines can increase corrosion rates and may reduce the effectiveness of a corrosion inhibitor (Lee, Sun and Jepson, 1993). Severe

slugging can even cause platform trips and plant shutdowns. More frequently, the large and rapid variation in flow causes unwanted flaring and reduces the operating capacity of the separation and compression unit (Havre, Stornes and Stray, 2000). The fluctuating pressure may induce wear on processing equipment and will lessen the longevity and raise the maintenance costs compared to production with an even flow. The well pressure will oscillate during severe slugging, which might reduce well performance (Godhavn, Fard and Fuchs, 2005). Slug flow decreases the average output by as much as 50%. This relative inefficiency results in substantial profit losses (Di Meglio et al., 2010).

Types of slugging flow

There are different types of slugging flow such as hydrodynamic slugging, riser-induced or severe slug flow and transient slug flow.

2.3.1 Hydrodynamic slugging

Hydrodynamic slug flow is caused by the growing liquid waves in a pipeline. This slug flow condition can merge to form larger slugs, and it can happen over a wide range of flow conditions (Pedersen, Durdevic and Yang, 2017).

2.3.2 Riser-induced slug

Riser-induced slug flow is a phenomenon associated with liquid blockage at the riser base (Brill et al., 1981). Its strong cyclic nature categorises it. The cycle is made up of an extended period of no gas inflow at the riser top, followed by a liquid slug arrival with a length longer than the height of the riser and finally the breakthrough of gas surge (Hoffmann, Hirsch and Pitz-Paal, 2016). The slug cycle time, which depends on the flow conditions and the system size, can range from minutes to hours (Taitel et al., 1990).

The five stages in the riser-induced slug flow (severe slug flow), as presented in Figure 1-1, are as follows (Malekzadeh, Henkes and Mudde, 2012):

1. Riser base blockage: At a low production, the riser will operate in the hydrodynamic slug flow regime where the liquid falls back and blocks the riser initiating the riser-induced slug flow cycle.
2. Slug growth: Liquid builds up at the riser base inducing slug growth in the riser direction and upstream to the flow-line. The gas flowing into the pipeline will build up enough pressure at the back of the slug upstream to make up for the increasing hydrostatic head.
3. Production of liquid: The riser-induced slug grows until the riser is filled with liquid. Immediately when the slug gets to the riser top, liquid slug production into the separator begins.
4. Fast liquid slug production: Immediately when the slug tail in the pipeline reaches the riser base, the hydrostatic head in the riser starts decreasing, which prompts accelerated liquid production at the riser top.
5. Blowdown of gas: This happens after all the liquid has been produced and the excess gas released.

Riser-induced slug flow can take place if one of the following four conditions are fulfilled:

1. The severe slug number (π_{ss}), which is a function of the flow condition of gas/liquid and the length of the flow-line, must be less than one because blockage of the liquid at the riser base can only happen if $\left(\frac{\mathrm{dp}}{\mathrm{dt}}\right)_{flowline} < \left(\frac{\mathrm{dp}}{\mathrm{dt}}\right)_{riser}$. The pressure gradient $\left(\frac{\mathrm{dp}}{\mathrm{dt}}\right)_{flowline}$ is the rate of increase in pressure at the pipeline upstream of the riser base because of gas compression while the latter gradient, $\left(\frac{\mathrm{dp}}{\mathrm{dt}}\right)_{riser}$, is the rate of increase in pressure at the riser base because of the liquid head increase caused by the liquid flowing into the riser (Malekzadeh, Henkes and Mudde, 2012). As illustrated in Appendix A, a severe slug flow number can be written as:

$$\Pi ss = \frac{\left(\frac{\mathrm{dp}}{\mathrm{dt}}\right)_{flowline}}{\left(\frac{\mathrm{dp}}{\mathrm{dt}}\right)_{riser}} = \frac{P_s}{(1-\alpha_F)\rho_L g L_F} GLR \qquad 2\text{-}1$$

where

P_s is the pressure at standard conditions in Pascal units.

α_F is the liquid holdup fraction in the pipeline upstream of the riser base.

ρ_L is the density of the liquid.

ρ_G is the density of the gas

g is the gravitational acceleration.

L_F is the length of the pipeline upstream of the riser base, and

GLR is the gas-liquid ratio at standard conditions.

In deriving this equation, It is assumed that (a) the riser is a vertical riser, (b) the riser and pipeline have the same diameter and (c) $\rho_G \ll \rho_L$.

Thus, for a severe slug flow to occur, $\pi_{ss} < 1$, which is known as the Boe criterion. The Boe criterion expresses that a decreasing gas-liquid ratio (GLR) will reinforce severe slugging (Boe, 1981). This happens in a field's late life, where the breakthrough of water will decrease the GLR.

2. The pipeline topography has a low point at the riser base where the liquid blockage may occur.
3. The flow line is operated either in the annular or stratified flow pattern but not in slug flow. This condition is not strong enough, as some cases exist where a severe slug-like cycle happens with a hydrodynamic slug flow in the upstream pipeline of the riser base.
4. An uneven riser flow, which indicates that a decline in production will induce a higher pressure drop instead of a lower pressure drop over the riser. This happens below a specific flow condition where the pressure drop becomes gravity dominated instead of friction dominated. In this case, low production yields an increased liquid holdup in the riser, which gives the hydrostatic head increase. A rough indication of the onset of an unstable flow is when the densimetric gas Froude number

$$Fr_G = \sqrt{\frac{\rho_G}{(\rho_{L-}\rho_G)}\frac{V^2_{SG}}{gD}} \text{ is lower than one} \qquad 2\text{-}2$$

The summary of the criteria for severe slug flow is illustrated in the flow regime map for an upstream pipeline of the riser base as depicted in Figure 2-5. Severe slug flow usually happens in a field's late-life or during a production turndown when the riser system is in the hydrodynamic slug flow regime and at low gas production.

As presented in Appendix A, the determined severe liquid slug length is L_R/Π_{ss} and the time period of the cycle is given as

$$\Delta t = \frac{L_R}{V_{SLs}} \frac{1}{\Pi_{ss}} \qquad 2\text{-}3$$

where V_{SLs} is the pipeline superficial velocity in standard conditions and L_R is the height of the riser.

During a severe slug flow, much energy is lost because of the gas and liquid velocities' abnormal variation in the line.

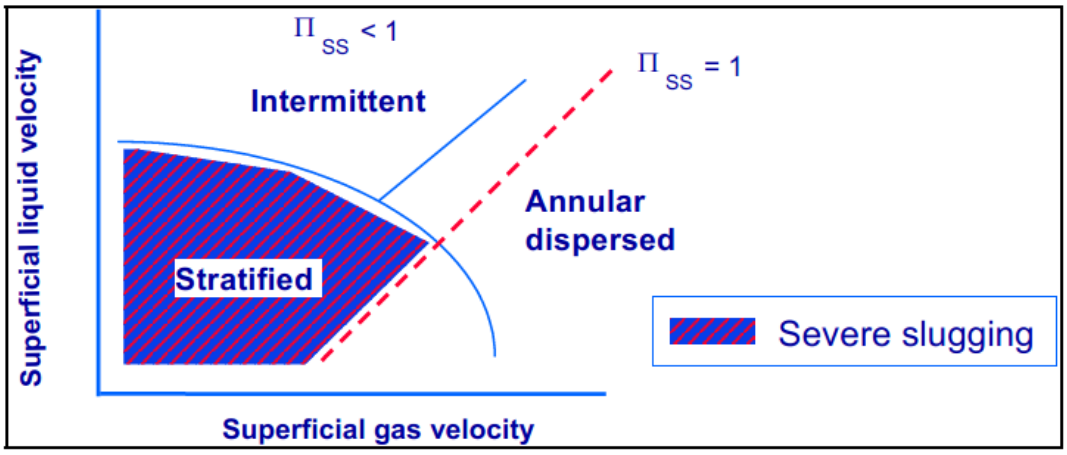

Figure 2-5: Flow regime map of the pipeline at the riser base illustrating where slug flow can occur

2.3.3 **Transient slugs**

The transient slugs' behaviour produced via the riser is shown in Figure 2-6 During phase 1, the slug is getting close to the riser. The slugs have already been initiated at the earlier phase. In phase 2, the slug velocity reduces because the slug pressure is not high enough to push the slug into the riser, and the

hydrostatic pressure must be compensated for (Taitel et al. 1976). The pressure, therefore, builds up in the pipeline. In phase 3, the maximum pressure is attained, and the slug moves into the riser. In phase 4, the slug reaches the top of the riser. The hydrostatic pressure does not have to be compensated for anymore, so the slug accelerates. In phase 5, a gas surge induced by the high pressure behind the slug follows the slug. Examples of transient slugging are growing slugs, terrain slugs, start-up slugs, ramp-up slugs and surge.

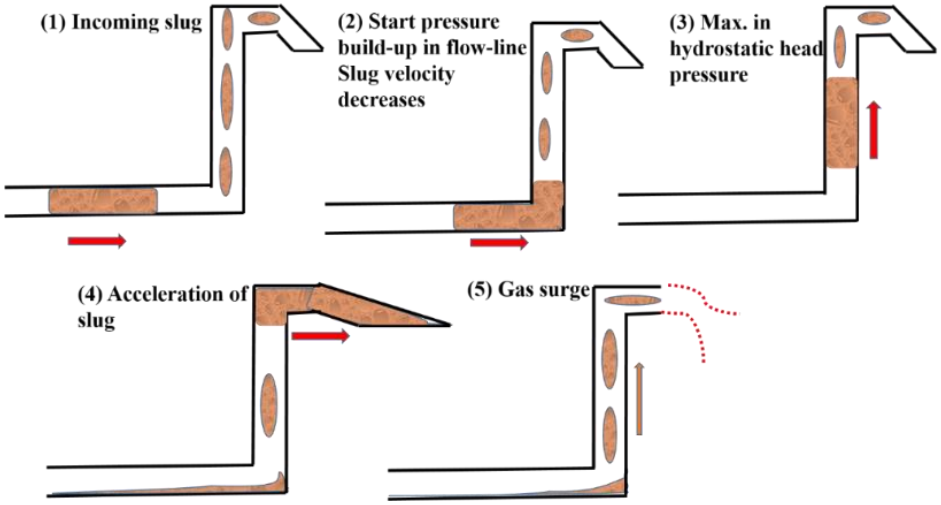

Figure 2-6: The five transient slugs' phases entering the riser (Malekzadeh, Henkes and Mudde, 2012)

2.3.3.1 Terrain slug flow

As presented in Figure 2-7 a terrain slug occurs in the low-points of the pipeline during low production rates. Severe slug flow is a significant case of terrain slug flow. Terrain slug flow is distinct from that of hydrodynamic slug flow because it is induced by undulations of the terrain and can originate at flow conditions outside or within the theoretical edges of the intermittent slugging regimes (Sivertsen, 2008). With changing undulations, a slug's build-up on the vertical slope may continue to move further into the topside section (downstream) running in the stratified flow regime section of the flow map. Primarily, a slug's size can increase at the vertical slopes and disappear or decrease in size at the horizontal slopes. There are several criteria that need to be satisfied for a terrain slug to occur which are almost the same as for severe slug flow. For instance, the flow

in the upstream region has to be stratified while the flow in the topside region has to be unstable (Brasjen et al., 2014).

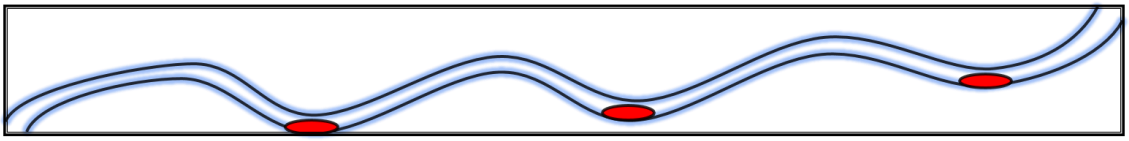

Figure 2-7: Accumulation of liquid in the low-points of the pipeline inducing terrain slug flow (Brasjen et al., 2014)

2.3.3.2 Ramp-up slug flow

The liquid holdup will normally increase with a decreasing production rate in a pipeline system. Below a specific production rate, the liquid holdup will rapidly increase. The accumulation of the liquid at the low flow rate is because of the variation of friction dominated flow to gravity dominated flow that can take place for vertical (upwards) inclined systems. As illustrated in Figure 2-8 a drop in pressure against a flow curve shows a minimum when the increase in the liquid holdup occurs.

During ramp-up, a steady-state liquid holdup difference between the high and small flow rates will be produced at the outlet as a liquid surge or liquid slug. However, for pipeline-riser systems, they are normally called liquid slugs while in trunk-lines, liquid surges are preferable. The reason for this is because there are larger diameters in wet-gas trunk-lines than in a flow-line. Consequently, the trunk-line slug liquid body does not cover the entire cross-section of the pipe; rather the excessive liquid holdup is produced as a holdup wave providing additional liquid production (the surge) when the wave surfaces at the outlet (Harun, Cochran and Choate, 2002). The ramp-up slugs' size can be computed accurately with transient and steady-state pipeline instruments.

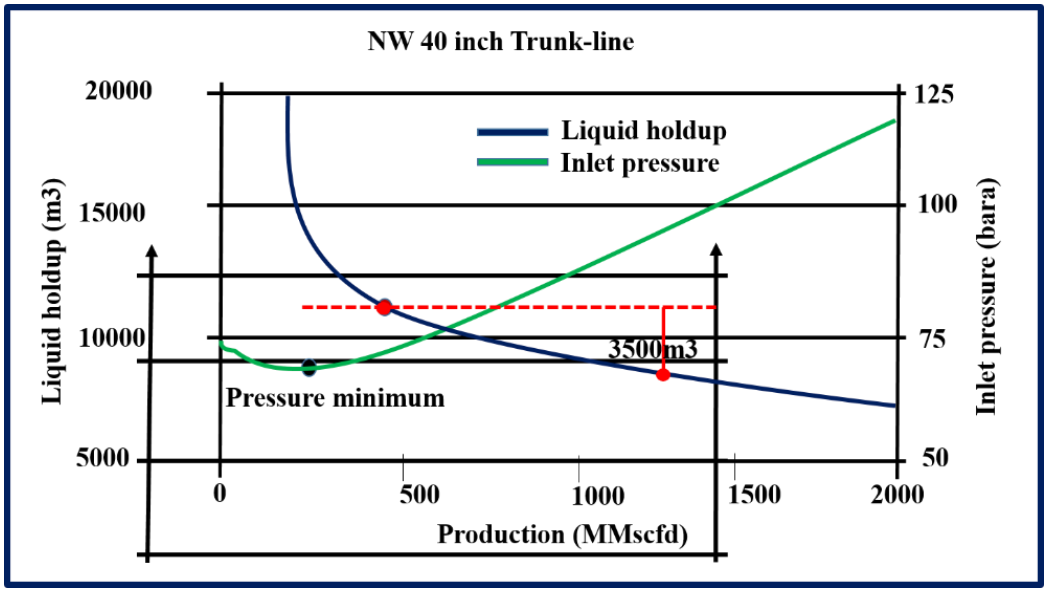

Figure 2-8: Ramp-up from 500 MMscfd - 1500 MMscfd (40" trunk-line)

2.3.3.3 Start-up slug flow

During normal steady-state production, the liquid holdup is distributed according to a specific profile across the pipeline. After shut-in, the liquid holdup will be circulated across the pipeline in a way that the low point will be covered with liquid while other sections of the pipeline will be filled with gas. If there are low-points comparatively close to the outlet, the liquid accumulated may yield huge start-up slugs (Storkaas and Godhavn, 2005). The accumulated liquids in the dips upstream at shut-in will likely expand and be recirculated along the pipeline during its transportation downstream and is unlikely to reach the outlet as a concentrated start-up slug.

2.3.3.4 Growing slug flow

Considering the field data from the 15 inches long pipeline producing fluids from BP's Prudhoe Bay field in Alaska, Brill et al. discovered that slugs could become up to 450m in a pipe (Brill et al., 1981). In 1994, Hill and Wood recorded slugs becoming as large as 600m in a 28 inch, 5 km pipeline at Prudhoe Boe (Hill and Wood, 1994). Thus, the logic behind this large slug growth is that the pipeline stabilises to stratified flow immediately when a slug is produced. The initiation

stage of a slug happens at irregular intervals, possibly because of the brief-duration fluctuation of the flow entering the pipeline.

Growing slug flow can originate when the gas/liquid interface of stratified flow is stable with regards to small disturbances (i.e. the liquid/gas velocities are very small to meet the Kelvin-Helmholtz criterion for instability to occur), whereas slugs, once formed, persist (K.Bendiksen and M.Espedal, 1992).

A conventional horizontal flow regime map in a low-pressure system is presented in Figure 2-9 the upper curve between the intermittent (slug) and stratified slugging regime illustrates the Kelvin-Helmholtz transition (KH stability curve). The lower curve shows the transition to growing slug flow (steady slugging curve), which means it demonstrates that the liquid holdup of stratified flow is equal to the hydrodynamic slugging liquid holdup. Thus, from the shaded region, a slug can grow so large that the difference in the liquid holdup between hydrodynamic and stratified slugging is produced as the liquid surge. However, after the slug production, the pipeline liquid holdup increases once more until it reaches the stable stratified flow level. Hence, a new slug originates after the occurrence of enough large flow disturbance (Elgsæter, 2006).

As pressure increases, the stable slugging curve moves nearer to the Kelvin-Helmholtz stability curve. At high pressure, the stable slugging curve is above the Kelvin-Helmholtz stability curve in the flow regime map. This implies that at a certain region, the waves at the interface will be present but will not initiate hydrodynamic slugging. This region is also known as a large-wave region. Immediately when the stable slugging curve has been crossed, the slug becomes stable although it will be hydrodynamic slugging (not growing slugging).

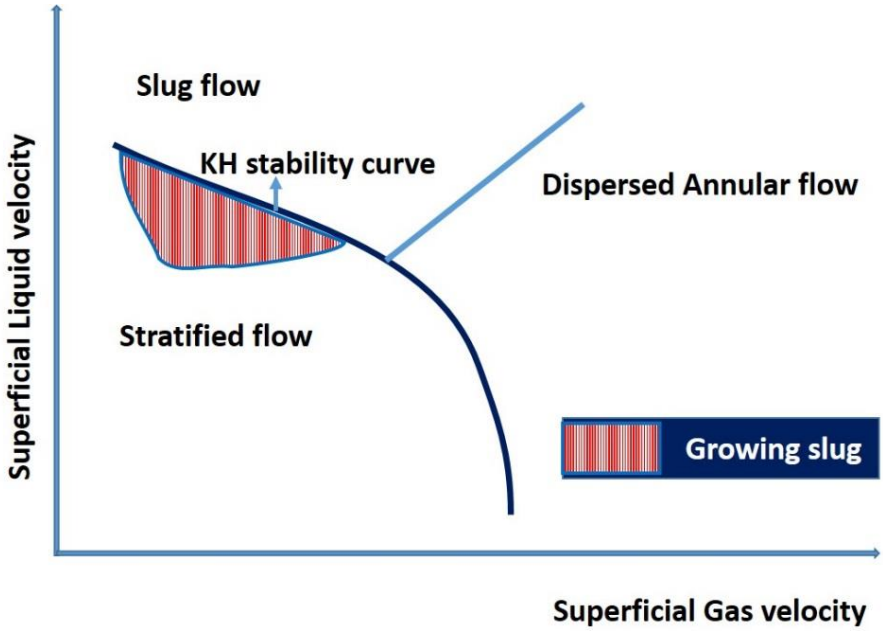

Figure 2-9: Typical horizontal pipe flow pattern in a low-pressure system (Schroeder et al., 2019)

2.4 **Slug flow mitigation and control methods**

Slugging mitigation/control strategies vary from field to field and are largely divided into three categories: slug mitigation by system configuration, system operation, and system control.

2.4.1 **System configuration**

These involve additional or modification of the normal process flow equipment to accommodate the multiphase slug management.

2.4.1.1 Multiple pipelines

The increment of the pipeline liquid holdup increases slug flow problems. This usually occurs in an uphill onshore system or pipeline-riser system at a downturn in production. To solve this slugging problem, multiple pipelines in smaller diameters are used, instead of a single large-diameter pipeline (Yocum, 1973). This will allow the operator to use one pipeline instead of two when production slows.

2.4.1.2 Slug catcher or large separator:

Building a slug catcher large enough to take in the largest slugs of liquid that may occur. This requires that there are no weight and space limitations. These may be good techniques for onshore but not for offshore applications (Rezzónico and Carp, 2007).

2.4.1.3 Subsea equipment:

Using subsea equipment can help prevent slug flow. However, subsea equipment application, testing, and development is a challenging area for offshore production systems.

2.4.2 System operation

System operation involves various routine activities to support the fluid flow to the receiving facility. This slug mitigation strategy relies on pipeline-riser configurations for its effectiveness.

2.4.2.1 Riser base gas-lift:

A riser-base gas-lift can be used late in the life of a field when the GLR is low. The liquid holdup in the riser will increase when the GLR is low, which increases the hydrostatic head. A riser base gas-lift can remove the severe slug flow as well as reduce the hydrostatic head in the riser if the gas flow rate is significantly high.

Sarica and Tengesdal developed a new type of natural riser base gas-lift. If liquid begins to build up at the riser base causing severe slug formation, upstream gas will pass through the blockage of liquid, and be injected naturally into the riser as shown in Figure 2-10 (Sarica and Tengesdal, 2000). As a result, the slug formation will be prevented.

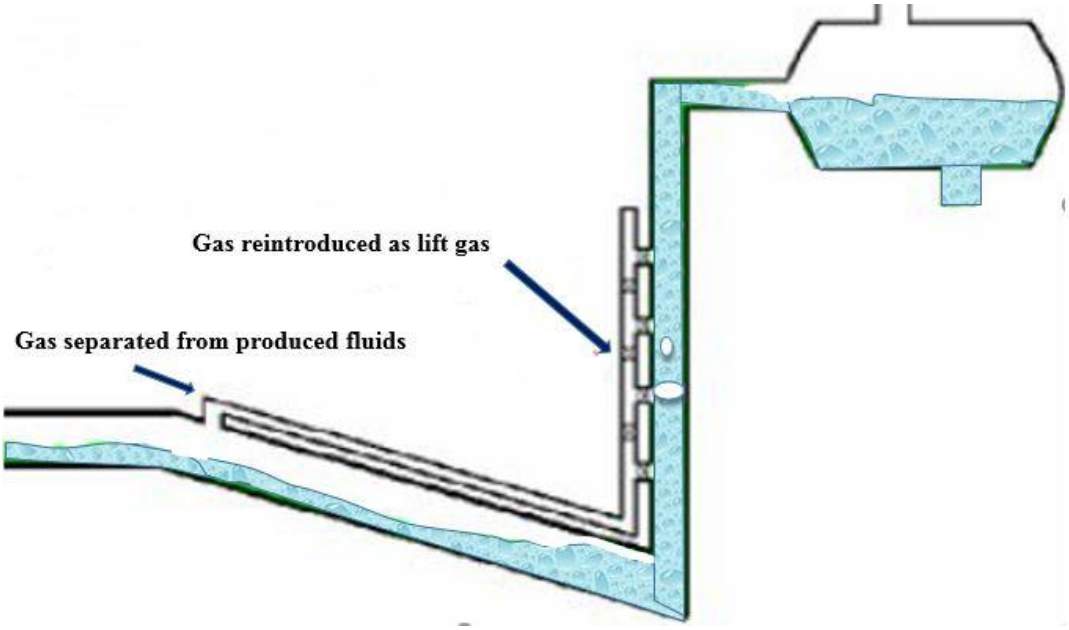

Figure 2-10: Severe slugging mitigation through natural riser base gas-lift (Tengesdal, Sarica and Thompson, 2003)

2.4.2.2 Outside slug regime operation:

Multiphase flow operations may encounter various forms of slugging, for instance, severe slugging, operational slugging, and hydrodynamic slugging. How this slugging occurs depends on the liquid volume rate and on the flow rate. An operator may try to operate only outside a slug flow regime, which will not be easy because different types of slugging have different occurrence mechanisms.

2.4.2.3 Slow ramp-up or start-up

Slow ramp-up or start-up involves the slow bean-up of the well-choke due to the inventory of fluid in the pipeline at start-up or moving from one flow rate to the next to achieve a stable flow. The distribution of the fluid inventory along the pipeline length and near the riser base plays a key role in a smooth start-up or ramp-up operation. Although this method has been adopted as a standard start-up operational procedure for many oil producers, it may take time for the system to respond to different choke settings and different flow rates.

2.4.2.4 Restricted turndown ratio

Restricted turndown ratio involves applying a high minimum flow restriction due to the tendency of liquid to hold up at a very low production rate. This strategy is more effective in the early stages of a field's life. However, it places some constraints on operational flexibility and impacts the need to carry out a slow start-up.

2.4.2.5 Normal and by-pass pigging

Normal and by-pass pigging involves the use of pigs to reduce the liquid holdup/inventory in a pipeline especially after a shutdown or before start-up. This will mitigate/reduce the effect of the start-up or ramp-up slug. The use of pigs here is different from its use for asset integrity and maintenance. The pigging operation generally reduces the upset at the receiving facility during start-up (Van Spronsen et al., 2013).

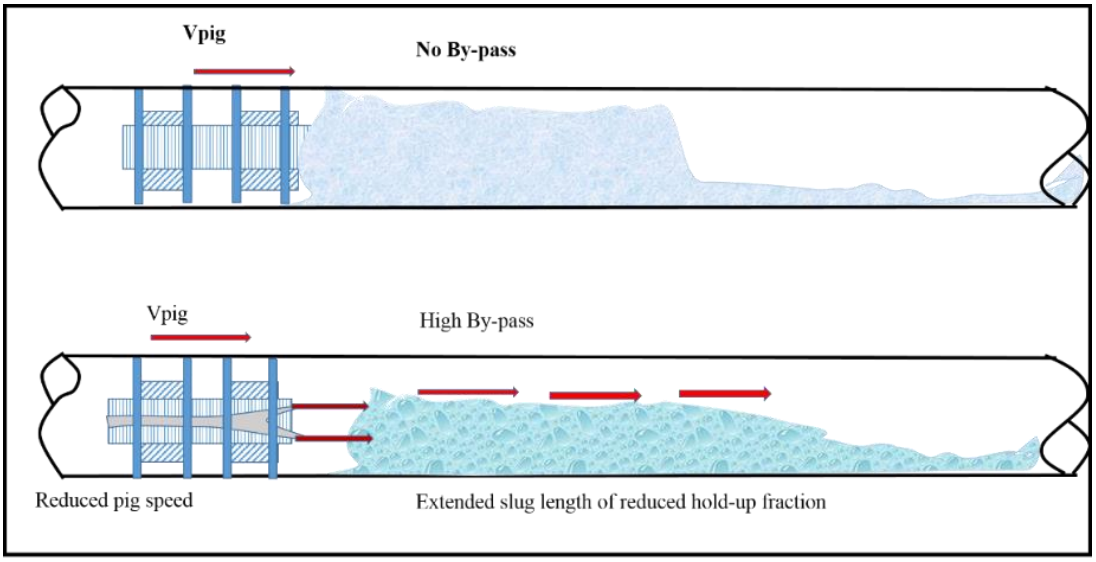

Figure 2-11: Slug flow mitigation by pigging (Van Spronsen et al., 2013)

The normal and by-pass pigging arrangement is for the management of the pig generated volume and the pig residence time. This strategy is in use at the Leman to Bacton trunk-line in the southern North Sea. This pipeline is pigged at a frequency of three per day such that the liquid holdup in the pipeline will not exceed the Bacton slug catcher capacity.

2.4.3 **System control**

System control involves the use of passive and active control strategies to mitigate the effect of multiphase flow slugging. This generally relies on the choke valve (e.g. smart choke) or a control valve as the final control element to respond to an error function (the difference between a controller set point and a measured variable) (Kovalev, Seelen and Haandrikman, 2004; Ogazi et al., 2009).

Various modifications in the control architecture have been used in the oil and gas industry. The strategy relies on high-speed responses of the control systems to perturbation variables and the elimination of lags in the transmission of signals. The benefit of this type of control/mitigation strategy cannot be compromised in that some forms of slugs are transient and will require fast responses to the unstable fluid behaviour.

The control methods can be categorised into two parts: passive control and active control.

Passive control: In this type of control, there are no actuators deployed. Thus, the slugging is handled by process changes.

Active methods: Here, the slugging is handled by manipulating the actuators.

In most cases, the actuators are deployed, while process changes are in use as well. Thus, this can be classified as an active control (Pedersen, Durdevic and Yang, 2017).

The main aim of these slugging control techniques is to ensure that the peak gas and liquid production levels at slugging production do not exceed a specific maximum rate. This maximum is selected such that the processing facility's capacity is not exceeded. Hence, slugging control will:

1) Enhance a field's life, as it can handle typical fields' end of life slugging.
2) Enhance the processing facility's stability.
3) Minimise compressor trips and separators flooding.
4) Increase the processing facility's production capacity.

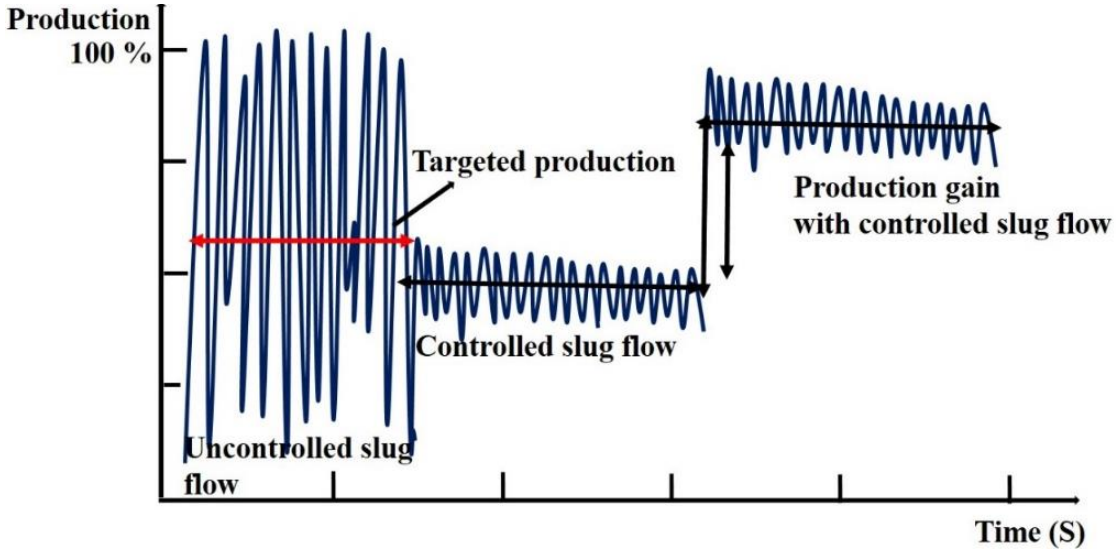

Figure 2-12: Production capacity's increase because of slug control by passive or active control (Yaw et al., 2014)

2.4.3.1 Passive method

The control or mitigation of riser slugging by introducing physical adaptions in the process has been explored for decades (Pedersen, Durdevic and Yang, 2017). The earliest studies established various process changes that are still in use today to control slugging (Yocum, 1973). The passive methods can be grouped into three classes:

1. Use of a liquid mixing device, which helps mix the flow at the riser base to prohibit liquid build-up, thereby prohibiting stratified flow from inducing severe slug flow.
2. Deployment of multiple risers as a substitute for a single riser.
3. Reduction of the incoming line diameter close to the riser to ensure an even flow regime.

Research on passive methods has been explored (Xing et al., 2013a), where various flow conditioners were examined. Flow conditioner is described as a

passive approach where a device is situated in the pipeline to alter the existing regime of the flow upstream of the riser (Pedersen, Durdevic and Yang, 2017).

In Table 2-1, a summary of the different passive methods is discussed based on their benefits and limitations.

1. Slug catcher: The slugging catcher is the most commonly used passive slugging control method. They act as a buffer and aid in gas and liquid pre-separation. The slug catcher acts as a physical low pass filter in such a way that the high frequency fluctuating inflow will be filtered out to a steady outflow. An early-stage separation approach is investigated and deployed to mitigate the multiphase flow entirely from the conveying pipeline (McGuinness and Cooke, 1993). The target was to separate the gas, water and oil in the separator on the top of the well. This approach is promising but very costly if the price of several single-phase pipelines is compared to that of a single multiphase pipeline. However, it is very costly to deploy a slug catcher in deep-water, and for the early stage separators, there is seldom any well structure above sea level. The greatest drawback of the deep-water slug catcher is that it is not cost-effective.

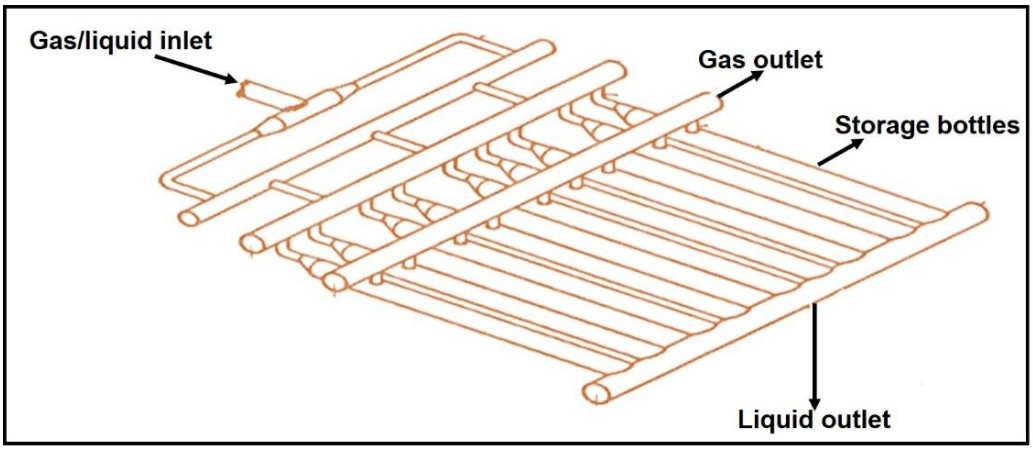

Figure 2-13: Schematic diagram of a slug catcher (Pierro et al., 2019).

2. Choking: In 1996, Jansen et al. proffered permanent choking as an efficient approach to handling slugging (Jansen, Shoham and Taitel, 1996a). This approach is almost the same as the venturi-shaped pipe. The

aim is to alter the flow by inducing backpressure. This approach reduces production.

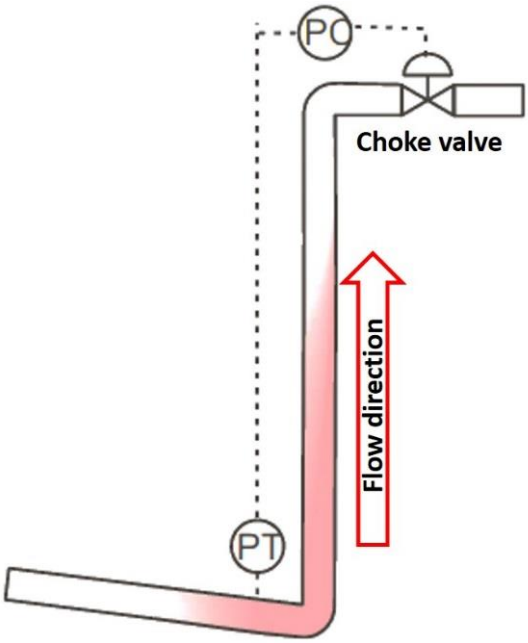

Figure 2-14: Slug mitigation using the manual choking method (Pedersen, Durdevic and Yang, 2017)

3. Multiphase flow homogenisation: in 1998, Hassanein and Fairhurst proposed a method of slug handling by reducing the force of non-homogeneous gas and liquid into a homogeneous one, thereby stabilising the multiphase flow. The target was to minimise the surface tension of the gas and liquid by introducing a surfactant that could alter the fluid into foam, thereby homogenising the fluid (Fairhurst, 1998a). The primary drawback of this approach is that the separation of the fluid at the separation process topside may lower the quality of the product (Pedersen, Durdevic and Yang, 2017).
4. Venturi-shaped device: The venturi-shaped device is situated near the riser base. This device can cause a drop in pressure, which causes a mixing effect, converting the stratified flow to turbulent flow (Almeida, A., 1999a; Pedersen, Durdevic and Yang, 2017). This drop in pressure also reduces production and induces the pigging operation's problems. Almeida and Gonalves introduced this idea in 1999. The venturi-shaped

device includes a convergent nozzle section accompanied by a divergent diffuser section.

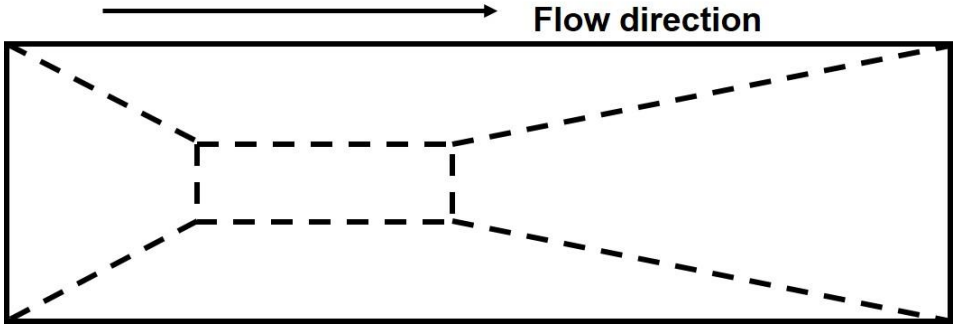

Figure 2-15: Venturi-shaped device (Pedersen, Durdevic and Yang, 2017)

5. Self-gas lifting: This method is a synthetic approach to reducing the cycles of slug and the pressure fluctuation amplitude. The weight of the liquid is minimised in this method by introducing a lesser pipeline feeding from the primary pipeline to the riser, where a one-way rectifier is connected to the riser to guarantee unidirectional flow (Pedersen, Durdevic and Yang, 2017). The gas will build up for a smaller period because of the feeding to the riser. Moreover, an external gas-lift supply is not required. Sarica and Tengesdal implemented this method in 2000; it demonstrated that a stable start-up transient is possible where blow outflow usually occurs (Sarica and Tengesdal, 2000). The drawback of this approach is its pigging difficulties and the extra pipeline cost.

   In 2002, Tengesdal et al. examined the prospect of preventing gas compressibility in the pipeline via gas separation upstream of the riser base and reinjecting the gas back into the riser (Pedersen, Durdevic and Yang, 2017). The reinjected gas minimises the hydrostatic pressure induced by the liquid in the riser. Thus, the formation of slugging is prevented, and in the case of slugging, the amplitude of the pressure will be minimised.

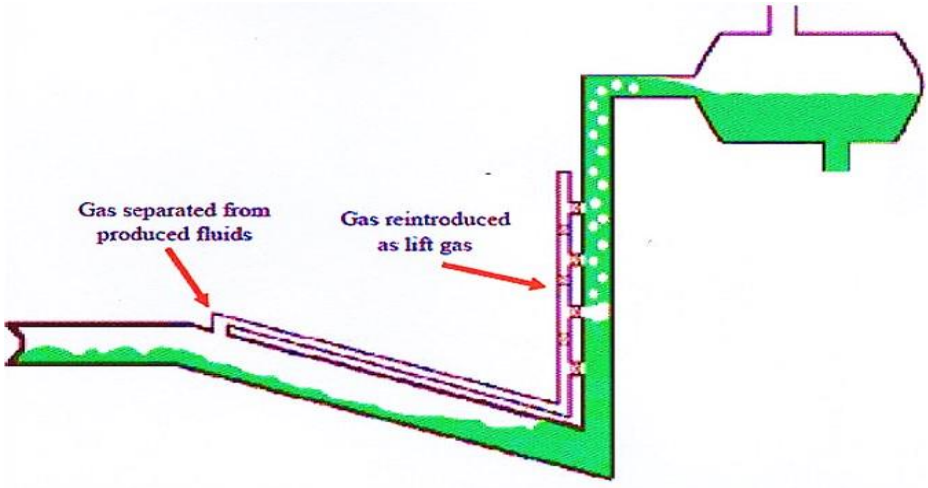

Figure 2-16: Schematic diagram of gas-lift for slug flow mitigation (Okereke and Omotara, 2018)

6. The pipeline as a flow conditioner: In 2007, Makogan patented another flow conditioner. The pipeline design upstream of the riser base was introduced to function as a flow conditioner by attaching a tiny trapezium bend to the pipeline (Taras, Makogon and Brook, 2013). They established that this device could attenuate severe slug flow because of the small mini-plugs. The amount of any liquid slugging could be less to be conveyed by the gas pressure accumulating behind it. Hence, the severe slug flow in the riser could be altered or changed into a plug flow. Therefore, the approach was to reduce the severe slugs to plugs instead of entirely eliminating them.

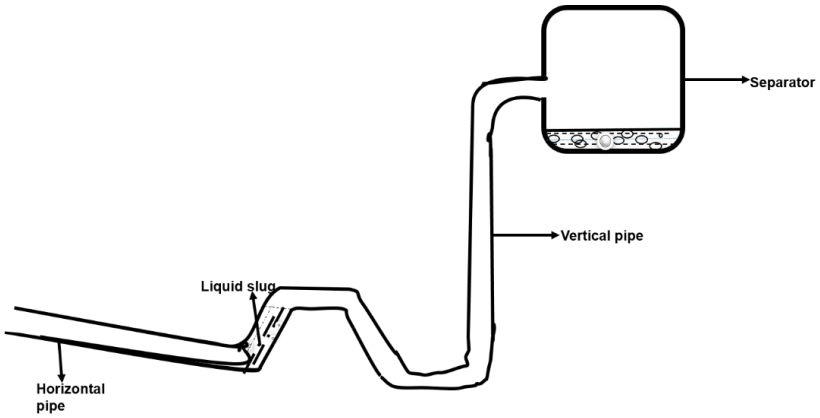

Figure 2-17: A rough sketch showing pipeline as a flow conditioner (Taras, Makogon and Brook, 2013)

7. Helix-shaped pipe: In 2007 Adedigba proved that the region of slug in the flow map can be minimised by applying a helically shaped pipeline due to its ability to alter the flow regime downstream of the helical pipeline section. Moreover, Adedigba determined that the most effective way of minimising the slug region is by introducing the helix at the upstream section of the riser (Adedigba, 2007; Pedersen, Durdevic and Yang, 2017).

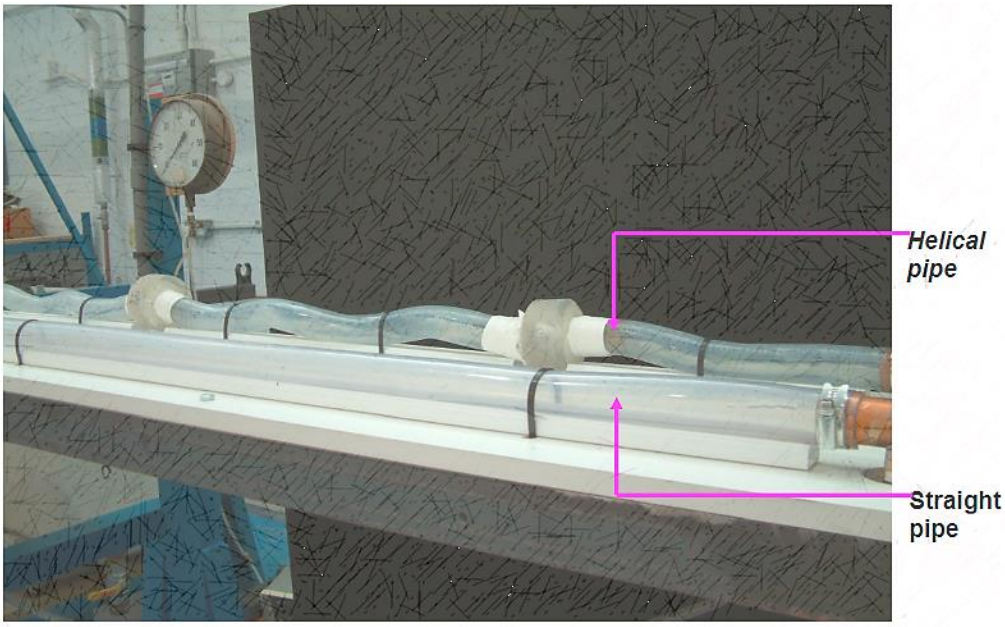

Figure 2-18: Pictorial representation of the helical pipe for slug mitigation (Adedigba, 2007).

8. Wavy pipe implementation: Here, a wavy pipe is introduced at the pipeline nearer to the riser base. Thus, small artificial slugs are formed to handle the large slugs introduced by the build-up at the riser base. A minimised operating slug flow region has been established experimentally. A numerical study was also carried out to establish the optimal dimensions and position of the wavy pipe using a CFD model (Xing et al., 2013).

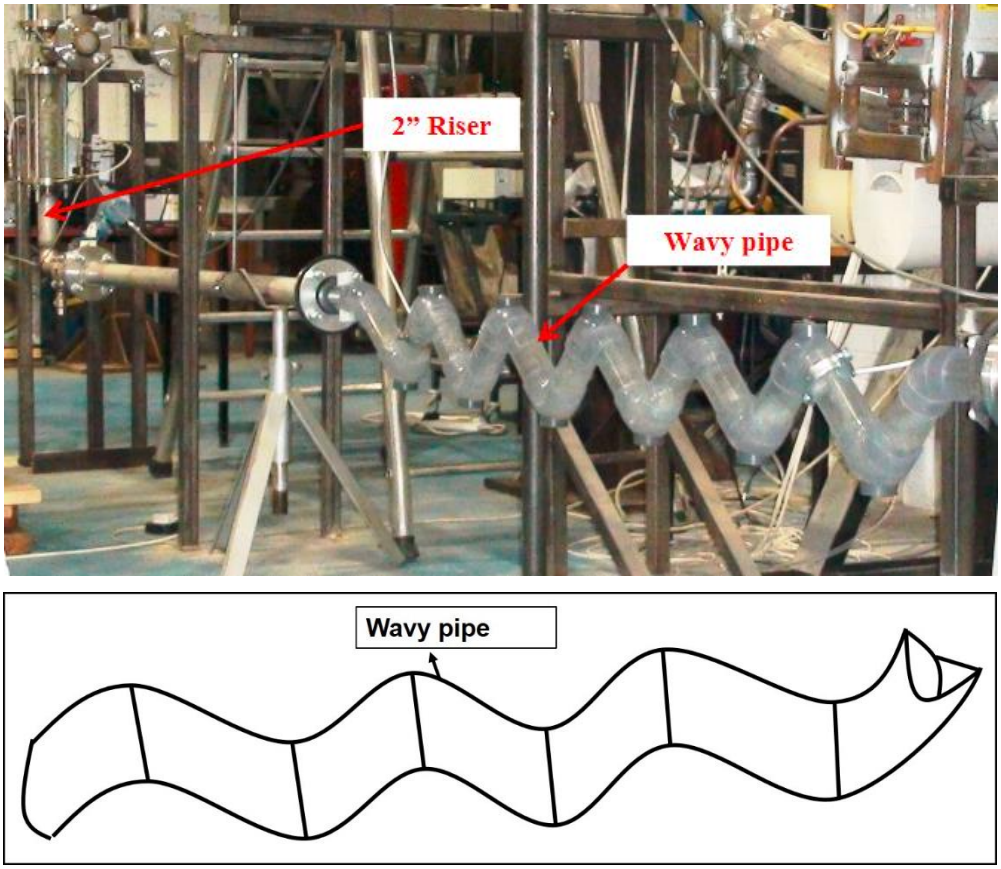

Figure 2-19: Schematic diagram of a wavy pipe for passive slug flow mitigation (Xing et al., 2013).

Table 2-1: The comparison of different passive control methods based on their benefits and limitations

Researcher	(McGuinness and Cooke, 1993)	(Almeida, A., 1999b; Almeida, A., 1999a)	(Fairhurst, 1998b)	(Jansen, Shoham and Taitel, 1996b; Sarica and Tengesdal, 2000).	(Adedigba, 2007; Taras, Makogon and Brook, 2013).
Year	1993	1996-1999	1998	2000-2002	2007-2013
Approach	The flow fluctuations are physically filtered	Backpressure increment	Homogenising the multiphase fluid	Hydrostatic pressure reduction	The flow regime is altered upstream of the riser

Stable zone	Determined by the size of the slug catcher	All	All	Not all	Not all
Benefits	Removes slug at the initial stage	Simple and economical	No multiphase	Flexible to disturbance and it works for some vertical sections	Causes no issues for pigging operations, simple
Drawback	Expensive maintenance and installation	Limits production rate	Not good for separation	Expensive maintenance and installation	Expensive installation

2.4.3.2 Active slug control methods

Active slug control is a method where some measurements such as temperature, flow transmitters, and pressure are used to control the actuators in a feedback loop. The sensor's position differs depending on the structure being investigated although it is usually located at the top of the platform.

The effects of input and output have been investigated recently. The system input and output controllability can be estimated quantitatively through the estimation of the minimum achievable peaks of various transfer functions of the closed-loop system (Pedersen, Durdevic and Yang, 2017; Postlethwaite, 2005).

2.4.3.2.1 Active choking

Choking the valve is the most examined actuator to control slugging because choke valves are simple, relatively cheap and have flexible application solutions. However, it is impossible to use a choke valve for slugging control without limiting the production rate.

Theoretical examination (Storkaas, 2005), partial differential equation (PDE) model analysis (Storkaas and Skogestad, 2007) and ordinary differential equation model analysis (Jahanshahi, Skogestad and Helgesen, 2012) have been used to examine the input/output controllability analysis of a topside control

choke valve incorporating different measurements to find the best control feedback loop for stability. All the studies carried out determined that both the flow and pressure measurements at the top side had drawbacks and recommended using the two measurements together in a single-input-multiple-output (SIMO) cascade control for a well-pipeline-riser system. A subsea control choke valve was also recommended as the manipulated variable, both in a layout as the only actuator, and in a layout merging the topside and subsea control valve as the actuators in a multiple-input single-output (MISO) control systems. A controllability analysis on the gas lifting oil well and a well-pipeline-riser system was performed by Jahanshahi (2013) and Jahanshahi et al. (2012). They concluded that riser base measurements are the most suitable for a single-input-single-output (SISO) control valve (topside) control. It is always true that the choke valve rate downstream is suitable if the riser base pressure is readily available. They deduced that combining flow rate and riser base pressure in a well-pipeline-riser system yields the best results (Jahanshahi, 2013; Jahanshahi, Skogestad and Helgesen, 2012). The flow rate and topside pressure combination when subsea pressure measurements are not available also provide successful results. The drawback of the topside pressure measurement is connected to the non-minimum phase system inverse response due to the low Signal to Noise Ratio (SNR) and right half plane zeros (Jahanshahi, 2013). The performance of the observer as investigated in the work of Meglio (2012) using the measurement of topside pressure was not determined by the unstable zero induced by the controlled variable, as presented in the work of (Storkaas, 2005). Sivertsen and Skogested (2005) and Helgesen (2010) also investigated different topside measurement cascade control (Helgesen, 2010). To date, investigations on which control variable to use for the optimal performance of a closed-loop system is ongoing. The pressure drop over the riser was proposed in Hedne Pal and Linga Harald, (1990) and Di Meglio et al., (2012), as a controlled variable.

2.4.3.2.2 Topside choke valve

Choking the pipeline at the riser base has been proven to be effective in slug elimination (Almeida, A., 1999). However, it is not cost-effective to have such a

low-point choke valve deployed subsea. Thus, the deployment of a choke valve at the riser base is rare. The placement of a choke valve topside is more prevalent than at the riser base in offshore designs. The anti-slugging control deploying choke valve topside has been investigated for decades. Schmidt first proposed it in 1979. However, this minimises the velocity of the gas in the riser and also hinders the gas tail from entering the riser base (Farghaly, 1987). Havre and Dalsmo (2001) demonstrated through OLGA simulation that topside choke valve manipulation with feedback control from a pressure measurement can suppress slug flow. It was concluded that feedback control could enhance the production rate compared to permanent choking.

Ogazi, (2011) considered the separator gas-outlet control valve at the topside as an alternative for the actuator of anti-slug control. He demonstrated through simulations that flow stability is possible with a gas outlet valve as it successfully stabilises the flow at a higher choke valve opening than the topside choke valve before the separator. It was determined that even though the gas outlet valve can stabilise the flow at a higher opening, the riser base pressure is lower when using the choke valve upstream of the separator. Controllability analysis of an input-output was carried out to determine which of the two topside control valves is the most suitable, and it was established that both choke valves are capable of stabilising the flow at a higher opening. Molyneux and Kinvig, (2000) patented a control method of slug flow elimination by manipulating the separator's gas outlet (Almeida, 1999b). The outlet gas valve is usually dedicated to level and pressure.

Jahanshahi et al. (2013) used feedback linearisation to fabricate the control law, establishing a model-based nonlinear control (Jahanshahi, Skogestad and Grøtli, 2013). Both topside pressure and riser base pressure were used in the controller design. The controller stabilised the slugging flow with a high valve opening and avoided the low choke valve opening production limitations (Jahanshahi, Skogestad and Grøtli, 2013).

Ogazi et al. (2010) examined the possibility of using a large valve opening to increase the production rate while removing the slugging and also working in the

unstable open-loop slug flow region by shifting the bifurcation point with a feedback loop. Ogazi et al. (2010) concluded that total oil production increase compared to ordinary choking would significantly increase as the well pressure decreases. This control system is more profitable for brownfields than new fields.

Stasiak et al. (2012) also introduced a topside control system for reducing either the pressure or the flow fluctuations, while still keeping the choke valve opening higher than the valve opening at the initial stage of the limit cycle. Thus, the control seems to repress the fluctuations while still keeping the choke valve opening operating within a high acceptable opening value (Stasiak, Pagano and Plucenio, 2012).

Havre, (2007) patented a dynamic feedback controller, deploying a control choke valve at the topside as an actuator and the differential pressure over the valve, flow or topside pressure as controlled variables. At any sudden drop, an action is taken to determine whether there is a liquid blockage present in the flow-line (if the sudden drop is large enough). If there is any blockage of liquid predicted or observed, the choke valve opening will be increased. The actual measurement drop estimates the changing proportion of the choke valve opening. However, further valve manipulations are restrained until the expiration of the time penalty. Pedersen et al. (2014) investigated similar techniques where a controller was deployed in conjunction with a supervisor which decides if the pressure has changed too much in the pipeline-rise. Pressure fluctuations are used as a controlled variable for the supervisor. A switching PID controller was combined with the supervisor for two objectives: the elimination of slugging flow and increasing production. Through choke valve manipulation, the slugging was removed, and a 7.8 percent production rate increase at steady-state recorded compared with the constant fully opened valve. The investigation determined that this controller gets the best open-loop bifurcation point with a fixed valve opening. However, the production rate can be increased by implementing a changing choke valve opening to shift the bifurcation point more into the uneven open-loop region.

Because proportional integral derivative (PID) is the most common controller used in industry; many investigations have considered PID schemes but have inculcated more enhanced tuning methods. Godhavn (2005) suggested three PI tuning techniques to eliminate slugging. The tuning techniques deployed various controlled variables for the feedback signals such as a pressure PI controller for pressure stabilisation, a volumetric flow PI for the flow stability and a volumetric flow/pressure cascade PI controller where the inner loop takes care of the flow stability, and the outer loop ensures pressure stability. Thus, the cascade system is unnecessary since a steady pressure typically will induce a steady flow (meaning for the inlet flow, there is a fixed pressure source) (Pedersen, Durdevic and Yang, 2017). Hence, an additional feedback loop is unnecessary. For the pressure, subsea pressure measurement is needed, and for the volumetric flow, a densitometer or a flow transmitter at the topside is needed. Therefore, the tuning techniques are limited to a system configuration with many available measurements. Jahanshahi et al. (2014) developed a new internal model control tuned PID with a low pass filter controller (IMC-PIDF). This was developed as a Godhavn et al. (2005) tuning technique extension. The tuning technique developed was compared with some robust tuning techniques, and the controller efficiency could be enhanced further by an H_∞ loop shaping extension to enhance the robust performance and stability (Jahanshahi et al., 2014; Pedersen, Durdevic and Yang, 2017). In 2004, Eikrem et al. introduced a well PI controller which uses pressure measurement at the topside to calculate the well's downhole pressure (Eikrem et al., 2004). Since then, many investigations have been carried out on PID controllers in conjunction with observers for flow and pressure stabilisation. In 2006, Eikrem deployed Extended Kalman Filters (EKF) to estimate the masses in the system or measure pressure downhole (Eikrem, 2006). An observer (reduced order) is then implemented as another option to the EKF. Both observer techniques are deployed in conjunction with various controllers for the stability of the mass in the well, thereby controlling the condition of the system through feedback control of the valve topside (Pedersen, Durdevic and Yang, 2017).

2.4.3.2.3 External gas lifting

The two primary objectives of the external gas lifting technique are (a) aiding depleted reservoirs with a relatively low-pressure capacity to produce by injecting gas upstream of the well, and (b) mitigating riser-induced slug flow by introducing gas at the riser base. Jansen et al. (1996) concluded that the gas lifting could remove severe slug flow by increasing velocity, which reduces the riser liquid holdup. Thus, a large volume of gas is required for flow stability. Gas lifting reduces hydrostatic pressure in the vertical pipeline and then stabilises the flow in the direction of the gas superficial velocity (Jansen, Shoham and Taitel, 1996a).

Johal et al. (1997) proposed a new technique for gas lifting in a riser. The principal aim of the technique is for deep-water oil fields riser gas lifting. The study proposed the Multiple Riser Base Lift (MRBL) as a substitute for the conventional Riser Base Gas-Lift (RBGL) where Joule Thompson cooling can induce some setback for the gas at the control choke valves because of possible hydration (Johal, Teh and Cousins, 1997). The proposed technique reroutes an even multiphase fluid flow to the closest pipeline-riser system where severe slug flow is experienced. This technique is expensive, as it requires the installation of multiple transportation pipelines with the likelihood of rerouting each single multiphase fluid flow accordingly.

Krima et al. (2012) investigated many PI controllers for gas lifting using OLGA simulation to prevent hydrodynamic slugging (Krima, Cao and Lao, 2012). The controllers deployed various multiphase flow measurements as a controlled variable. However, the holdup transmitter at the topside was the best-controlled variable for the optimal control solution. Moreover, it was noted that a quality control design for the control valve at the topside minimises gas injection requirements.

2.4.3.2.4 Topside choking and gas lifting combination method

Pagano et al. (2008) investigated model-free multiple inputs multiple outputs (MIMO) PI controller for both topsides choking and gas lifting for the well. The

choke valve at the top side was used for topside pressure stability, and the choke valve manipulating the inlet of the gas lifting was controlled for the injected gas in the production pipe stability. The primary aim was to deploy a Variable Structure Control law (VSC) that implements sliding bifurcation on the system to control the limit cycles. This approach was based on Angulo et al. (2005). The work demonstrated that Hopf Bifurcation is commonly induced by low gas rate inflow. The measurements at the downhole are not essential for the control scheme. The controller also demonstrated that it could work for well restarting, where it minimises the start-up time without inducing start-up slugs (Pedersen, Durdevic and Yang, 2017).

2.4.3.2.5 ABB's Optimize:

ABB's Optimize technique fits a flow control valve at the riser top, upstream of the production separator. Maintaining a constant pressure at the pipeline inlet is its fundamental control mode (Havre and Dalsmo, 2002). It is designed to mitigate the occurrence of severe slugging. The ABB Optimize technique is illustrated in Figure 2-20.

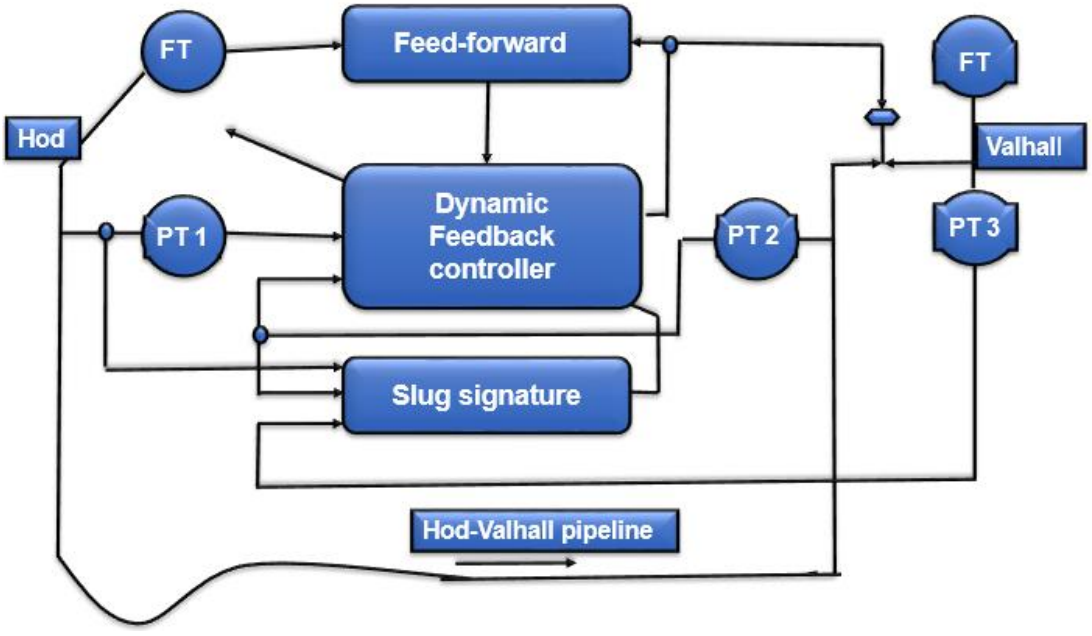

Figure 2-20: Schematic of ABB's Optimize to control slug flow in the Hod-Valhall pipeline (Havre and Dalsmo, 2002)**.**

2.4.3.2.6 Flow rate control: Shell's Slug Suppression System

Shell's Slug Suppression System (S^3) control technique depends on the liquid flow and total volumetric flow control (Kovalev, Cruickshank and Purvis, 2003). The valve of the liquid is controlled to ensure that the level setpoint is maintained and the valve of the gas is controlled to ensure that the total volumetric flow set point is maintained; all these are done in total volumetric control mode. The flow meters in the liquid and gas outlet flow measure the actual flow rates. The variable to be controlled is the sum of flow meters' output. A pressure controller regulates the volumetric flow set point in conjunction with other algorithms (Kovalev, Cruickshank and Purvis, 2003). These regulations rely on the actual pressure and pressure set point in the mini-separator and other factors relying on the flow-line size. One of the drawbacks of this technique is that it requires a lot of space and has a high operating cost.

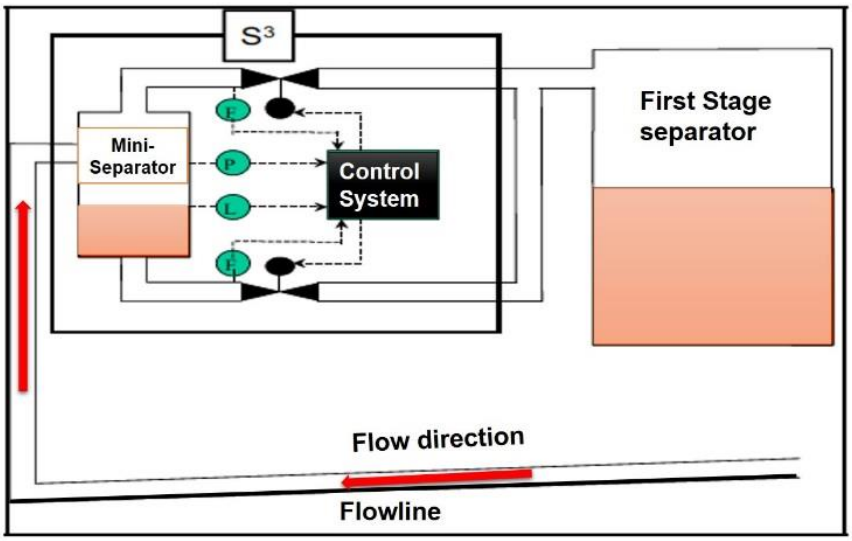

Figure 2-21: Schematic diagram of the S3 deployed between the first stage separator and the pipeline (Kovalev, Cruickshank and Purvis, 2003).

2.4.3.2.7 Shell's vessel less S^3:

One of the reasons behind the development of S^3 without a separator is to minimise costs. The mini separator function was replaced by the down-comer,

two T-junctions and a stratifier (Kovalev, Seelen and Haandrikman, 2004). The stratifier enhances liquid/gas separation in the T-junction and the down-comer harbours the liquid slugs' inflow, which helps to create enough time for the control valve to react. The level transmitter measures the liquid level in the down-comer. The rest of its operations are the same as the standard S^3. The major setback for this approach is that it requires the retrofit of the existing system to install a new set of devices.

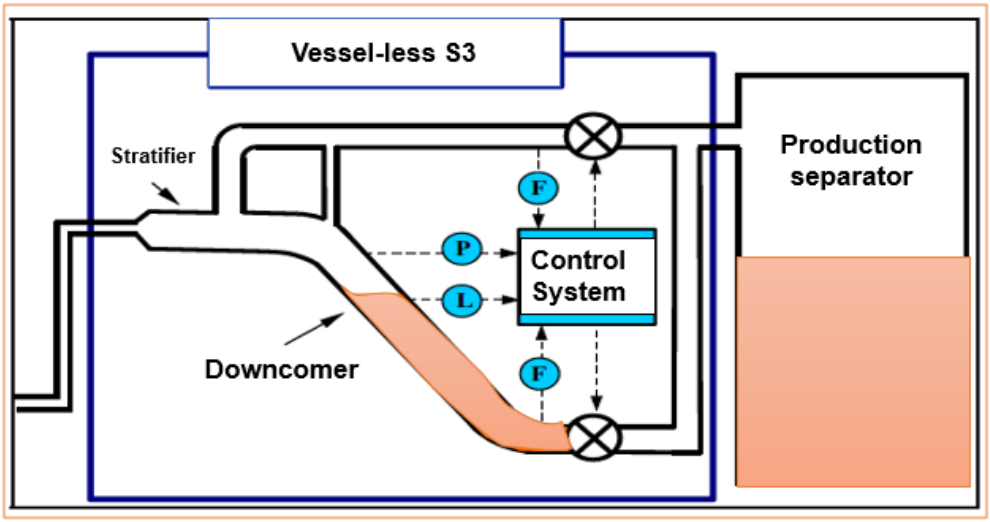

Figure 2-22: Schematic diagram of Vessel less S^3 (Kovalev, Seelen and Haandrikman, 2004)

2.4.3.2.8 Statoil's choke:

Statoil has built a slug cascade controller. The system contains two traditional PID controllers. The cascade controller merges the flow and pressure controller. The outer control loop maintains constant pressure at the inlet by adjusting the inner control loop setpoint (Storkaas and Godhavn, 2005). The quicker inner control loop adjusts the choke valve to ensure the desired flow. The controller can be switched into a flow controller by deactivating the outer control loop pressure, and it can be switched into a pressure controller by deactivating the inner control loop flow.

The reason for the flow controller is to make the multiphase fluid volumetric flow stable via the choke. In this control mode, the choke valve is issued by a flow controller (FIC) with feedback from (F) the volumetric flow via the choke and (F_{SP}) setpoint defined by the operator (Storkaas and Godhavn, 2005).

The volumetric flow is given by

$$F = g(v_{pos})\sqrt{\Delta P/\rho} \qquad 2\text{-}4$$

where ΔP is the choke differential pressure, ρ is the multiphase fluid density traveling via the choke and it is measured by the gamma densitometer, F is estimated volumetric flow, and g is a function of the choke valve v_{pos}.

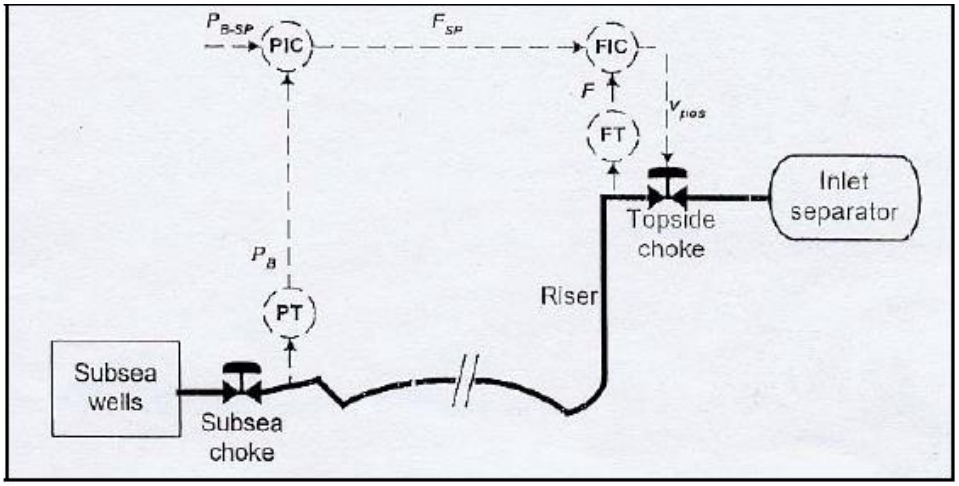

Figure 2-23: Schematic diagram of Statoil's slug controller (Storkaas and Godhavn, 2005)

2.4.3.2.9 Intelligent choke:

The intelligent choke technique consists of a choke fitted at the riser top upstream of the first stage separator. A PID controller, which controls the downstream first stage separator liquid level, determines the choke opening. The outlet liquid valve of the separator controls the liquid level, though when the level becomes more than the present value, the intelligent choke activates and begins to close. Hence, the peak levels in the production of liquid because of slugging arrival can be minimised (Kovalev, Cruickshank and Purvis, 2003).

Nevertheless, the intelligent choke cannot mitigate gas surge (because of pressure accumulation upstream of the choke valve) following the surge of liquid. Another drawback of this technique is that the intelligent choke PID tunings are highly dependent on the outlet gas and liquid valves of the first stage separator. The effectiveness of the choke will also diminish if multiple pipelines are linked to the same first stage separator.

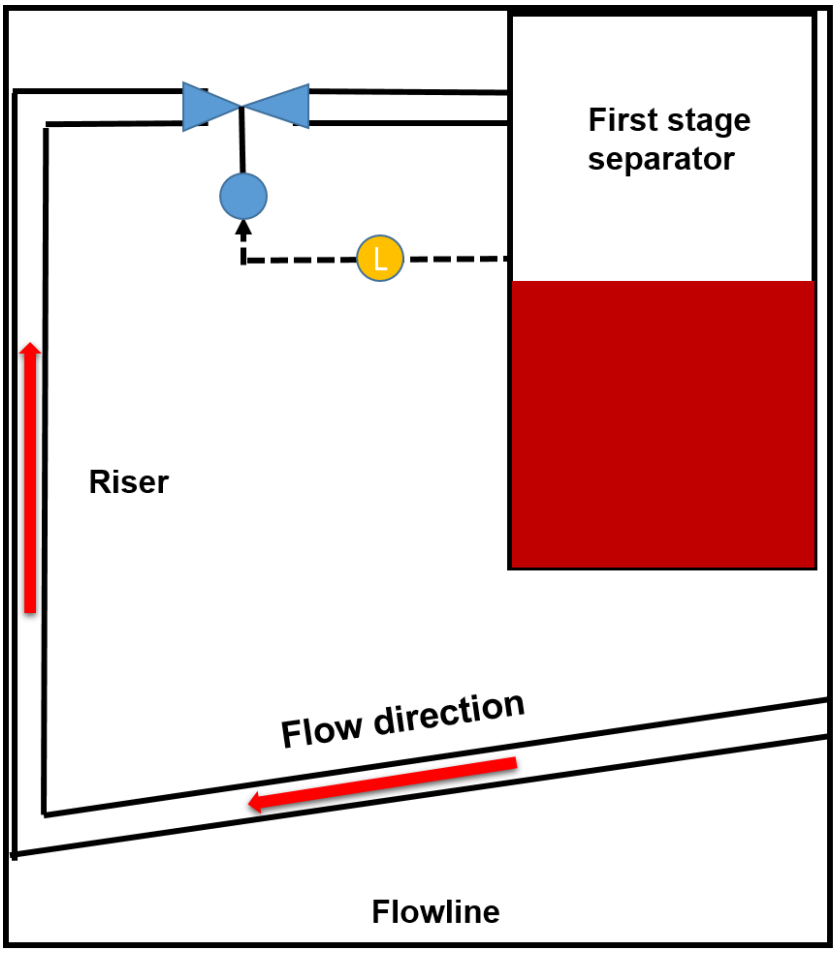

Figure 2-24: Schematic diagram of an intelligent choke (Yaw et al., 2014).

2.4.3.2.10 Slug control using only topside measurements

The solutions to slug flow mitigation/control proposed by some of the investigators required at least one or two subsea measurements (Zhou et al., 2018). This comes with many disadvantages. In most cases, these subsea measurements are not readily available, and their addition to an existing pipeline/flow-line requires additional cost. Subsea measurement equipment must

be regularly inspected, calibrated, checked for maintenance and possibly replaced due to wear. Thus, these are not cost-effective (Ehinmowo and Cao, 2016).

2.4.3.2.11 Single topside measurements:

Storkaas, 2005 applied a controllability analysis to slug flow suppression. He assumed that to achieve efficient control performance that the use of upstream pressure is the best and only measurement that can be used in a single loop controller for slug attenuation. Thus, the riser base pressure signal is suitable for slug control, but it requires an instrument from subsea, which is not always available. Also, due to operational and high capital costs associated with subsea instruments, operators and researchers have been considering the use of topside measurements to determine if topside measurements can be more beneficial in the control system. From the analysis conducted on mass or volumetric flow rate, it was observed that theoretically, it could be possible to stabilise the system, but because of issues of low-frequency performance and disturbance, it is not possible to use mass or volumetric flow rate in practical operations. Other controllability analyses deduced that the pressure measurements at the riser top are not suitable for use in control process stability because of the zeros and poles located near one another at the right half of the imaginary plane (RHP).

The mini-loop experiment was developed and carried out by Sivertsen and Skogstad in 2005 to test various control strategies using a PI controller with measurements of subsea pressure; it was observed that control with this variable gave good results. A further analysis was made using only a single topside measurement for control, but it was concluded that using only a single topside measurement for control caused problems (Sivertsen and Skogestad, 2005).

Sivertsen et al. (2010) designed a controller-based only on the use of a single topside pressure measurement. During an experiment conducted on a medium scale rig riser, it was observed that achieving stability with this type of controller is not possible. Another approach was a measurement of topside density,

which was observed to be noisy if applied directly to the control (Storkaas, 2005).

2.5 Combination of topside measurements:

2.5.1 Control using Cascade Configuration

The idea of controlling slugging flow using a cascade configuration arose due to the inability of using topside measurement as a single variable in achieving effective control performance. Considering the controllability problems observed using topside measurement, the cascade method was implemented with the hope that it would be a better solution (Storkaas, 2005).

In the cascade system, two controllers were applied to work together and produce a single output. These two controllers were arranged into two loops in such a way that the inner loop took care of the fast dynamics of the system to prohibit it from affecting the signal output while the outer loop took care of the system's slow dynamics. A master controller (outer loop) determined the inner loop setpoint known as the slave controller (Arrieta, Vilanova and Balaguer, 2008).

Godhavn, Fard, and Fuchs (2005) researched a cascade controller at the SINTEF petroleum flow laboratory with a control system deploying only topside flow-line pressure and volumetric flow rate for slugging control. The flow-line pressure feedback control was successful in mitigating riser slugging and could stabilise both the flow in the riser and flow-line pressure.

From the mini-loop experiment developed by Sivertsen and Skogstad (2005) to test various control strategies using a PI controller with measurement of subsea pressure, it was observed that control with this variable was successful. A further analysis was made using only a single topside measurement for control, but it was concluded that using only a single topside measurement for control caused problems. A combination of topside measurements was further considered to investigate its capability of stabilising the flow. A cascade controller was developed and tested using the topside measurements of

pressure and mass flow rate. It was first investigated using a simplified riser slug model in simulations, and it was determined from the result that the controller managed to suppress the flow. From the experiment carried out in a mini two-phase loop, the obtained results were unsatisfactory because of volume flow estimation using holdup measurements which need to be heavily filtered (Sivertsen and Skogestad, 2005c).

Fard et al. (2006) carried out a simulation investigation of a cascade slug controller using the same topside measurements as proposed in Sivertsen and Skogestad (2005a), and Sivertsen and Skogestad, (2005b). The SINTEF test loop model which was deployed by Godhavn et al. (2005) was implemented in OLGA. The investigators concluded that tuning the controller was more problematic than the controllers deploying only the measurements from the seabed. From the simulation analysis, the investigator deduced that the cascade controller deploying this topside measurement was partially successful in that before the controller could be switched on, the stable operation was first achieved by manually choking the system. Stability is not possible if the controller is switched on in an unstable flow condition. Nevertheless, when the controller is switched on in a stable flow condition, it managed to maintain the flow stability to a higher valve opening with a lower flow-line pressure compared to manual choking.

Sivertsen et al. (2010) performed a further experiment to evaluate/analyse the effectiveness of using a cascade control configuration to attenuate or eliminate severe slug flow, which was carried out in a multiphase medium-scale rig riser. The following variables were tested in a cascade configuration (Sivertsen, Alstad and Skogestad, 2009):

1) The topside volumetric flow rate in the inner loop and topside choke valve opening in the outer loop.
2) The topside volumetric flow rate in the inner loop and pressure in the outer loop.

3) The topside density in the inner loop and topside choke valve opening in the outer loop.
4) The topside density in the inner loop and the topside pressure in the outer loop.

The measurements of the combinations used in cascade control mentioned above were able to suppress the slugging flow, but after some time, the system became unstable again. It was also deduced that the controller could suppress the slugging flow only when the controller is activated on a particular flow condition otherwise stability will not be achieved. Moreso, there was no structured approach when testing the performance of the controller in that some of the results obtained were when the controller was already activated. Because of that, the time required to stabilise the flow was not estimated. Due to the lack of an effective systematic approach during the experiment, repeatable flow behaviour was not obtained because of the inability to start the analysis during a severe slugging flow regime. As a matter of fact, this type of chaotic (nonlinear) system will affect the results significantly due to flow hysteresis. This type of control system is not adequate for use in the industry.

Esmaeilpour, (2013), investigated cascade control deploying topside pressure with density. One of the objectives in the work was to run the closed-loop deploying a cascade control system with topside density and pressure as the control variables. The idea was to tune this control system by trial and error and thereby examine the controllability features compared to the single loop system. The control variable of the inner loop was the outflow density, and the control variable for the outer loop was top pressure. The conductance probe was the device deployed to measure the outflow density. It was observed that the conductance probe used to measure density is not a suitable measuring device for it. It was deduced that the density signal could not be an appropriate signal for control because the density signals are very noisy and do not indicate a good response to step changes. To achieve effective cascade control using density

as a control variable in the inner loop, clearer and more accurate density signals are essential.

2.5.2 **Inferential Slug Control**

Cao et al., (2013) invented a novel method to suppress the slugging flow called Inferential Slug Control (ISC). This method was known for its effectiveness to detect and suppress hydrodynamic slugging flow in real-time, in a subsea production facility. This technique implements multiple topside measurement signals to suppress slugging flow in the offshore pipeline-riser system (Tandoh, Cao and Avila, 2016).

The topside measurements that were fed into the controller are the pressure at the outlet of the riser, the separator pressure topside, the separator pressure of the three-phase, the topside separator liquid level, the topside separator gas outlet flow rate, the topside separator liquid outlet flow rate, the mass flow rate riser outlet measurement from the Coriolis meter, the density measurement of the riser outlet from the Coriolis meter, the riser outlet soft count from the Gamma meter, and the riser outlet hard count from the Gamma meter.

This idea of applying a linear combination of all available topside measurements in designing a slug control system has been investigated both in OLGA simulations and in experiments. The benefits of this approach are numerous such as:

1) An increase in oil production: The Principal Component 1 (PC1) which denotes the combinations of measurements most sensitive to slug flow when used as the controlled variables; the control choke valve will be maintained at a larger valve opening to suppress the flow, increasing the production rate.
2) Sensitivity to slugging flow: The more measurements available, the more sensitive the system will be to slugging flow.

3) Simple and easy to implement: The PC1 variable can be designed by deploying any available topside measurements in as much as the measurements will react to slugging flow.

However, ISC gain is determined by trial and error although its measurement combination coefficients can be estimated systematically. More so, the gamma densitometer used in ISC has been demonstrated to be a suitable parameter for slug detection and control. It is a clamped-on, non-invasive, non-intrusive measurement, so the installation is inexpensive. Nevertheless, due to its radioactive nature, it is not well utilised in offshore systems.

Furthermore, the higher the measurement instrument deployed, the higher the system uncertainty becomes because each measurement adds to the total system uncertainty, minimising the accuracy of the system.

In 2015, a systematic approach was investigated and proposed by Ehinmowo and Cao to determine the minimum control gain for a slug flow controller. The study on flow stability at a large valve opening used active feedback control; the gas flow rate was used as the input variable for a purely catenary riser (Ehinmowo and Cao, 2015). The input variable (gas flow rate) was used successfully to stabilise the flow, but determining this variable practically is not easy.

Tandoh, Cao and Avila, (2016) extended the work proposed by Ehinmowo and Cao, (2015) to design a controller gain of the inferential slug controller on a U-shaped riser to make the method more feasible for a real system. In the study, the liquid density, total liquid mass flowrate, riser top pressure, and gas mass flow rate were the topside measurements used due to their ready availability. One of the benefits of the approach is that it can be used to determine the control gain of the ISC.

2.6 **Machine Learning**

Machine Learning (ML) is a data analysis method that automates analytical model building (Lee et al., 2019). It is a part of Artificial Intelligence (AI) that allows the

system to learn automatically from the data, identifies the patterns and gives out the output without human assistance or intervention.

Machine learning has evolved from the study of pattern recognition and computational learning theory. It is an effective method utilized in the data analytics field so as to predict one thing by designing and developing some algorithms and models. The analytical models enable the data scientists, analysts, engineers and researchers to produce valid, and reliable results (Carvalho et al., 2019).

2.6.1 **Neural Networks**

Neural Networks are one of the machine learning models that functions similarly to that of the human brain. The aim of the neural networks is to carry out those logical functions the human brain can execute such as being teachable and problem-solving (Livieris and Pintelas, 2019).

Neural Networks are comprised of computational units also known as the layers of neurons. These layers of neurons are also linked in different layers. These neurons process the data until the output is acquired (Henríquez and Ruz, 2018).

Neural networks have been successful in solving supervised learning-related problems in different domains such as image classification (Fernandes Junior and Yen, 2019), natural language processing (Morchid, 2018), and speech recognition (Lee, Lee and Chang, 2019).

An Artificial Neural Network (ANN) can have one of three types of topology namely single layer, recurrent layer, and multilayer. A single-layer ANN has no hidden layer. Recurrent Neural Networks (RNNs) have at least one feedback layer in the network. A Multilayer Neural Network (MLNN) is comprised of an input layer, a hidden layer (one or more) and an output layer.

Different types of ANN models have been designed for various ranges of industrial applications such as classification and image processing, optimization, associative memory, pattern recognition, control, and modeling.

Table 2-2 summarises the learning strategy, functions and topology of various ANNs used in the engineering industry ranging from Multilayer Perception (MLP), Wavelet Neural Network (WNN), Radial Basis Function (RBF), Probabilistic Neural Network (PNN), Extreme Learning Machine (ELM), Cellular Neural Network (CNN), Committee Machine (CM), Adaptive Resonance Theory (ART), Cerebellar Model Articulation Controller (CMAC), Elman, Kohonen, and Hopfield.

Table 2-2: Functions, learning approach and topology of various ANN

ANNs	**Learning Approach**	**Topology**	**Functions**
MLP	Supervised	Multilayer feedforward	Classification, function approximation, pattern recognition, control, and modeling
WNN	Supervised	Three-layer feedforward	Classification, function approximation, forecast
RBF	Supervised	Three-layer feedforward	Classification, function approximation
PNN	Supervised	Four layered feedforward	Classification, pattern recognition
ELM	Supervised	Three-layer feedforward	Classification, function approximation
CNN	Supervised	Multilayer	Classification, optimization
CM	Supervised/unsupervised	Experts	Classification, function approximation, pattern recognition, control, and modeling.
ART	Unsupervised	Recurrent	Classification, optimization
CMAC	Supervised	Multilayer	Function approximation, control, and modeling
Elman	Supervised	Recurrent	Pattern recognition, Time series forecast
Kohonen	Unsupervised	Single-layer	Classification, associative memory, pattern recognition
Hopfield	Supervised	Recurrent	Optimization, image processing, associative memory, classification

2.6.2 **How Neural Networks works**

Assume that Neural Networks (NNs) act as a black box that accepts input information (e.g. fluid flow in oil and gas pipelines) and processing it into outputs (e.g. the flow regimes of the pipeline). A neural network is made up of multiple small units known as neurons and these neurons are categorised into various layers. Layers are neurons columns that are linked to one another through their neurons.

Each and every neuron is linked to another neuron layer through connectors known as weighted connections. The weighted connections are regulated with a real-valued number associated with them. Each neuron takes the value of neurons connected in their layers multiplied with a connection weight. The neuron's bias value is the sum of every connected neuron. The neurons bias value is passed through an activation function $[(f)x]$ which transforms the value mathematically and designate it to the adjacent layer connected neuron. The major challenge of neural networks is getting the correct neuron values (weights) in order to estimate the right results. Finding the correct neuron weight is accomplished through machine learning (Kolasa et al., 2018).

The networks predict the correct results by looking for some specific features before making predictions. Although, sometimes the network is wrong and predicts the incorrect output. For example, if an image is relatively similar to another image, the network could predict the wrong answer. To avoid such a scenario, the network is first equipped with some feedback mechanism called back-propagation algorithm. This allows the network to regulate the connections back to the network. Using back-propagation algorithms enables the network to move back and cross-check the network to ensure that all the connections are properly weighted and the biases are correct (Bisoyi et al., 2019).

Secondly, neural networks can be made to be a Recurrent Neural Network (RNN). These incorporate signals that move in both directions as well as between and within layers. RNNs are basically designed to identify data sequential

features and use the patterns to classify or predict the next similar one (Lin et al., 2019).

2.6.3 **Training a Neural Networks**

The supervised learning method under Machine Learning (ML) umbrella is normally used during the training of NNs (Kulkarni and Rajendran, 2018). This method is essentially where each training model is assigned the values of the expected output and the input data. It applies the past learned event to new data using classified or labeled samples to make predictions of future events. Using known training dataset analysis, the supervised learning algorithm gives an inferred function to predicts the output values. The algorithm can also cross-check its output value with the targetted or correct output and find errors so as to adjust the model appropriately (Nicola and Clopath, 2017).

In contrast, neural networks can be trained using an unsupervised learning method (Liu, Gong and He, 2019). Unsupervised algorithms are implemented when the data adopted to train the network is neither labelled nor classified. This type of learning process studies how the network can infer a function to depict a hidden structure from unclassified or unlabelled data. The network does not predict or figure out the correct output, rather it analyses the given data and produces some inference from the data to depict the hidden structures from the unclassified or unlabelled data.

2.6.4 **Support Vector Machines (SVM)**

The Support Vector Machine (SVM) was designed and developed in 1995. The Support Vector Machine (SVM) was by Vapnik and co-workers to solve classification associated problems based on structural risk minimization and statistic learning theory (Yan et al., 2018). However, the SVM method has been extended to solve prediction and domain regression problems. As presented in Figure 2-25, the data x was mapped by SVM from the input space to feature space via $\phi(x)$ the nonlinear mapping. To identify the separating hyperplane that

maximizes the separating margins of two distinct classes in the feature space, ca onstrained optimization approach is adopted.

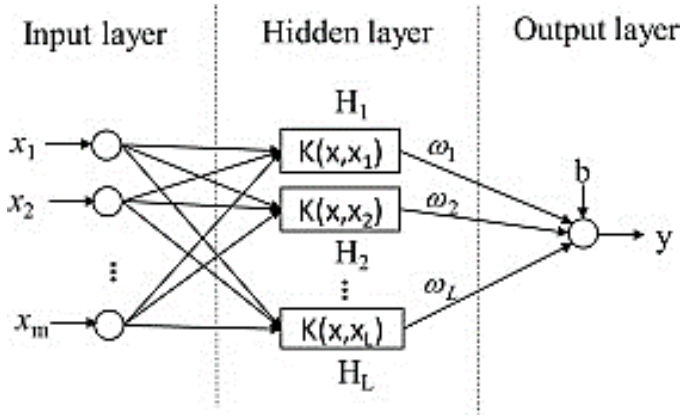

Figure 2-25: The SVM structure (Yue et al., 2019)

2.6.5 **Support Vector Machine (SVM) for classification**

Assuming we have n training samples $X^* = (x_1, x_2, \dots, x_n)$ and the targeted output $Y = (y_1, y_2, \dots, y_n)$, each sample input is a vector $X = (x_1, x_2, \dots, x_m)^T$ containing m variables. A transfer function $\phi(x)$ is used to map the input vectors into an L-dimensional feature space. $\frac{2}{\|\omega\|}$ is the distance between two distinct classes in the feature space. To minimize the training errors and maximize the separating margin ξ_i gives (Hou et al., 2018)

$$\min \frac{1}{2}\|\omega\|^2 + C\ \sum_{i=1}^{n} \xi_i \qquad 2\text{-}5$$

$$s.t \begin{cases} y_i\ (\langle \omega, \phi\ (x_i)\rangle + b)\ \geq 1 - \ \xi_i \\ \xi_i\ \geq 0 \end{cases}$$

where $\boldsymbol{C}$ is the user-specified variable which provides a trade-off between the training error distance and the separating margin while ξ_i is the slack parameter.

Using the Karush-Kuhn-Tucker (KKT) theorem the following dual problem is solved:

$$\min \frac{1}{2}\sum_{i=1}^{n}\sum_{j=1}^{n} y_i y_j \alpha_i \alpha_j \left\langle \phi(x_i), \phi(x_j)\right\rangle - \ \sum_{i=1}^{n} \alpha_i \qquad 2\text{-}6$$

$$s.t.\begin{cases}\sum_{i=1}^{n} y_i\,\alpha_i\ = 0\\ 0\ \le \alpha_i\ \le C\end{cases}$$

where α_i (Lagrange multiplier) corresponds $(x_i y_i)$. The kernel function $K(x_i, x_j) = \langle \phi(x_i), \phi(x_j) \rangle$. The SVM classifier decision function is defined as

$$y = f(x) = \text{sign}\,(\sum_{i=1}^{n} \alpha_i y_i K(x, x_i) + b) \qquad 2\text{-}7$$

Some other optional SVM kernel functions are as follows:

Linear kernel: $K(x, x_i) = \langle x, x_i \rangle$ 2-8

Polynomial kernel: $K(x, x_i) = (\langle x, x_i \rangle + p)^d \quad d \in m, p > 0$ 2-9

RBF kernel: $K(x, x_i) = exp\,(\frac{\|x, x_i\|^2}{2\sigma^2})$ 2-10

Sigmoid kernel: $K(x, x_i) = \tanh(\varphi \langle x, x_i \rangle + \theta) \quad \varphi > 0, \theta > 0$ 2-11

2.7 **Summary**

Slug control is a challenging problem. Several primary slugging elimination techniques have been examined, and they are categorised into active and passive slug control methods. The most common active slugging control methods are the feedback control of a riser/well-artificial gas lifting and topside choke valve feedback control of a riser/well. The primary aim of every slug control method is the elimination of severe slugging and production optimisation.

Although much effort and money have been spent over the past decades in slug control investigations in both industrial and academic sectors, getting the most accurate, economical, optimal and robust remedies is still an unsolved problem. As the potential hydrocarbon resources minimise with time, the motivation for exploring deeper hydrocarbons is on the increase. Hence, slugging problems will become more common in the future due to the use of longer risers and wells.

The use of topside measurements for slugging control is possible, but further work is required in finding the best topside measurements for flow stabilisation.

The subsea solution is better regarding robustness. The deployment of riser base pressure as the controlled variable for flow stabilisation is robust and easy. The main drawback of this idea is its requirement for subsea equipment, which is usually difficult and expensive.

Furthermore, slug control/mitigation research is still ongoing and will become more crucial in the future.

CHAPTER THREE

3 Experimental setup and procedure

3.1 Introduction

This chapter describes the general setup and methods deployed in carrying out the experiments and the experimental data acquisition processes. Specific set-up is described in the relevant chapters. The experimental setup used in this work is located in the oil and gas centre laboratory at Cranfield University. The three-phase test facility is equipped with a standard industrial scale multiphase flow system to investigate different complex flow behaviours existing in process plants and oil and gas systems. The facility is equipped to safely and constantly process multiphase flow under various flow conditions in real-time. The chapter starts by giving a general overview of the experimental facility and the operating conditions. Furthermore, the illustrations of the various sections of the facility are used for the in and outflow processing in the riser system.

3.2 Multiphase flow facility overview

The three-phase test facility in the oil and gas centre is a completely computerised high-pressure test rig structured to control and measure the flowrate of gas-liquid mixtures in the fluid metering section of the facility into the test section. Next, the gas-liquid mixtures are separated into their individual phases in the separation section. The oil and water are cleaned in their respective coalescers after the final separation in the horizontal three-phase gravity separator before being sent back into the storage tanks, and the air is released into the atmosphere. Figure 3-1 presents a schematic diagram of the three-phase test rig for more details. This test rig is operated using the DeltaV (Fieldbus based supervisory, control and data acquisition) software provided by Emerson Process Management (Lao, 2014).

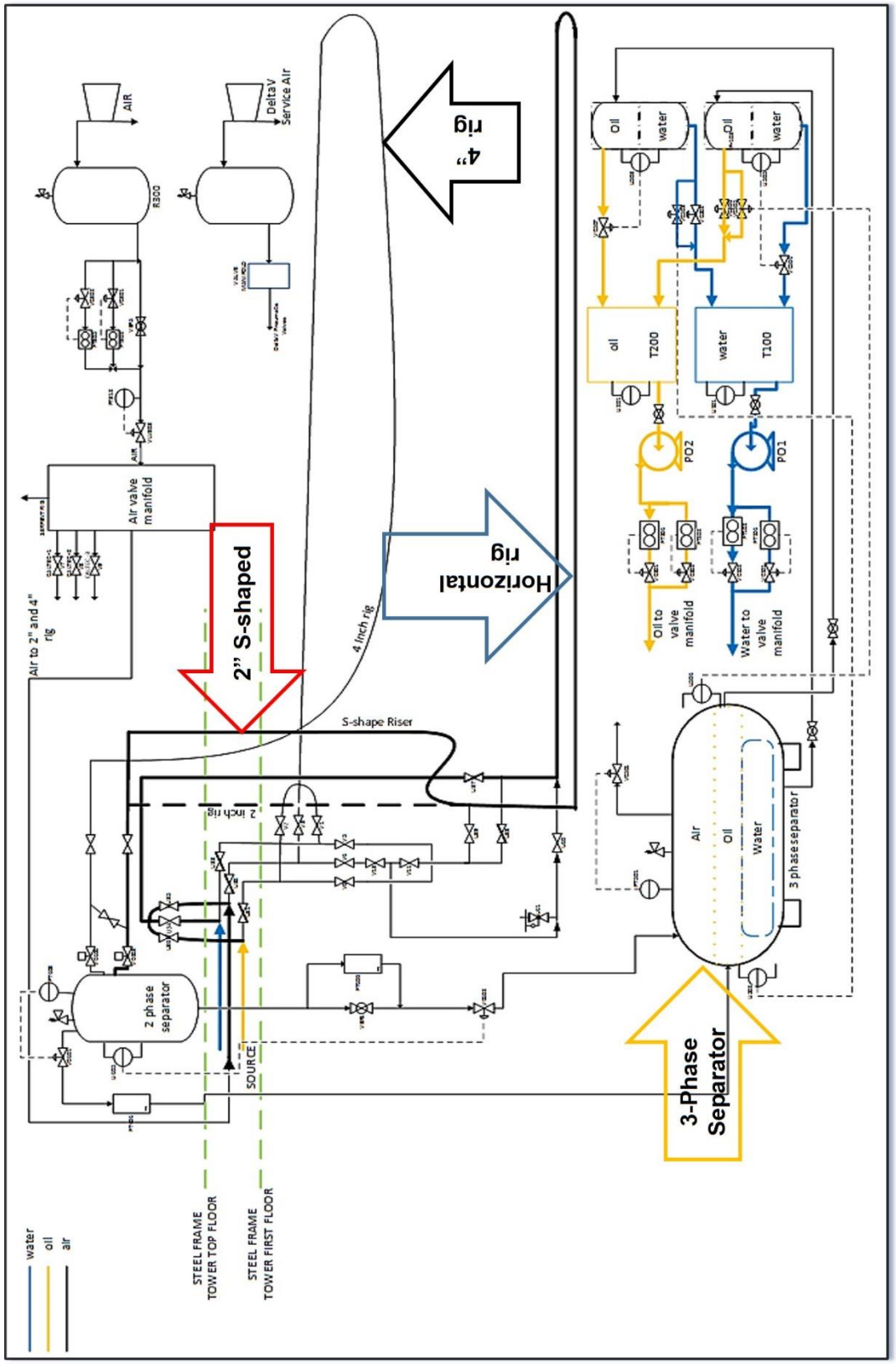

Figure 3-1:Schematic of the Three-Phase Test Facility: Overall Structure (Ogazi, 2011)

There are different types of test loops in the facility, which include the following:

- The 4” riser flow loop is made up of a 55 m horizontal, 10.5 m vertical, 2° downward attached pipeline, and a catenary riser. The flow loop exits to a two-phase vertical separator at the topside of the steel frame tower where the air and liquid are separated.
- The 2” flow loop is made up of a 40.0 m horizontal pipeline connected to a 10.5 m vertical riser. This loop exits to a vertical two-phase separator.
- The 4” horizontal flow loop is a diverted section of the 4” riser loop. It is made up of a horizontal 4” pipe section and exits to the 3-phase separator on the ground floor.
- The 12” horizontal flow loop is also a diverted section of the 4” riser loop that is made up of a 10m long 4” pipe connected to a 16 m long horizontal 12” pipe via an enlargement section. The 12” pipe exits to the 4” horizontal flow loop via a reducer section. Fluids from this loop will go to the 3-phase separator by part of the 4” horizontal flow loop.

There is another test section called the Caltec Involute Separator (I-SEP) test section, which is connected to the 3-phase flow facility with a multiphase fluid inlet and two outlets, one for gas and the other for liquids. The inlet is connected to the top of the 4” riser flow loop. The gas and liquid outlets join the gas and liquid outlets of the top two-phase separator, respectively. All the sections are isolated with manual ball valves to prevent them from interfering with each other.

The equipment and the pipes in the test rig are made with hardened steel and, the test rig is rated up to 20 bar although the maximum air pressure from the compressors was limited to only 7 bar.

The test facility has four separate sections, which include the following:

- Metering and fluid supply
- Valve manifold
- Test area
- Separation

3.3 Metering and flow supply section

The metering and flow supply section of the facility discretely stores, provides and supplies the multiphase flow measurements used in the experiments. It is made up of three distinct sources, which include oil, water, and air sources.

In this work, all the experiments were carried out using water and air because water and air are immiscible fluids. They hardly mix together to form a single phase. Typical examples of pipeline system fluid flow are oil-gas, water-salt-water, gas-oil, oil-water, and oil-gas-water. These examples of fluid flow are known as multiphase flow. Hence, since air-water are immiscible and multiphase fluid, they are good surrogates for systems with oil-water-gas (Srinivas, Ramana Murthy and Sai, 2015).

3.3.1 Air supply

Air is provided through a collection of two parallel linked compressors. When the compressors are run parallel, a 1410 m^3/hr FAD at 7 bar maximum air flowrate can be supplied. The air from the two compressors is accumulated in an 8-m^3 capacity receiver to minimise compressor pressure variations. The air from the receiver passes through a channel of three filters (coarse, medium, fine) and then through a cooler where condensates and debris in the air are removed from the air before it enters the fluid meters. The compressors are started manually and stopped at the end of each use. However, in case of an emergency, the compressors can be remotely shut down from the control room with an emergency button.

3.3.2 The supply of oil and water

Tap water and a dielectric oil (refer to Table 3-1 for their typical physical properties) are used in the rig. The water is provided through a 12.5 m^3 capacity water repository, while oil is provided from a bonded oil repository of the same capacity. The water repository is placed inside the laboratory while the oil repository is situated outside the laboratory. The oil/water is furnished into the flow loop by two pumps (multistage Grundfos CR90-5). Both oil/water pumps are

similar and have a capacity of 100 m^3/hr @ 10 bar. Speed is controlled with frequency variable inverters. The DeltaV is also used to operate the pumps remotely.

Table 3-1: The typical physical properties of the liquids used in the 3-phase rig (obtained at a temperature of 20°C)

	Density kg/m^3	Viscosity mPa s	Surface tension mN/m	Conductivity µS/cm
Dielectric oil	811	7.0	19	N/A
Tap water	998	1.0	71(32) Dielectric oil/distilled water 11.6	310 (540)

3.3.3 **Fluid metering**

The oil, water, and air flow rates are regulated using their individual valve controls. The one-inch Rosemount 8742 Magnetic flow meter (roughly 7.36 l/s) and three-inch Foxboro CFT50 Coriolis meter (roughly 30 kg/s) are deployed to meter water flowrate. A three-inch Foxboro CFT50 Coriolis meter (roughly 30 kg/s) and 1-inch Micro Motion Mass flow meter (roughly 9.47 kg/s) were used to meter the oil flow rate. One-inch and ½-inch diameter of Rosemount Mass Probar flow meters were used to meter the air flowrate. However, the lower air flowrate (1 Sm^3/h to roughly 150 Sm^3/h) was estimated using the lesser air flow meter while the higher air flowrate of about 155 Sm^3/h to 4250 Sm^3/h) was estimated using the larger flow meter.

3.4 **Test section**

This section describes the riser systems, measuring equipment and two-phase separator. There are two loops in the test area, the 4-inch loops, and a 2-inch flow loop.

3.4.1 **The 2” test rig**

The water flows through a 40.0 m 2-inch test loop horizontal pipeline connecting to a 10.5 m vertical riser. The oil supply is linked directly to the riser base. The air

supply can mix with the water before going into the horizontal loop or directly to the base of the riser. A 2-inch Endress and Hauser (E+H) Coriolis meter was positioned at the end of the riser. The riser top is then linked to the two-phase separator via a 2-inch horizontal section. Thus, the 2-inch valve was positioned on the 2-inch horizontal area, which was controlled by the flow conditions in the test area.

The two-phase separator liquid level and the pressure can be regulated using a radar gauge level and pressure controller through the DeltaV control system if required. The disassociated oil-water mixtures and air, therefore, pass through their individual lines respectively back to the gravity three-phase separator.

A 1-inch Rosemount Vortex flow meter is used to meter the air from the vertical 2-phase separator while a 2-inch Micro Motion Mass flow meter is used to meter the water/oil mixtures. The by-pass flow-line with a valve is positioned along the 2-inch flow meter to aid experiments that need high liquid flow rates. However, if the overall liquid flow rate (i.e. oil and water) is less than 7 kg/s, the by-pass valve will be closed so that the flow meter can record the flow rate going back to the three-phase separator. The by-pass valve is open only if the rig is operating at an overall liquid flow rate above 7 kg/s.

3.4.2 **The 4-inch test rig**

This test loop is a catenary shaped riser with 55 m of an upstream pipeline, inclined downward at 2° with about 10.5 m of riser height. The fluid is supplied into the loop through the three individual single-phase sources for water, oil, and air. Thus, the fluids supplied mix together via the mixing point of the loop before entering the pipeline that connects at the base of the riser. The loop exits through the two-phase vertical separator installed at the top side of the loop.

3.5 **Phase separation section**

An 11.12m^3 horizontal three-phase separator separates the air, water, and oil on reaching gravity. The two-level displacer type level and pressure controllers,

which are managed by the DeltaV control system, regulate the pressure, gas-liquid interface level, and the water-oil interface levels.

The air is released into the atmosphere after being separated and cleaned in the three-phase separator. The oil and water from the three-phase separator enter the 1.6 m^3 coalescers. The liquids are cleaned further before being sent back to their respective repository tanks. There are two flow control valves of distinct sizes (3 inch and 1-inch valves) for each of the oil and water return lines. A split range flow control scheme maintains the stability of the gas-liquid and oil-water interfaces in the three-phase separator.

3.6 **Data acquisition method**

The supervisory control and data acquisition software (SCADA) DeltaV regulates the test loop system. Emerson Process Management supplied the software. The measuring equipment process data are linked to the DeltaV control system. All the level, flow and pressure controllers are managed and regulated through the DeltaV system. The signal sampling rate is 1 Hz for all signals maintained and regulated by the DeltaV control system. All the signals generated are saved in the historian database of the DeltaV system. All the data are retrieved from DeltaV after the completion of each experiment.

CHAPTER FOUR

4 Identification of Gas-Liquid Flow Regimes - Virtual Flow Regime Maps

The accurate prediction of flow regimes is vital for the analysis of behaviour and operation of gas/liquid two-phase systems in industrial processes. This chapter investigates the feasibility of a non-radioactive and non-intrusive method for the objective identification of two-phase gas/liquid flow regimes using a Doppler ultrasonic sensor and machine learning approaches. The experimental data is acquired from a 16.2-m long S-shaped riser, connected to a 40-m horizontal pipe with an internal diameter of 50.4 mm. The tests cover the bubbly, slug, churn and annular flow regimes. The power spectral density (PSD) method is applied to the flow modulated ultrasound signals in order to extract frequency-domain features of the two-phase flow. Principal Component Analysis (PCA) is then used to reduce the dimensionality of the data so as to enable visualisation in the form of a virtual flow regime map. Finally, a support vector machine (SVM) is deployed to develop an objective classifier in the reduced space. The classifier attained 85.7% accuracy on training samples and 84.6% accuracy on test samples. Our approach has shown the success of the ultrasound sensor, PCA-SVM, and virtual flow regime maps for objective two-phase flow regime classification on pipeline-riser systems, which is beneficial to operators in industrial practice. The use of a non-radioactive and non-intrusive sensor also makes it more favorable than other existing techniques.

4.1 Introduction

Two-phase gas-liquid flow is encountered frequently in industrial operations such as nuclear power plant steam generators, boilers, chemical reactors, and petroleum transportation (Julia and Hibiki, 2011). The different types of interfacial structures between different phases of fluids, known as multiphase flow regimes, can be geometrically complex and varying. The flow can be steady or intermittent,

turbulent or laminar, gas/liquid segregated or mixed. Gas can flow within the liquid as bubbles or liquid can flow within the gas as droplets (Falcone et al., 2002).

The governing flow regime is influenced by many parameters such as gas/liquid superficial velocities, gas/liquid densities, gas/liquid surface tension, gas/liquid viscosities, pipe diameter, and pipe incline (Thorn, Johansen and Hjertaker, 2013). Traditionally, flow regime maps are used to illustrate the dependence of the flow regime on two quantities, which are usually the superficial gas and liquid flow rates (Gioia Falcone, Geoffrey Hewitt, 2009). Yet, characterising and measuring two-phase flow is still challenging due to its inherently complex nature. Thus, the problem of flow regime identification remains relevant.

Flow regime identification methods can either be subjective techniques (direct observation) or objective techniques (scientific or indirect determination) (Rouhani and Sohal, 1983). Subjective or direct techniques involve the operator visually interpreting an image of the flow to classify it into a flow regime. Objective or indirect determination is a two-part process. The operator must first utilise a suitable experimental methodology to measure flow parameter features correctly and then analyse the flow features objectively to categorise the flow regime (Juliá et al., 2008).

Currently, gas/liquid two-phase flow regime identification is mainly accomplished by subjective means such as direct visual observation and via cameras (Peddu, Chakraborty and Kr. Das, 2017). Hence, the accurate classification of flow regimes is yet to be standardised, and it mostly depends upon the interpretation of individual visual views, which leads to inconsistency in flow regime identification due to human subjectivity. The main drawback of visual observations is that the pictures are often confusing and challenging to interpret, in particular when handling high flow velocities even with high-speed cameras. Moreover, flow channels are often opaque, so flow identification by visual means is impossible (Barnea, Shoham and Taitel, 1980). Although there are numerous flow regime identification approaches already studied for two-phase gas/liquid flow, industrial acceptance remains difficult to interpret. Subjective techniques

cannot facilitate industrial automation, where many important decisions depend on the governing flow regime.

Significant efforts have already been made to develop flow regime identification using objective methodologies. Several research studies have used a phase distribution measurement approach. One of these methods is the use of invasive-point sensors such as pitot tubes, fibre-optic or electrical probes, and hot-wire anemometers (Barnea, 1987). The major drawback to these methods is that the sensors disturb the flow fields during the measurement of void or pressure fluctuations (Dyakowski, 1996). Hence, non-invasive means should be deployed to differentiate the boundaries between diverse flow regimes.

Objective flow regime identification using a clamped-on, non-invasive sensor is of great interest in many industries. Non-invasive methods are highly attractive as they eliminate the need for immersion of instrumentation in the flow. Jones and Delhaye (1976) investigated and summarised different measuring methods applied to a two-phase flow of which few are employed directly to characterise the flow regime. For instance, Barnea et al. (1980) used an enhanced electrical conductance probe in two-phase near horizontal, horizontal, and vertical flows to identify the flow regime.

Among the non-invasive sensors, radiation attenuation methods are more widely used in many industrial applications due to their reliability. Jones and Zuber (1975) studied an X-ray void measurement system for vertical two-phase flow in a rectangular channel; Salgado et al. (2010) achieved flow regime identification using gamma-ray Pulse Height Distributions (PHDS) and Artificial Neural Networks (ANNs); Blaney and Yeung (2008) analysed probability distributions using a self-organising feature map and gamma densitometer data for multiphase flow regime identification; Sunde et al. (2005) proposed an enhanced method, which compares the visualisation of the intensity of gamma-ray measurements at every flow condition. Generally, radiation attenuation methods based on gamma rays, X-rays and neutrons are already established online measurement systems. When compared with each other, the gamma densitometer has merits, such as

high penetration and cost-effectiveness (Chaouki, Larachi and Dudukovic, 1997). However, the major drawback to these methods is their radioactive nature, which is hazardous. The need to increase the gamma source strength with an increase in density or the pipe wall thickness requires increased radiation protection and hence restricts its portability.

Chakraborty et al. (2009) presented a novel ultrasonic method for two-phase flow void fraction measurement using an ultrasonic sensor and two signal processing techniques established on the time series analysis approach: logical signal space partitioning and symbolic filtering. Although the theory on symbolic dynamic filtering was established, identification using pulse-echo mode is not a full classification method of flow regimes, but rather of flow patterns (Jha et al., 2012). It was noted that more research needs to be carried out on experimental and computational work before applying the method in the industry. Another drawback to this method is that the set-up is invasive even though the ultrasonic method itself is non-intrusive. As an extension of the work by Chakraborty et al., (2009), Jha et al. (2012) presented the concept of implementing ultrasonic pulse echoes in a clamped-on set-up in connection with symbolic dynamic filtering for deployment in the industries.

Regardless of the prospect of using ultrasonic pulse-echo for flow regime identification, the method is based on computational models. The computational models apply a set of non-linear equations that are frequently simplified for flow regime identification. In practice, the simplified equations are difficult to implement since the knowledge of various flow parameters is required, such as pipe thickness and pipe diameter. The accuracy of these equations is also compromised when flow parameters deteriorate with time (Meribout et al., 2010). In addition, the ultrasound pulse-echo method is limited by the maximum velocity that it can measure due to the Nyquist criterion (Evans and McDicken, 2000).

Doppler ultrasonic sensors can also measure flow velocity. This technique is ubiquitous in the medical field. The method utilises the shift in frequency due to flow velocities to predict the flow regime (Übeyli and Güler, 2005). The

applicability of Continuous Wave Ultrasonic Doppler (CWUD) in two-phase flow velocity measurement was investigated by Kouam et al. (2003). They suggested the use of frequency resolution methods to resolve the issue of the presence of coloured noise in velocity measurement, which otherwise poses a severe problem to the classical frequency estimators.

In the present work, a non-intrusive and non-radioactive method for the objective identification of a two-phase gas/liquid flow regime is proposed using CWUD signals and Machine Learning (ML) approaches. Many ML solutions to objective flow regime identification have already been proposed, such as Xie et al. (2004), Hanus et al. (2017), Wang and Zhang, (2009) and Trafalis et al. (2005). In this work, to better facilitate the applicability to industrial practice, Principal Components Analysis (PCA) is used to visualise the information from intrinsic flow regime features in 2-dimensional space. To this end, a mapping is created so that in 2-dimensions, the mapped samples can be found clustered according to their respective flow regimes. Support Vector Machine (SVM) is then applied to the samples in the 2-dimensional space to create boundaries between the clusters. This leads to a *virtual flow regime map* that serves as a visual aid to human operators for objective flow regime identification. In summary, the main contributions of this chapter are as follows: (i) we explore the feasibility of visualizing frequency-domain features from ultrasonic Doppler signals in a 2D virtual flow regime map; and (ii) we make the first known effort towards the applicability of continuous wave Doppler ultrasound and the SVM to objectively identify flow regime in an S-shaped riser. By using safer and more advanced techniques for two-phase flow measurement and instrumentation, industries can enhance production, achieve better process performance, and hence, have economic advantages.

In this chapter, the problem of the accurate prediction of flow regimes is considered. The feasibility of a non-radioactive and non-intrusive method for the objective identification of two-phase gas/liquid flow regimes using a Doppler ultrasonic sensor and machine learning approaches is investigated. This meets

objective 2 given in Section 1.6 which is to determine the applicability of CWDU for flow regime identification.

This chapter is organised as follows: Section 4.2 presents the sensor principle and the algorithm for CWUD. In Section 4.3, the experimental method used in this study is described. Signal analysis using ML approaches is discussed in Section 4.4 In Section 4.5, the results and discussion of the analysed data are presented, and finally, a summary of this chapter is given in Section 4.6.

4.2 Measurement Sensor and Algorithm

The Doppler shift (or Doppler Effect) is the frequency variation of an acoustic wave when movement exists between the acoustic receiver and the source, where the change in frequency is proportional to the acoustic source velocity (Weinstein, 1982). Thus, the velocity of the acoustic source is obtained by calculating the frequency shift between the acoustic receiver and the source (see Figure 4-1(b)). In the ultrasonic Doppler flowmeter, illustrated in Figure 4-1(a), a fixed-frequency acoustic beam is released continuously from the transducer into the flow. The beam is then reflected by the moving scatterers in the fluid, which could be bubbles in the flow (Chivers and Hill, 1975). Another ultrasonic transducer receives the scattered acoustic beam so that the velocity of the fluid can be estimated with the frequency shift based on the Doppler Effect. Mathematically, the principle behind this sensor is as follows.

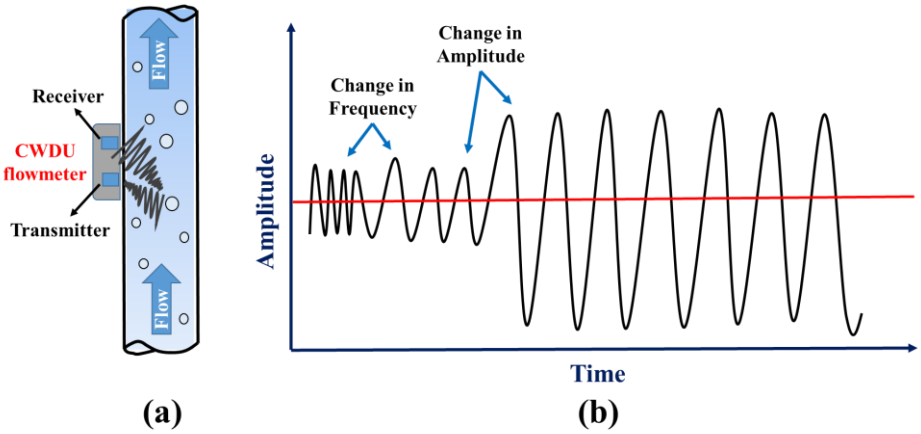

Figure 4-1: Ultrasound Doppler principle (Meire and Farrant, 1995)

First, assume that the signal transmitted is

$$x_t(t) = \varepsilon_t \cos(\omega_t t) \quad 4\text{-}1$$

and that the corresponding received signal from one of the scatterers is

$$x_r(t) = \varepsilon_r \cos(\{\omega_t + \omega_d\}t + \theta_1) \quad 4\text{-}2$$

where $\omega_t = 2\pi f_t$ is the angular frequency of the transmitted signal, $\omega_d = 2\pi f_d$ is the amount of shift in the angular frequency, and θ_1 is the phase shift based on the scatterer distance between the receiver and the transducer (Cobbold, 1989).

Multiplying the two signals electronically results in:

$$x_t(t)x_r(t) = \varepsilon_t \varepsilon_r \cos(\omega_t t)\cos(\{\omega_t + \omega_d\}t + \theta_1) \quad 4\text{-}3$$

$$x_t(t)x_r(t) = \frac{\varepsilon_t \varepsilon_r}{2}[\cos(\omega_d t + \theta_1) + \cos(\{2\omega_t + \omega_d\}t + \theta_1)] \quad 4\text{-}4$$

The resulting signal is then low-pass filtered to remove the $2f_t$ source frequency, leaving only the desired Doppler signal (Cobbold, 1989):

$$x_d(t) = \frac{\varepsilon_t \varepsilon_r}{2}\cos(\omega_d t + \theta_1). \quad 4\text{-}5$$

Additional signal processing may be needed since the received signal has reflected an ultrasound of amplitude greater than the signal backscattered from the moving scatterers. Finally, the relationship between the Doppler shift f_d and the velocity of the scatterer can be described as follows (Sanderson and Yeung, 2002):

$$f_d = 2f_t \frac{v}{c}\cos\theta \quad 4\text{-}6$$

where f_d is the Doppler frequency shift, f_t is the transmitted ultrasound frequency, v is the flow velocity average, and θ is the angle between the flow velocity and the ultrasound beam.

The Continuous-wave ultrasonic Doppler (CWUD) used in this work is DFM-2, a commercial non-invasive flowmeter developed by United Automation Ltd. It generates the ultrasonic signals, calculates the Doppler frequency shifts of the

ultrasonic signals reflected from the discontinuities or scattered like bubbles in the flowing fluid, and evaluates the velocity of the flow. More specifically, the flow meter has two separate crystal transducers embedded, which transmit and receive ultrasonic signals continuously at 500 kHz (Kremkau, 1975). The received output signals are then filtered and further processed by the flowmeter electronics. The flow meter's standard features include an isolated 4 – 20 mA output signal which can be converted into a 0-5 volt analogue signal, proportional to the flow velocity. In this study, the analogue signal was sampled by using NI PCI-6040E, a NI data acquisition system. To achieve a suitable bond between the external conduit surface and the sensor, a glycerine gel was applied to avoid air cavities trapped between the sensor and the conduit surface. Other specifications of the flow meter used in the experiment are given in Table 4-1.

Table 4-1: Continuous Wave ultrasonic Doppler flowmeter specifications

Model	Doppler Flow Meter 2 (DFM-2).
Maker	United Automation Ltd., Southport, U.K.
Analogue Output	Active 4-20 mA.
Velocity range	0 to 19.99 feet per second velocity by Liquid Crystal Display (LCD).
Repeatability	1 % of reading.
Indicator	Sufficient signal strength only when green Light Emitting Diode (LED) is on.
Temperature	Instrument 0 to 50^0C. Standard sensor -30 to 70^0C. HT Sensors are available up to 120^0C.

The detailed experimental specifications are given in the following section.

4.3 Test Rig and Experimental Procedure

4.3.1 Two-phase flow test rig set-up

The experiment was carried out on a 2-inch S-shaped riser of the three-phase flow loop at Cranfield University oil and gas centre. The 2-inch flow loop is made up of a 40-m horizontal pipeline, 5.5-m vertical lower section, 1.5-m down-comer, 5.7-m vertical upper section, and 3.5-m topside section. This test rig is operated using the DeltaV (Fieldbus based supervisory, control and data acquisition) software provided by Emerson Process Management. The schematic diagram of the test rig is presented in Figure 4-2. The air used was supplied from a bank of

two compressors connected in parallel. When both compressors are run in parallel, a maximum air flow rate of 1410 m^3/hr FAD at 7 bar can be supplied. The air from the two compressors accumulates in an 8-m^3 capacity receiver to reduce the pressure fluctuation from the compressor. Air from the receiver passes through a bank of three filters (coarse, medium, fine) and then through a cooler where debris and condensates present in the air are stripped from the air before it enters the flow meters. The water flow rate was supplied from a 12.5-m^3 capacity water tank. The water was supplied to the flow loop by two multistage Grundfos CR90-5 pumps. The water pump has a duty of 100 m^3/hr at 10 bar. The speed control is achieved using frequency variable inverters. The water pumps are operated remotely using DeltaV, a fieldbus based Supervisory, Control, and Data Acquisition software (SCADA). The water flow rate was metered by a 1-inch Rosemount 8742 magnetic flow meter (up to 7.36 l/s) and 3-inch Foxboro CFT50 Coriolis meter (up to 30 kg/s).

After the experiment, air and water were separated in an 11.12-m^3 horizontal three-phase gravity separator. After the separation in the three-phase separator and cleaning, the air was exhausted into the atmosphere while water from the three-phase separator entered a 1.6-m^3 coalescer, where the water is further cleaned before returning to the storage tank.

The 2-inch S-shaped flow loop test facility used in this experiment has a 54.8-mm internal diameter, 40-m length, and 1.5-m downcomer. The 2-inch S-shaped flow loop test section has a transparent pipe for flow regime observation. The air flow-rate was adjusted by controlling the valves through the DeltaV to achieve the desired flow regime.

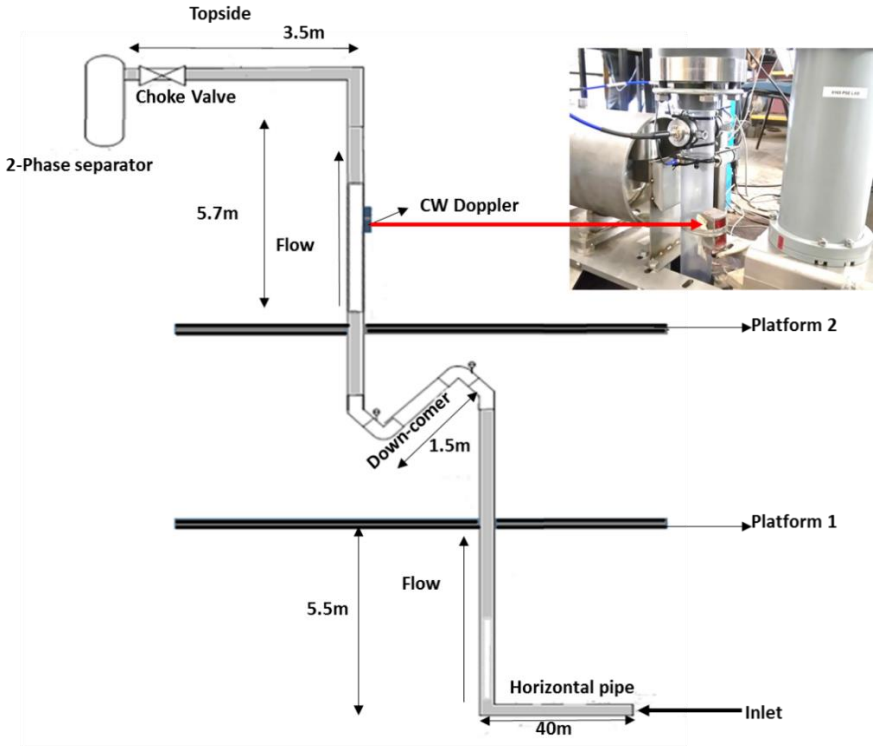

Figure 4-2: Schematic diagram of S-shape rig

A clamp-on non-intrusive CWUD transducer with an excitation voltage of ±10V, operating at a carrier frequency of 500 kHz was attached to the top-side of the S-shaped riser as illustrated in Figure 4-2. The ultrasound beam incident angle was 58° with respect to flow direction on the S-shaped riser. It is essential to place the ultrasonic sensor on the pipe at least 10 diameters away from tees, valves and bends to prevent measurement errors from cavitation, swirls, and turbulent eddies. A gel coupling agent was applied between the pipe wall and the Doppler transducer to make the ultrasound energy transmission easier. The electronics of a CWUD flow meter was adapted to record the voltage signals of the Doppler frequency shift for further analysis (see Figure 4-3).

Ultimately, the process variable being measured by the ultrasound Doppler is the average flow velocity. Based on the pipe scale and flow velocity range, it was estimated that the value of the flow velocity fluctuates at a frequency no more than 2 kHz. Hence, in the LabVIEW data acquisition system, a sampling

frequency of 10 kHz is appropriate with respect to the Nyquist criterion, since this is five times the estimated upper limit frequency of the flow velocity fluctuations.

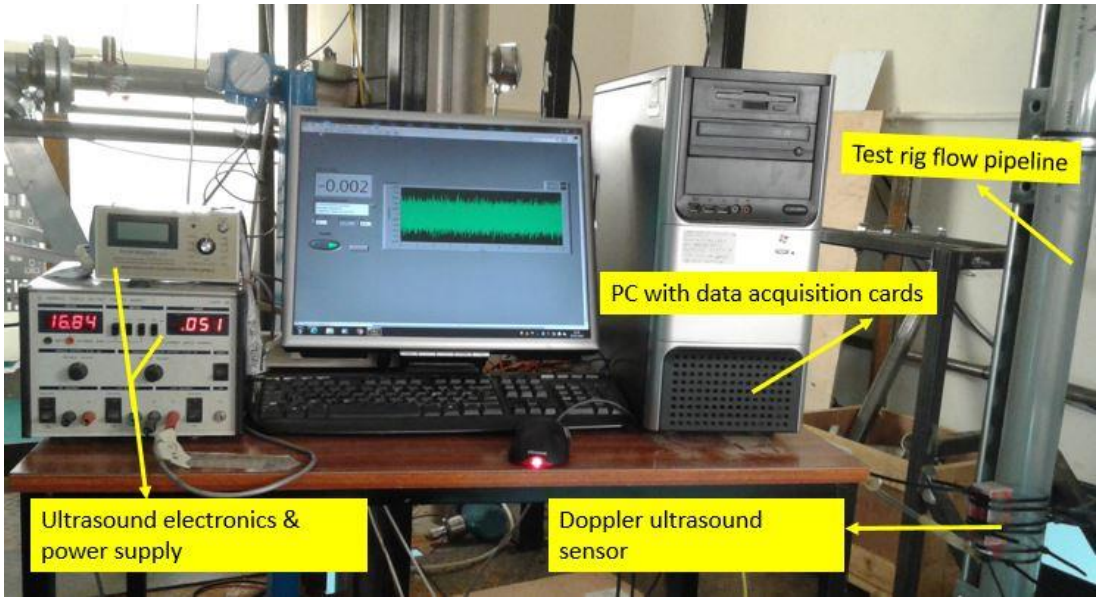

Figure 4-3: Doppler ultrasonic sensor and its auxiliary instruments

4.4 Flow regime classification methodology

4.4.1 Feature extraction from ultrasonic Doppler signals

Feature extraction is the most crucial step for any flow regime identification method. This step aims to find any information from the measurement data that can be used to best distinguish among flow regimes. For high-frequency data, such as the ultrasonic Doppler signals, features can be extracted either from the time domain or frequency domain. In this work, the widely used frequency-domain Power Spectral Density (PSD) features are adopted (De Kerret, Béguin and Etienne, 2017).

Given a stationary discrete-time signal $x(n)$, the power spectral density function $P_x(f)$ of this signal is defined as the Fourier transform of the autocorrelation sequence $R_x(k)$ (Xie, Ghiaasiaan and Karrila, 2004):

$$P_x(f) = \sum_{k=-\infty}^{\infty} R_x(k) \exp\left(-2\pi i k \frac{f}{f_s}\right) \quad \text{4-7}$$

where f_s is the sampling frequency. Since the signal is only measured on a finite interval $[0, \dots, N-1]$, Welch's method is adopted to obtain the PSD, which is given as

$$\hat{P}_x(f) = \sum_{k=-N+1}^{N-1} \hat{R}_x(k) \exp\left(-2\pi i k \frac{f}{f_s}\right) \quad 4\text{-}8$$

where the autocorrelation is (Xie, Ghiaasiaan and Karrila, 2004):

$$\hat{R}_x(k) = \frac{1}{N} \sum_{n=0}^{N-1-k} x(n+k)x(n). \quad 4\text{-}9$$

Using Welch's method in the same way Abbagoni and Yeung (2016), the PSD features were analysed from each sample of ultrasonic Doppler signals at various gas-liquid flow rates as presented in Figure 4-4. A total of 130 data samples of different superficial gas and liquid velocities were recorded. Different flow regime labels were assigned to each data sample by visual observation, and ambient temperature conditions were recorded at the same time. Each data sample acquired consists of Doppler frequency shift signals recorded for a period of 900s. The data set was subdivided into 70% for training (91 samples) and 30% for testing (39 samples). With a sampling frequency of 10 kHz, a Hanning window with a length 1,024 and a 75% overlap was used in the Welch method.

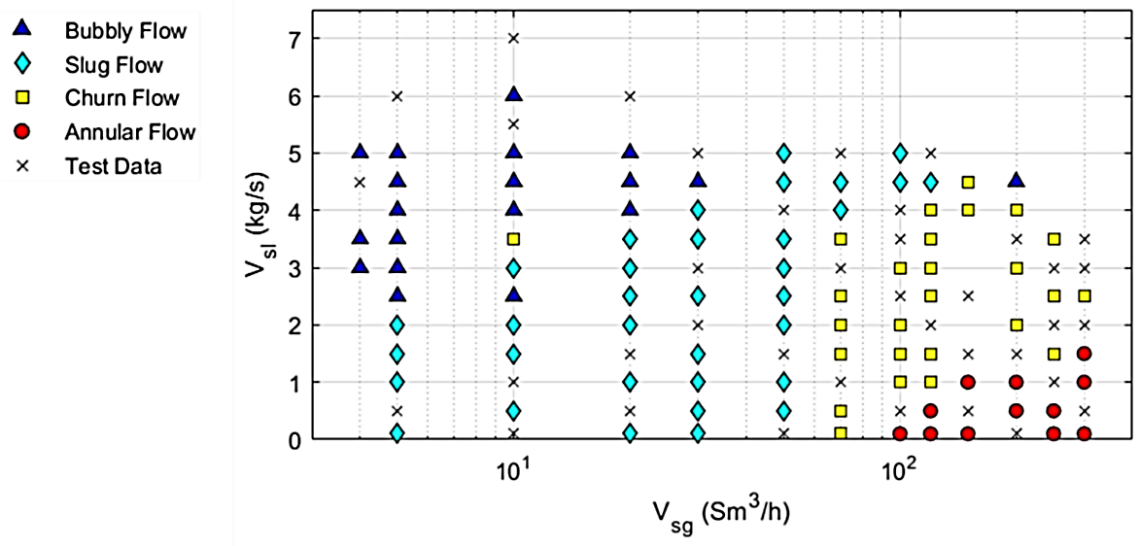

Figure 4-4: Gas and liquid flow rates of all samples from the experiment

Typical power spectral estimates from each flow regime are presented in Figure 4-5. The relevant frequency spectrum ranges from 0 to 1200 Hz. In this range, the PSD spectrum is distinct in each flow regime. To obtain the actual features that can distinguish between the flow regimes, 10 frequency bands of a length of 120 Hz were taken from the power spectrum, and, following Abbagoni and Yeung (2016) the mean PSD was computed on each band. Also, the maximum peak of the PSD, the mean weighted frequency $\bar{f}$ of the spectral power, and the variance of the spectral power equation σ_f^2 were computed for each sample. The last two are computed as

$$\bar{f} = \frac{\sum_i f_i P_x(f_i)}{\sum_i P_x(f_i)} \quad 4\text{-}10$$

$$\sigma_f^2 = \frac{\sum_i (f_i - \bar{f})^2 P_x(f_i)}{\sum_i P_x(f_i)} \quad 4\text{-}11$$

In total, 13 features are obtained from the power spectrum of ultrasound signals: the mean PSD for each of the 10 frequency bands, the maximum peak of the PSD, $\bar{f}$, and σ_f^2. This approach is commonly used to distinguish each flow regime using features in the frequency-domain (Abbagoni and Hoi, 2016; Drahoš and Čermák, 1989). This present work takes the further step of taking these features and visualising them in 2-dimensional space before the flow regime is classified by an efficient pattern recognition technique.

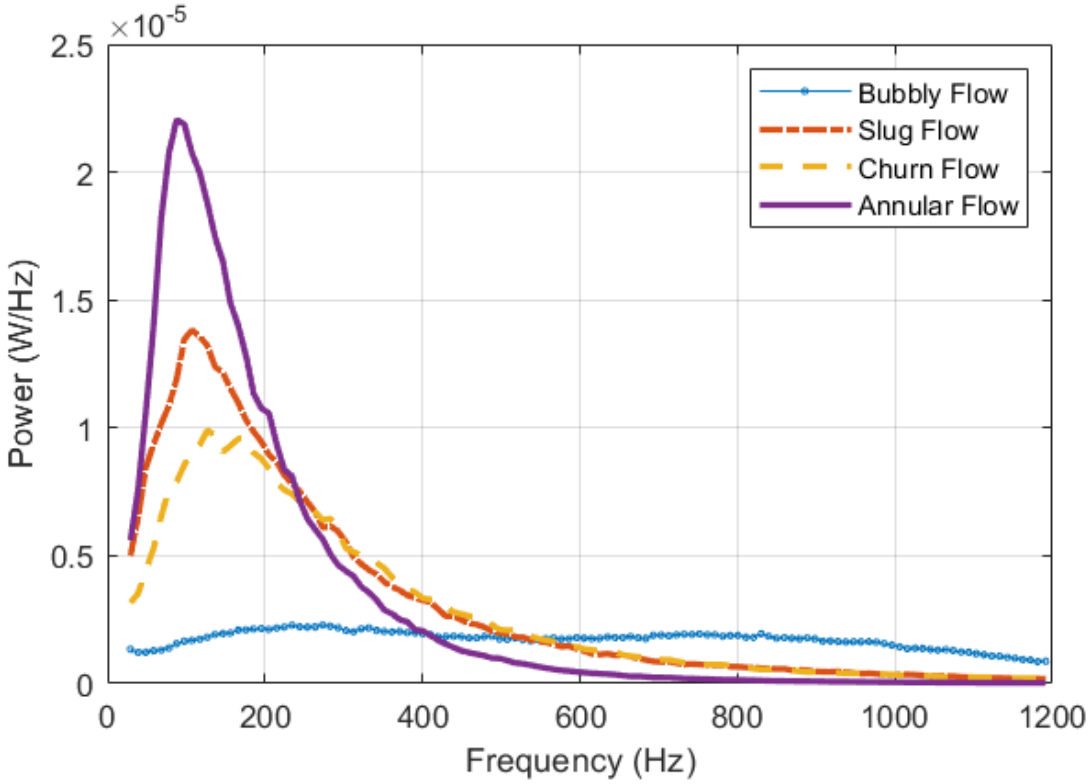

Figure 4-5: Typical power spectra of one frequency band of each flow regime

Table 4-2: Ultrasonic signal PSD frequency band

Frequency band		
Doppler signal PSD frequency bands		
Band name	Frequency range (Hz)	Mean power
B_1	0–120	P_{B1}
B_2	120–240	P_{B2}
B3	240–360	P_{B3}
B4	360–480	P_{B4}
B5	480–600	P_{B5}
B6	600–720	P_{B6}
B7	720–840	P_{B7}
B8	840–960	P_{B8}
B9	960–1,080	P_{B9}
B10	1,080-1,200	P_{B10}

4.4.2 **Dimensionality Reduction for Visualization**

In unsupervised machine learning, dimensionality reduction is a family of methods used to express the same information from a high-dimensional data set using only a few dimensions. In the previous subsection, the information as expressed in 13 features (dimensions) was taken from ultrasound Doppler signals for flow regime identification. Here, the same information is to be retained using only two dimensions by performing a dimensionality reduction method. Since this step is unsupervised, the information about the flow regime labels of the samples is not used yet. Nonetheless, the benefit of reducing the data to two dimensions is the ability to *visualise* the information in a 2-dimensional space. This leads to the realisation of a *virtual flow regime map* completely from ultrasound Doppler data.

In our work, Principal Components Analysis (PCA) is used for linear dimensionality reduction, which is by far the most popular (Van Der Maaten, Postma and Van Den Herik, 2009). In PCA, the information is retained in a set of latent variables that are linear combinations of the original set of features. The PCA algorithm is outlined as follows.

Given a M-dimensional data set of N samples, $x_i \in \Re^M, i = 1,2, \dots N$, PCA proceeds by first normalising the data to zero mean and unit variance, yielding $\bar{X} \in \Re^{M \times N}$. The sample covariance matrix of this data set is computed as

$$\Sigma_{xx} = \frac{1}{N-1} \bar{X}^T \bar{X} \in \Re^{N \times N}. \quad \text{4-12}$$

The eigenvalue decomposition of the covariance matrix can be written as

$$\Sigma_{xx} = V \Lambda V^T \quad \text{4-13}$$

where $V \in \Re^{N \times N}$ is the matrix of eigenvectors on each column, and $\Lambda \in \Re^{\mathrm{N} \times \mathrm{N}}$ is the diagonal matrix of decreasing eigenvalues. The columns of matrix V represent the principal directions that successively explain the maximum variance in the data, while the eigenvalues in Λ are scaling factors equivalent to the data variance values themselves. The projection matrix is given by:

$$P = V\Lambda^{-1/2} \in \Re^{N\times N}. \quad \text{4-14}$$

By using only the first two columns of P, denoted as matrix P_2, the dimensionality of the data is reduced to two while preserving as much information possible. The projections are then applied to the covariance matrix to obtain latent variables L as

$$L = P_2^T \Sigma_{xx} \in \Re^{2\times N} \quad \text{4-15}$$

After the application of Eq. (4-15), each training sample is now represented by every column of L, which has two features that can be plotted in a 2-dimensional space. A machine learning technique for classification can then be used to create decision boundaries objectively between the samples in 2-dimensional space.

4.4.3 **Support Vector Machine for Classification**

This present work proposes the use of a Support Vector Machine (SVM) for objectively classifying flow regimes in an S-shape riser using 2-dimensional features from the ultrasonic Doppler data.

Cortes and Vapnik (1995) originally proposed the SVM for binary classification. Given N data samples of features $x_i \in \Re^M$ each belonging to either of two classes, labelled $y_i \in \{+1, -1\}$, the aim of binary classification is to learn a mapping function that can be used to predict the unknown class of a new sample. SVM solves this by searching for a linear separating hyperplane in the M-dimensional feature space that maximises the margin of separation between samples from each opposing class. This separating hyperplane can then serve as a decision boundary between classes. To separate nonlinear classes, kernels can be used to first transform the original feature space using nonlinear projections prior to seeking the separating hyperplane (Cristianini and Shawe-Taylor, 2014). The idea of “maximum margin of separation” is the logic offered by the SVM approach, which replaces the human subjectivity in flow regime classification. Hence, using SVM, an objective flow regime classifier can be developed.

More specifically, the dual formulation of kernel binary SVM classification is posed as the following convex quadratic programming problem (Cristianini and Shawe-Taylor, 2014):

$$\max \sum_{i=1}^{N} \alpha_i - \frac{1}{2} \sum_{i=1}^{N} \sum_{j=1}^{N} y_i y_j \alpha_i \alpha_j K(\boldsymbol{x}_i, \boldsymbol{x}_j) \qquad \text{4-16}$$

$$\text{subject to} \quad \sum_{i=1}^{N} y_i \alpha_i = 0,$$
$$0 \leq \alpha_i \leq C, \quad i = 1, \ldots, N$$

where $\boldsymbol{x}_i \in \Re^M, i = 1,2, \ldots, N$ is the N training samples with M features, α_i are Lagrange multipliers, $K(\cdot\,,\cdot)$ is a kernel function, $y_i \in \{+1, -1\}$ are the known labels for each sample, that is positive or negative, and C is a regularisation parameter. To project the data into the kernel feature space, the widely used radial basis kernel function is adopted:

$$K(\boldsymbol{x}, \boldsymbol{x}') = \exp\left(\frac{-\|\boldsymbol{x} - \boldsymbol{x}'\|^2}{k_w}\right) \qquad \text{4-17}$$

where k_w is the kernel width. The advantage of SVM over other pattern recognition models is that the solution to Eq. 4-16 is unique and can be calculated efficiently. On the other hand, ANNs require an iterative gradient descent solution, which may converge to local minima. Our application area has no issue with large data sets since the number of training samples is only in the order of 10^2, and the number of features is in the order of 10. This setting is ideal for an SVM solution. Once the problem in Eq. 4-16 is solved, the optimal values α_i^* are obtained, wherein the ith training samples $\boldsymbol{x}_i$ that correspond to $\alpha_i^* > 0$ are deemed *support vectors*. Support vectors participate in creating the boundaries between two classes, defined by the decision function:

$$f(\boldsymbol{x}) = \sum_{i \in SV} y_i \alpha_i^* K(x_i, x) + b_i{}^* \quad \text{4-18}$$

where SV is the set of support vectors, and b^* is a bias term calculated so that $y_i f(\boldsymbol{x}_i) = 1$ for any i with $0 < \alpha_i^* < C$ (Cristianini and Shawe-Taylor, 2014). For any test sample $\boldsymbol{x}$, the function $y = \text{sign}(f(\boldsymbol{x}))$ outputs either +1 or -1 to signify if the sample belongs to the positive or the negative class. Accordingly, the exact boundary between the two classes consists of points $\boldsymbol{x}$ where the SVM decision becomes indifferent, that is, $\text{sign}\big(f(\boldsymbol{x})\big) = 0$.

In the case of the experiment, samples belong to one of the four classes: (1) Bubbly Flow, (2) Slug Flow, (3) Churn Flow, or (4) Annular Flow. Thus, multi-class SVM needs to be implemented. Various strategies for multi-class classification have been proposed, such as one-against-one and one-against-rest. Here, an efficient one-against-one strategy proposed by Platt et al. (2000) called DAGSVM is adopted. It has been reported that DAGSVM retains the accuracy offered by other approaches, but it is faster to train and evaluate (Platt, Cristianini and Shawe-Taylor, 2000). Previously, DAGSVM has been adopted in the objective identification of two-phase flow regimes using electrical capacitance data (Wang and Zhang, 2009).

In this present work, DAGSVM is employed by training six binary classifiers, one for each possible pair of distinct flow regime classes, e.g. 1-vs-2, 1-vs-3, 1-vs-4, 2-vs-3, and so on. Training a binary classifier involves solving for a decision boundary between two classes in the form of Eq. (4-18). The classifiers are then arranged in a decision directed acyclic graph (DDAG) as presented in Figure 4-6. The DDAG structure is key to the efficiency of DAGSVM, which makes it advantageous over other multi-class classification strategies.

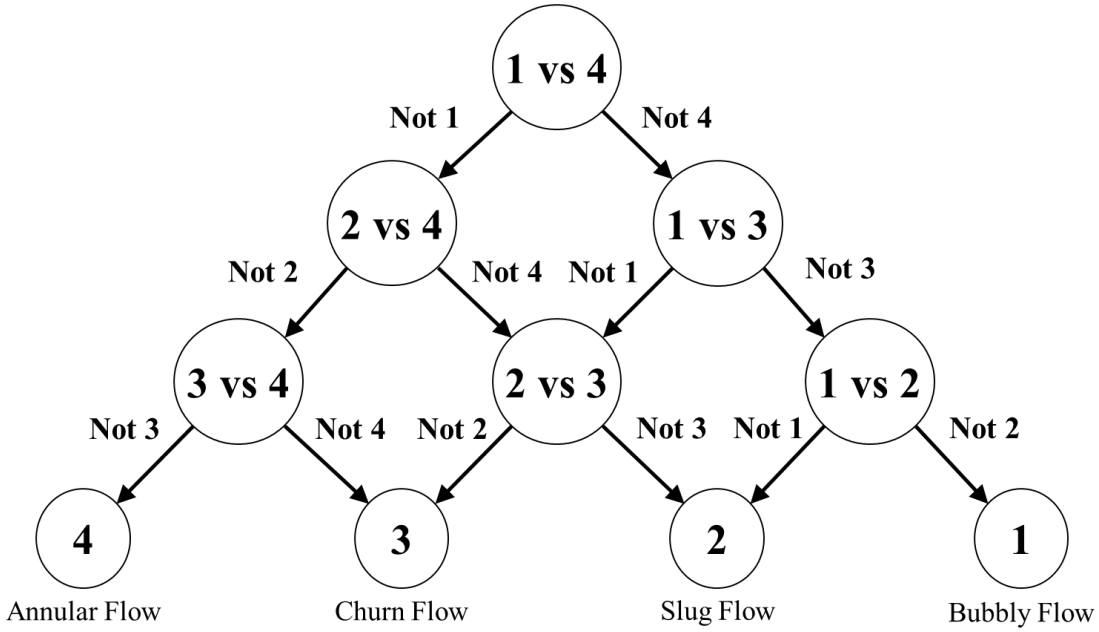

Figure 4-6: DDAG for Multi-class SVM classification

In the DDAG, any new incoming sample goes through the decision at each node, always starting from the 1-vs-4 node. Each node represents the binary decision of which class the sample is definitely excluded from, for example, the 1-vs-4 node classifies the sample as either “Not 1” or “Not 4”. The branch corresponding to the decision of the current SVM classifier is then traversed. As the downward traversal progresses, the sample is continuously being classified at every node visited by eliminating the excluded class, until only a single class is retained. At this point, the bottom of the DDAG is reached, and the sample has been assigned to a single flow regime. The implementation of DAGSVM used in this work is available online in Pilario, (2018).

By taking the 2-dimensional data from ultrasound Doppler signals after dimensionality reduction with the flow regime labels of each sample, the DAGSVM is used to create exact boundaries between the flow regimes. This completes the virtual flow regime map for use in objective flow regime classification. The summary of the methodology is given in Figure 4-7.

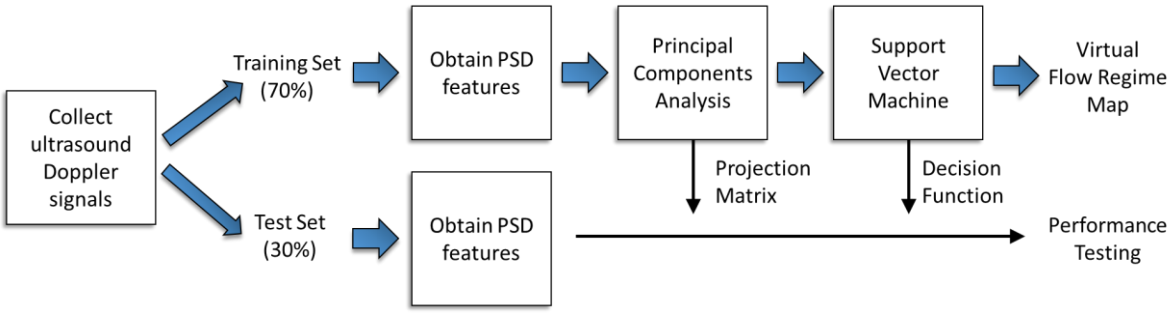

Figure 4-7: Proposed methodology for objective flow regime identification

4.5 Results and Discussions

Flow regime data samples were acquired experimentally from the S-shape riser system described in Section 4.5.2.1, and preliminary results are presented in Figure 4-5.

4.5.1 PCA Visualization

Figure 4-8 presents the resulting 2D visualisation of the ultrasound Doppler data for each training sample after applying PCA. The benefit of PCA visualization can be demonstrated by establishing the relationship between Figure 4-8 and Figure 4-4. These figures are similar in that they both represent a map where every point location is associated with a distinct gas-liquid flow rate value pair.

In Figure 4-8, Annular Flow samples (high gas flow rate and low liquid flow rate) are found at the lower left corner of the map, while Bubbly Flow samples (low gas flow rate and high liquid flow rate) are found at the right and upper right corners of the PCA map. The Slug Flow and Churn Flow samples are found in a specific order in the middle region. The gas flow rate increases from right to left in the PCA map, while the liquid flow rate increases from bottom to top. These directions correspond to the axes of the flow regime map in Figure 4-4. Because of this

relationship, PCA was able to discover the gas-liquid flow rate information of every sample using only the PSD features obtained from the ultrasound Doppler experiment. Thus, PCA can arrange the Doppler data meaningfully in 2D space, further enabling the construction of a virtual flow regime map.

However, there is no clear gap or boundary between the samples from different flow regimes in the PCA map. By comparing it with Figure 4-4, it was found that these samples lie mostly in the transition regions. Hence, a soft margin SVM can be used to establish the boundary between the various flow regimes by setting the value of C to be less than ∞. By further varying the SVM parameters, k_w and C, one can control the complexity of the boundaries between flow regimes. This investigation is carried out in Section 4.6.2.

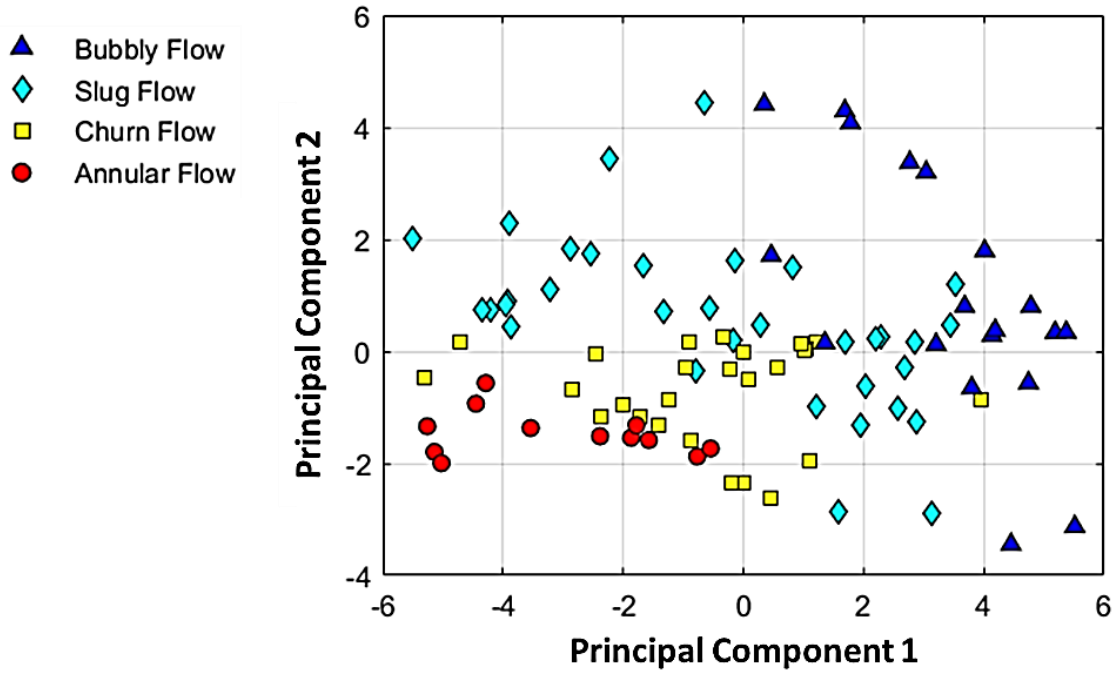

Figure 4-8: PCA visualisation of training samples of ultrasound Doppler signals

Another benefit of PCA visualisation of data is the detection of outliers. The consistency of the human expert in labelling flow regimes may be impeded by certain factors leading to the presence of outlier data samples. One obvious case

is the sample at 10 Sm^3/hr air flow rate and 3.5 kg/s water flow rate, which was observed to exhibit churn flow (see Figure 4-4), yet which is found between bubbly and slug flow regime samples. In the PCA visualisation of ultrasound Doppler data (see Figure 4-8), this specific data point lies at a position near (4.0, -1.0) on the 2D map, also between bubbly and slug flow samples. Hence, this data point is considered an outlier. Other outliers confirmed in the same way in our training dataset include those at air-water flow rates of 200 Sm^3/h, 4.5 kg/s and (10 Sm^3/h, 2.5 kg/s). Ultimately, the degree to which these outliers are tolerated by the subsequent SVM classification is dictated by setting appropriate parameters of k_w and C.

4.5.2 **SVM classification**

Figure 4-9 is a sample flow regime map for $k_w = 7$ and $C = 100$ where the samples of both the training and test data are superimposed. On this map, the background colours denote the results from the SVM classification, for example, SVM identified the Slug Flow regime for every point location in the S-shaped region between Bubbly and Churn Flow regime. Superimposed on this map are the training data samples (circles) and test data samples (triangles). By noting the mismatch between the sample colours and background colours, the training and test data classification accuracies are found to be 85.7% and 84.6%, respectively. Without counting the confirmed outliers in the training samples, the accuracy in the training data is 88.6%. These results depict the capability of the SVM approach for objective classification of two-phase flow regime based on Doppler ultrasound data.

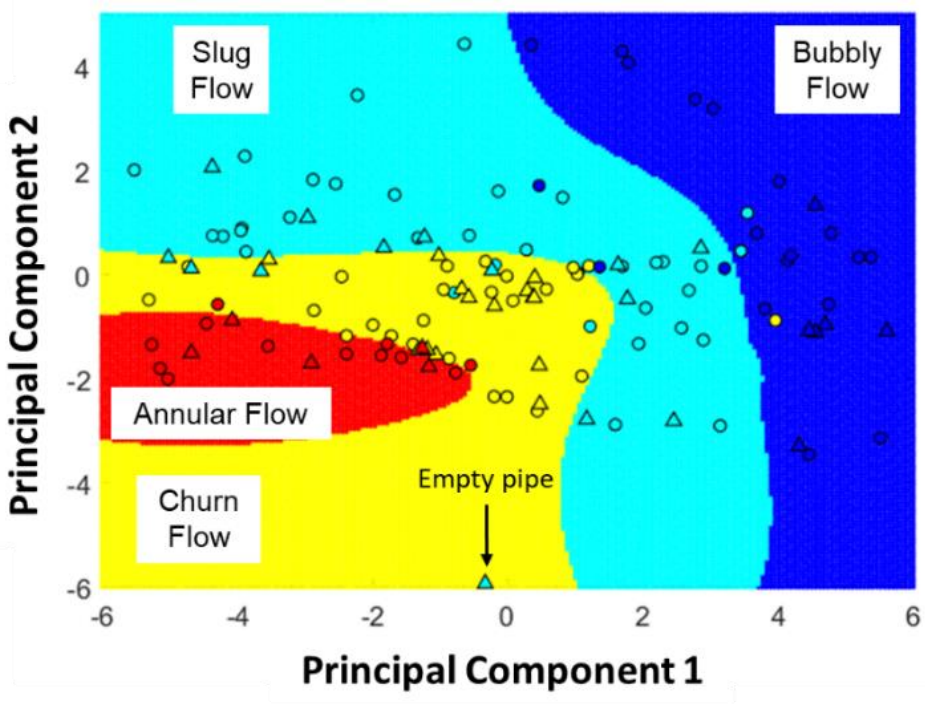

Figure 4-9: Virtual flow regime map using SVM at k_w=7 and C=100.

The background colours denote SVM identification results. A mismatched sample colour and background colour indicates misclassification. Legend: Circles – training samples; triangles – test samples

For completeness, a case of an empty pipe was included in the test samples. Interestingly, this sample was identified as churn flow by the SVM. Although this result is unexpected, the fact that the PCA mapping placed the empty-pipe ultrasound Doppler signal data at the bottom of the map validates that the direction of increasing the liquid flow rate occurs upward in the PCA visualisation.

4.5.3 SVM Performance at Different Parameters

The list of misclassified samples in Figure 4-9 is presented in Table 4-3. Some disparities in using the proposed identification method were observed. In particular, the objective classifier identifies some Slug Flow samples as Churn Flows samples. This misclassification is related to the parameter choice issues in the SVM objective classifier. Various settings for k_w and C give varying

classification performance. The SVM accuracy over a grid of parameter values, such as $k_w \in \{1,3,\ldots,9\}$ and $C \in \{1,10,\ldots,10^4\}$, is presented in Figure 4-10.

Table 4-3: List of Misclassified Samples in Figure 4-9

Misclassified Training Samples (13 out of 91)				
Vsg (Sm^3/h)	Vsl (kg/s)	SVM Classification	Actual Classification	Outlier?
10	2.5	Slug Flow	Bubbly Flow	Y
10	3.5	Bubbly Flow	Churn Flow	Y
20	2	Churn Flow	Slug Flow	N
20	4	Slug Flow	Bubbly Flow	N
30	4	Bubbly Flow	Slug Flow	N
50	2	Churn Flow	Slug Flow	N
50	3	Churn Flow	Slug Flow	N
50	4.5	Bubbly Flow	Slug Flow	N
120	1	Annular Flow	Churn Flow	N
120	4	Slug Flow	Churn Flow	N
200	4.5	Slug Flow	Bubbly Flow	Y
300	0.1	Churn Flow	Annular Flow	N
300	1.5	Churn Flow	Annular Flow	N
Misclassified Test Samples (6 out of 39)				
Vsg (Sm^3/h)	Vsl (kg/s)	SVM Classification	Actual Classification	
5	0.5	Churn Flow	Slug Flow	
20	0.5	Churn Flow	Slug Flow	
30	2	Churn Flow	Slug Flow	
50	0.1	Churn Flow	Slug Flow	
300	0.5	Churn Flow	Annular Flow	
0	0	Churn Flow	Empty Pipe	

Accurate classification of training data can be obtained by adjusting k_w and C towards the direction of overfitting (lower k_w and higher C). However, overfitting demonstrates poor generalisations of unseen test data. Concisely, overfitting makes the classification biased towards the training samples. On the other hand, at high k_w and low C, under-fitting occurs. In the case of under-fitting, the boundaries tend towards linearity at the expense of higher misclassification rates. In general, the only way to increase the level of confidence with the resulting flow regime map is to validate it against as numerous unseen test data samples as possible. With only the available data, the choice of $k_w = 7$ and $C = 100$ already

provide useful results for objective flow regime classification while striking a balance between overfitting and underfitting.

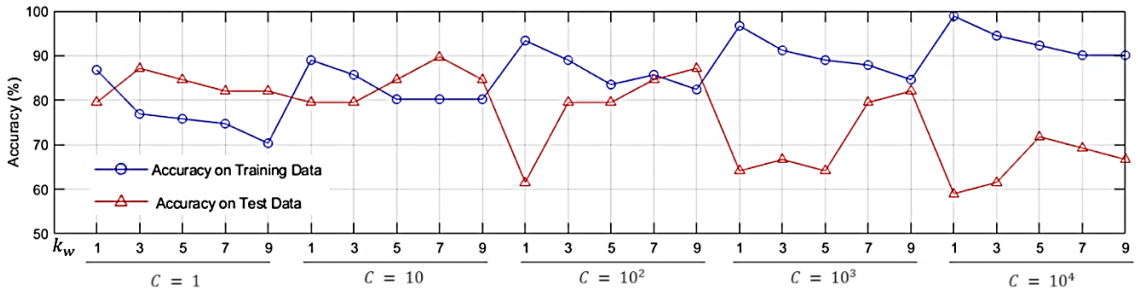

Figure 4-10: Accuracy of SVM classification at various parameter settings of kw and C

With the virtual flow regime map at hand, further analysis on the flow regime transitions and uncertainties can be performed. More importantly, online objective flow regime identification can be developed from the approach proposed in this work. Using a continuous feed of ultrasound Doppler-based flow velocity information, PCA-SVM can automatically visualise the frequency-domain features and classify the flow regime at every sampling instant. Hence, the proposed approach has broad potential for industrial applications.

4.6 **Summary**

In this present work, the necessity of objective, non-invasive and non-intrusive measurement methods for flow regime identification in industrial practice is highlighted. Specifically, this work proposes the use of non-invasive clamp-on Continuous Wave Ultrasound Doppler (CWUD) and machine learning approaches for objective two-phase gas/liquid flow regime identification. From the ultrasonic signals, Power Spectral Density (PSD) features were extracted and subjected to Principal Components Analysis (PCA) to project the data in 2-dimensional space. A multi-class Support Vector Machine (SVM) classifier is trained to establish exact boundaries between the flow regimes in the reduced data space. In the end, the objective classifier accuracy for both the training and testing data samples was 85.7% and 84.6%, respectively. More importantly, the

generation of virtual flow regime maps provided useful data visualisations of the Doppler signals, which can aid in detecting outliers and explain the decisions made by the SVM classifier. These results justify the suitability of our approach for flow regime identification in industrial practice.

To improve this work, the proposed approach must be tested against many other test rigs and configurations to determine if the generated virtual flow regime maps are capable of visualising flow regime patterns from the CWUD data. In addition, the feature extraction and dimensionality reduction steps are deemed the most important steps in the entire procedure. Many other techniques for these steps must be tested to see if various samples from different flow regimes can be clearly separated.

CHAPTER FIVE

5 Objective Identification of Gas-Liquid Flow Regimes - Neural Network

The problem of predicting the regime of two-phase flow is considered. An approach that classifies the flow regime by means of a neural net operating on extracted features from Doppler ultrasonic signals of the flow using either Power Spectral Density (PSD) and Discrete Wavelet Transform (DWT) is proposed. The features extracted are categorised into one of the four flow regime classes: the annular, churn, slug and bubbly flow regimes. The scheme is tested on signals from an experimental facility. The neural network used in this work is a feedforward neural network (FNN) with 20 hidden neurons. The network has four output neurons, which correspond to the element number in the target vector. When PSD features are applied, the network has 13 inputs. However, when features from DWT are applied, the network has 40 inputs. Using the PSD features, the neural network classifier misclassified three out of 31 test datasets in the classification and gave 90.3% accuracy, while only one dataset was misclassified with the DWT features, yielding an accuracy of 95.8%, thereby showing the superiority of the DWT in feature extraction of flow regime classification. This approach demonstrates the application of a neural network and DWT for flow regime classification in industrial applications, using a clamp-on Doppler ultrasonic sensor. The scheme has significant advantages over other techniques in that it uses a non-radioactive and non-intrusive sensor. This appears to be the first known successful attempt for the objective identification of gas-liquid flow regimes in an S-shape riser using Continuous Wave Doppler Ultrasonic (CWDU) and a neural network.

5.1 Introduction

Two-phase gas-liquid flows occur simultaneously inside the pipeline riser in a wide range of industrial and engineering processes, for example in nuclear energy, petrochemical and food-processing plants (Thorn, Johansen and Hjertaker, 2013) as well as in chemical reactors, steam boilers and their associated process piping and condensers (Firouzi and Hashemabadi, 2009). Two-phase flow system operations and design require accurate prediction of the system's pressure drops and that prediction is based on the proper knowledge of the nature of the flow regime that is obtainable in the two-phase flow system. Different two-phase flow regimes can result depending on the volume fractions, velocities and fluid's properties, as well as the pipe geometry (Cheng, Ribatski and Thome, 2008). In vertical or S-shape pipeline risers, the most frequently experienced flow regimes are annular, bubbly, slug and churn flow.

Usually, the flow regime can be identified using a flow map (Al-naser, Elshafei and Al-sarkhi, 2016). Flow regime input parameters based on physical mechanisms are usually gas and liquid superficial velocities, which are unmeasurable during online operations (Bin et al., 2006). The applicability of a flow map by which experimental data are acquired from the water-gas flow is limited. However, while the flow regime is influenced by many factors, only a few are considered in building the flow maps (Alssayh et al., 2013). Hence, the credibility of flow regime identification using flow maps is not guaranteed.

Flow regimes can be identified either through direct identification or indirect determination methods (Rouhani and Sohal, 1983). Direct identification methods require the operator to visually interpret the flow image in order to classify it into a flow regime. This method of flow regime identification in industrial plant pipelines is complicated as the industrial fluids flow in opaque steel pipes and often at high temperature and pressure. Gas-liquid, two-phase flow, direct identification with special equipment and instruments was investigated because of the flow regime map's limitations. There are two ways to obtain flow regime direct identification: one is direct observation, for instance using a high-speed

camera and adopting a visual method. This type of flow regime classification is based on subjective means, which may vary for different observers. The other is characteristic variable extraction from a two-phase flow fluctuation signal. The indirect determination method, also known as analytical determination, is a two-way process. First, the operator measures the flow parameter characteristics using a reliable experimental method. Then, the data is analysed objectively to determine the flow regime (Enrique et al., 2008).

Subjectivity is possibly the most significant issue in flow regime identification. Flow regime identification using visual means, even with the aid of high-speed cameras, is still at the operator's discretion. Some advanced approaches based on flow features such as void fractions are inserted into Probabilistic Density Functions (PDFs) in a quest to reduce subjectivity, which still requires the operator to describe the condition at which each flow regime occurs. Hence, this results in the retention of some level of subjectivity. The flow transitions also complicate flow regime delineation as the progression from one flow regime to another is not instantaneous but rather develops via intermediate regimes that exhibit mixed characteristics (Spedding et al., 1998).

The direct measurement technique, usually referred to as visual observation, is the most common and simplest method of flow regime identification. It is, however, the most subjective approach, with results being determined at the operator's discretion and hence resulting in a low level of replicability and repeatability by others. In 1969, Hewitt and Robert proposed the use of X-rays as an extension of the light photographs but operators did not widely accept this approach. This is due to the safety requirement, the relatively long exposure times and advances in technology (Hewitt and Roberts, 1969).

Statistical parameters such as void fractions were proposed as a means of flow regime identification around 1980 (Juliá et al., 2008). Using PDF in analysing this parameter allows for flow regime identification from experimental data. However, the rules regarding flow regime identification using statistical parameters are at the operator's discretion, thereby retaining the probability of

subjective analysis. Hence, the objective classification of the flow regime is not guaranteed (Julia et al., 2011). The PDF approach in comparison with the use of a high-speed camera shows that PDF has a poor performance in delineating between churn and slug flow but is effective in distinguishing between annular and churn flow (Omebere-Iyari and Azzopardi, 2007).

A significant advance in the objective identification of flow regime was established by the introduction of an Artificial Neural Network (ANN) (Cai et al.1994; Mi et al. 1998; Mi et al. 2001). A more successful objective process was established by classifying the flow regime indicators acquired through non-intrusive impedance probes and a Kohonen Self-Organising Neural Network (SONN) (Enrique et al., 2008). The classification using SONN was initially carried out using the PDF of the void fraction signals as an indicator. However, this approach has a significant disadvantage in that a longer observation period is required to acquire a reasonable statistical parameter of the void fraction signal. This was later enhanced when the Cumulative Probability Density Function (CPDF) of the impedance void meter signals was introduced (Lee, Ishii and Kim, 2008). The CPDF proved to be more stable because it is integral and faster than the PDF methods, as it needs fewer input data. Flow regime identification adopting a fuzzy and neural network methodology has been studied (Pan et al., 2016), but the signal variable characteristics used to depict the flow regime were obtained based on the statistical analysis method. However, the results were limited because the signal processing methods used were based on conventional linear techniques such as wavelet transform and Fourier analysis. The application and analysis of these methods based on nonlinear theory is a future research focus.

Flow regime identification using an ANN is reviewed (Mi, Ishii and Tsoukalas, 2001) with regards to its applications with electrical impedance sensors and pressure differential transducers as measuring devices. This choice is due to increasing interest in using an ANN with these measurement methods, in contrast to the use of a Support Vector Machine (SVM) (Rosa et al., 2010) or an image analysis of dynamic neutron radiograph videos (Tambouratzis and

Pázsit, 2009). The benefits and drawbacks of using impedance meters and pressure transducers as measuring devices in flow regime identification are as follows. Impedance sensors have a raw output signal that is proportional to the void fraction (Rosa et al., 2010). This feature, due to being closely related to the flow regime, requires less computational effort in mapping the signal features to the flow regime. The drawbacks are that they are not commercially available and not well developed for use in any scenarios other than indoor controlled environments operating with oil-gas or water-air mixtures. Pressure transducers are less expensive, readily available for a large range of operating temperatures and pressures, well developed and fulfill most of the operational safety regulations (Rosa et al., 2010). The drawback of pressure transducers is the possibility of pressure tap blockage.

Online flow regime identification plays a vital role in many areas of the industry and in scientific investigations relating to two-phase gas-liquid flow (Winters and Rouseff, 1993). It is established that the operation proficiency of this process is proximately related to precise measurement and the control of hydrodynamic parameters such as flow rate and flow regimes. For instance, in the subsea oil field transportation of gas-liquid flow, online flow regime identification is profitable to the refitting (modification) of operational methods and the enhancement of process proficiency. A two-phase gas-liquid cyclonic separator's modeling and redesigning can gain from the overall air-core motion measurement. In the petrochemical industries, the online monitoring of gas-oil flows is vital for safe operation in the fields of production and exploration (Muvvala et al., 2010). The sudden arrival of slug flows at the feed of three-phase separators installed on offshore production platforms results in severe transients to the control systems, which reduces the equipment's operating efficiency (Bordalo and Morooka, 2018). The likelihood of preventing such regimes can increase the number of information available for operators, such as industrial processes increasing the operational efficiency and security.

In this chapter, a non-radioactive and non-invasive method for the objective identification of two-phase gas-liquid flow regimes using CWDU and a

neural network is proposed. This also meets objective 2 given in Section 1.6 which is to determine the applicability of CWDU for flow regime identification. Flow regime objective identification using a clamped-on, non-radioactive and non-invasive ultrasonic sensor is of great interest to different branches of industry. Non-invasive and non-radioactive methods are highly attractive as they prohibit the need for the immersion of instrumentation in the flow and are less expensive to design, as they do not use radioactive elements. Moreover, the Operating Expenditure (OPEX) is less compared to radioactive instruments due to the excessive costs associated with safety, environmental and health issues. The ultrasonic technique is a promising alternative to complex, hazardous and costly techniques (Goncalves et al. 2011).

Artificial neural networks are considered an alternative tool for objective flow regime identification (Rosa et al., 2010) and since the early 1980s have been employed extensively for applications such as parameter estimation, fault detection, model-based control, dynamic modelling, process monitoring and adaptive control (Zhang, 2006). The key contributions of this chapter are as follows: (i) to develop ANNs for objective flow regime identification using Doppler ultrasonic data as input, (ii) to demonstrate that Doppler ultrasonic signals have the potential to provide reliable online information for the flow regime identification of gas-liquid two-phase flow and (iii) this appears to be the first known successful attempt for the objective identification of gas-liquid flow regimes in an S-shape riser using CWDU and a neural network.

This chapter is organised as follows: Section 5.2 describes the experimental method used in this study. Section 5.3 described the flow regime classification methodology. Section 5.4 discussed the ultrasonic sensor data collection and pre-processing. The spectral analysis and feature extraction from ultrasonic Doppler signals are discussed in section 5.5. Section 5.6 presents the flow regime classification with a neural network, after which section 5.7 presents the results and discussion of the analysed data. Finally, section 5.8 summarised this chapter's findings.

5.2 Test rig and experimental procedure

5.2.1 The multiphase flow test facility

The oil and gas centre at Cranfield University has one of the best multiphase test facilities in the UK approximating the industrial scale. It is fully automated with a state-of-the-art industrial standard distributed control system. This test rig is operated using the DeltaV (Fieldbus-based supervisory, control and data acquisition [SCADA]) software provided by Emerson Process Management. The test rig schematic diagram is shown in Figure 5-1.

The multiphase flow facility is a completely computerised high-pressure test rig structured to control and meter the flow rate of gas-liquid mixtures in the fluid-metering section of the facility into the test section and then the separation section, where the gas-liquid mixtures are further separated into their phases. The oil and water are cleaned in their respective coalescers after their final separation in the horizontal three-phase gravity separator and before returning into the repository vessel and releasing the air into the atmosphere. The air is supplied from the bank of two compressors connected in parallel. When both compressors are run in parallel, a maximum air flow rate of 1410m^3/hr FAD at 7 bar can be supplied. The air from the two compressors is accumulated in an 8m^3 capacity receiver to reduce the pressure fluctuation from the compressor. Air from the receiver passes through a bank of three filters (coarse, medium and fine), and then through a cooler where debris and condensates present in the air are stripped from the air before going into the flow meters. The water flow rate was supplied from a 12.5m^3 capacity water tank. The water was supplied into the flow loop by two multistage Grundfos CR90-5 pumps. The water pump has a duty of 100m^3/hr at 10 bar. Speed control is achieved using frequency variable inverters. The water pumps are operated remotely using DeltaV, a Fieldbus-based SCADA software. The water flow rate was metered by a 1-inch Rosemount 8742 magnetic flow meter (up to 7.36 l/s) and a 3-inch Foxboro CFT50 Coriolis meter (up to 30kg/s).

After the experiment, air and water were separated in an 11.12m^3 horizontal three-phase gravity separator. After the separation in the three-phase separator and cleaning, air is released into the atmosphere while water from the three-phase separator enters its 1.6m^3 coalescer, where it is further cleaned before returning to the storage tank.

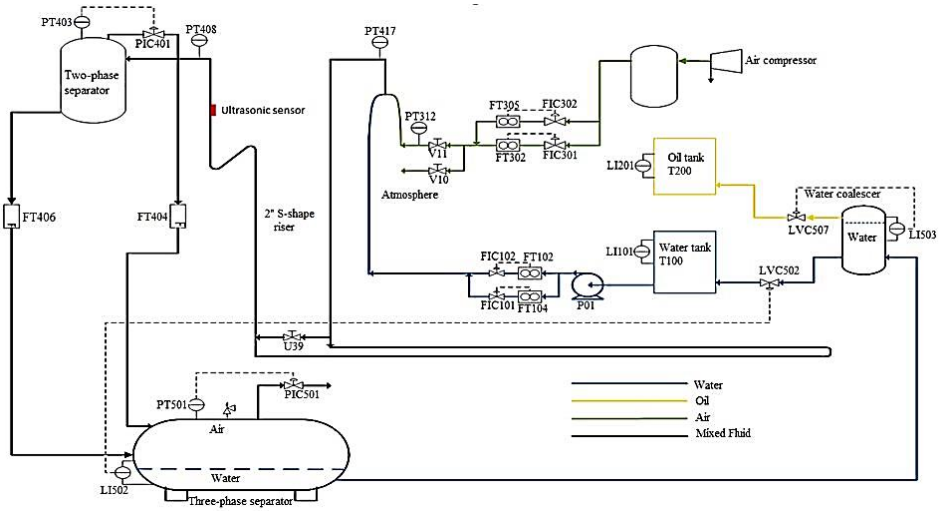

Figure 5-1: Schematic diagram of the multiphase flow test facility

Table 5-1: Experimental process and instrumentation list

Sensor tags	Description	Unit
PT312	Air delivery pressure	bar
PT403	Top separator pressure	bar
PT408	Riser top pressure	bar
PT417	Riser base pressure	bar
PT501	3-phase separator pressure	bar
PIC501	3-phase separator outlet air valve	%
FT102	Inlet water temperature	˚C
FT102	Inlet water density	Kg/m^3
FT102/104	Inlet water flow rate	Kg/s
FT305	Inlet air temperature	˚C
FT305/302	Inlet air flow rate	Sm^3/h
FT404	Top separator gas outlet	M^3/h
FT406	Top separator liquid outlet	Kg/s
LI101	Liquid tank level	m
LI502	3-phase separator water-oil level	%
LI503	Liquid coalescer level	%

5.2.2 **The S-shape riser multiphase flow loop**

The experiment was carried out on a 2-inch S-shaped riser of the three-phase flow loop at Cranfield University's oil and gas centre. The 2-inch flow loop is made up of a 40m horizontal pipeline, a 5.5m vertical lower section, a 1.5m down-comer, a 5.7m vertical upper section, and a 3.5m topside section. The 2-inch S-shaped flow loop test section has a transparent pipe for flow regime observation. The air flow rate was adjusted by controlling the valves through the DeltaV to achieve the desired flow regime.

5.3 **Flow regime classification methodology**

One hundred and twenty-five dataset measurements on the S-shape two-phase flow were collected and pre-processed for this work. Discrete wavelet transform and PSD were then applied to extract features from the pre-processed signals. The extracted features were randomly divided into training, validation and testing dataset in the ratio of 0.60:0.15:0.25, respectively. A feedforward neural network developed in MATLAB was applied to classify the two-phase air-water flow regimes using the extracted features. The output from the network was classified into the following flow regimes: slug flow, bubbly flow, churn flow and annular flow. This methodology is described in Figure 5-2 and further explained in the subsequent sections.

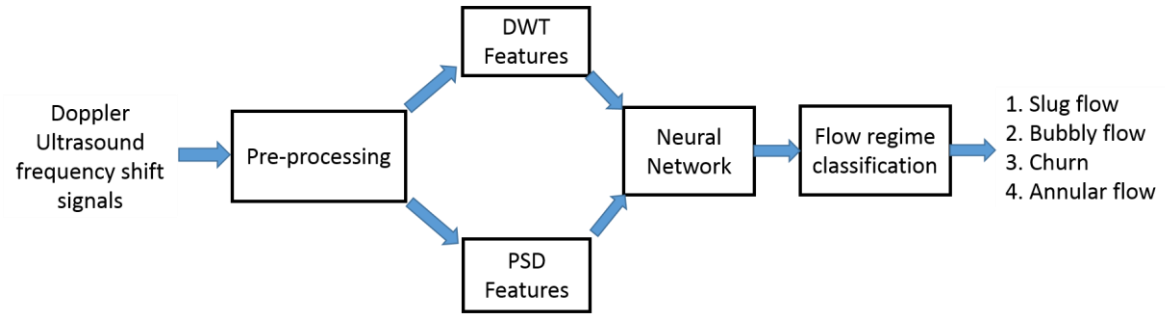

Figure 5-2: Methodology for objective flow regime identification

5.4 Ultrasonic sensor data collection and pre-processing

A clamp-on non-intrusive CWUD transducer with an excitation voltage of ± 10V, operating at the 500 kHz frequency was attached at the topside of the S-shaped riser. The ultrasound beam's incident angle was 58° with respect to the flow direction on the S-shaped riser. It is essential to place the ultrasonic sensor on the flow pipe at least 10 diameters away from the tees, valves and bends in order to prohibit measurement errors from cavitation, swirls and turbulent eddies. A coupling gel was applied between the pipe wall and the Doppler transducer to make the ultrasound energy transmission easier. The electronics of the CWUD flow meter were adapted to record the voltage signals of the Doppler frequency shift.

The LabVIEW data-acquisition system at 10 kHz sampling frequency was used to acquire the Doppler frequency shift voltage signals. Ultimately, the process variable that is measured by ultrasound Doppler is the average flow velocity. Based on the flow velocity range and pipe scale, it was estimated that the value of the flow velocity fluctuates at a frequency of not more than 2 kHz. Hence, in the LabVIEW data-acquisition system, a sampling frequency of 10 kHz is appropriate with respect to the Nyquist criterion, as this is five times the estimated upper limit frequency of the flow velocity fluctuations. The data were imported to MATLAB and pre-processed before feature extraction and flow regime classification.

5.5 Spectral analysis and feature extraction from ultrasonic Doppler signals

5.5.1 Spectral analysis

Spectral analysis is often used to analyse two-phase flow signals and estimate the oscillation period. The signals of a two-phase flow can be analysed from a time and frequency domain to extract the features of different flow regimes. In this study, PSD and DWT techniques were employed to extract the features of

two-phase flow signals obtained using CWDU (Shang et al., 2004). Power spectral density was applied in the analysis to obtain the periods of oscillation based on the signal fourier transform (Xie, Ghiaasiaan and Karrila, 2004). Discrete wavelet transform has the potential of denoising and analysing the signals in order to obtain the spectrum in the frequency-time domain.

5.5.2 **Power spectral density**

Power spectral density is an approach of estimating the features of the time-series signal of a stochastic process in the frequency components that are hidden in the process (Montgomery and Yeung, 2002). For high-frequency data, such as ultrasonic Doppler signals, features can be extracted from either the time domain or the frequency domain. In this work, the widely used PSD features from the frequency domain were used (De Kerret et al. 2017). Several works have been done on PSD application to a time-series signal such as a pressure fluctuation signal of two-phase flow (Abbagoni and Hoi, 2016; Sun & Zhang, 2008; Xie et al., 2004; Santoso et al., 2012). Assuming that a discrete-time signal $x(n)$ is stationary, the PSD function $P_x(f)$ of this signal is defined as the Fourier transform of the autocorrelation sequence $R_x(k)$ (Abbagoni and Hoi, 2016; Xie, Ghiaasiaan and Karrila, 2004):

$$P_x(f) = \sum_{k=-\infty}^{\infty} R_x(k) \exp\left(-2\pi i k \frac{f}{f_s}\right) \qquad 5.6$$

where f_s is the sampling frequency. As the signal used for this work is only measured on a finite interval $[0, \dots, N-1]$, Welch's method for obtaining the PSD was employed, which is given as

$$\hat{P}_x(f) = \sum_{k=-N+1}^{N-1} \hat{R}_x(k) \exp\left(-2\pi i k \frac{f}{f_s}\right) \qquad 5.7$$

where the autocorrelation is (Xie, Ghiaasiaan and Karrila, 2004):

$$\hat{R}_x(k) = \frac{1}{N}\sum_{n=0}^{N-1-k} x(n+k)x(n). \quad 5.8$$

In this chapter, using Welch's method in the same way as Abbagoni and Yeung (2016), the PSD features from each sample of ultrasonic Doppler signals at various gas-liquid flow rates were analysed. One hundred and twenty-five data samples of different superficial liquid and gas velocities were recorded. Different flow regime labels were assigned to each data sample by visual observation at the same ambient temperature conditions. Each acquired data sample consists of Doppler frequency shift signals recorded for a period of 900s. The dataset was subdivided into 60% for training, 15% for validation and 25% for testing. In this work, a sampling frequency of 10 kHz was used, while in the analysis using Welch's method, a Hanning window of length 1,024 and a 75% overlap were employed.

Typical power spectral estimates from each flow regime are presented in Figure 5-3. It was observed that the relevant frequency spectrum ranges from 0-1200 Hz. In this range, the PSD spectrum is distinct in each flow regime. Therefore, to obtain the actual features that serve to distinguish between the flow regimes, the band of length 120 Hz on the spectrum was taken to compute the mean PSD ($P_{B1} - P_{B10}$) on each band ($B_1 - B_{10}$), as shown in Table 5-2. In addition, for each sample, the maximum peak of the PSD, the weighted mean frequency $\bar{f}$ of the spectral power and the spectral power variance equation σ_f^2 were computed. The last two are computed as

$$\bar{f} = \frac{\sum_i f_i P_x(f_i)}{\sum_i P_x(f_i)} \quad 5.9$$

$$\sigma_f^2 = \frac{\sum_i \left(f_i - \bar{f}\right)^2 P_x(f_i)}{\sum_i P_x(f_i)}. \quad 5.10$$

In total, 13 features were obtained from the power spectrum of ultrasound signals: the mean PSD for each of the 10 frequency bands, as shown in Table 5-2, the maximum peak of the PSD, $\bar{f}$ and σ_f^2. This approach is commonly used for distinguishing each flow regime using features in the frequency domain (Abbagoni and Hoi, 2016; Drahoš and Čermák, 1989). These features were further visualised in 2-dimensional space using PSD, before classification by the neural network, as shown in Figure 5-3. The liquid and gas flow rates of all samples from the experiment are shown in Figure 5-4.

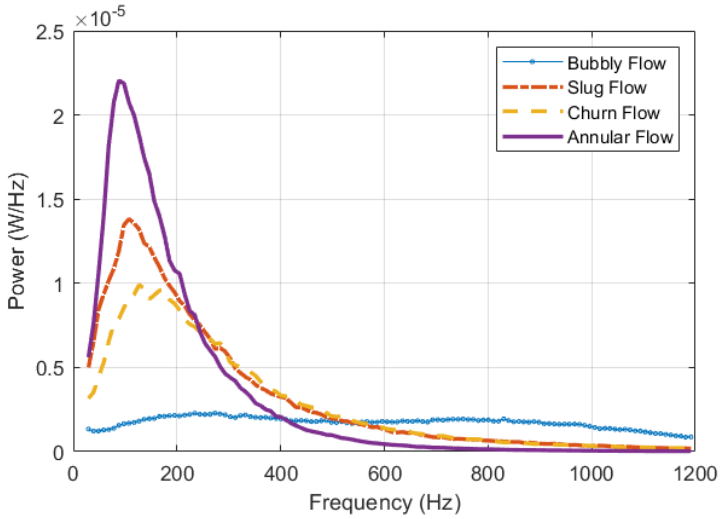

Figure 5-3: Typical power spectra of each flow regime

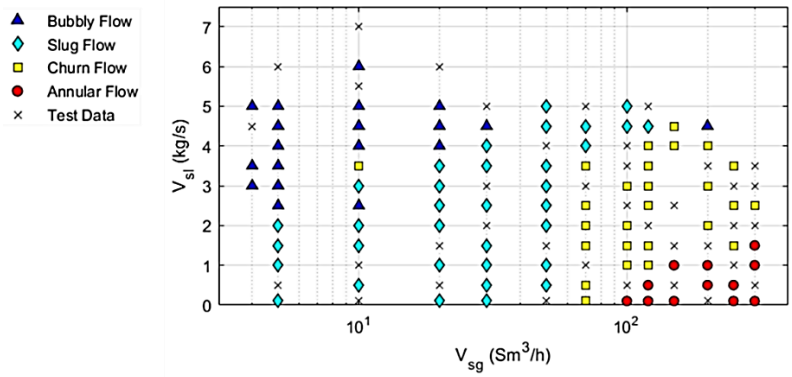

Figure 5-4: Liquid and gas flow rates of all samples from the experiment

Table 5-2: PSD frequency bands

Frequency band		
Doppler signal PSD frequency bands		
Band name	Frequency range (Hz)	Mean power
B_1	0–120	P_{B1}
B_2	120–240	P_{B2}
B3	240–360	P_{B3}
B4	360–480	P_{B4}
B5	480–600	P_{B5}
B6	600–720	P_{B6}
B7	720–840	P_{B7}
B8	840–960	P_{B8}
B9	960–1,080	P_{B9}
B10	1,080–1,200	P_{B10}

5.5.3 **Discrete wavelet transform**

The DWT input decomposes signals into sub-bands with smaller bandwidths and slower sample rates. The application of signal decomposition using DWT is not new. However, its applicability is based on the ability to regulate the wavelet coefficients in order to identify the signal characteristic that distinguishes them from the original time signal (Subasi, 2005). In this work, the decomposition of Doppler ultrasound signals from a two-phase flow was carried out using DWT.

The signal was decomposed by wavelet transform into a set of wavelets bases. These basis functions are obtained by the contractions, dilations and shifts of a unique function called wavelet prototype. Continuous wavelets are functions generated from a single function ψ by translations and dilations (Cohen and Kovačević, 1996; Rioul and Vetterli, 1991).

$$\psi_{a,b}(t) = \frac{1}{\sqrt{|a|}}\psi\left(\frac{t-b}{a}\right) \qquad 5.11$$

where *b* is a real-valued function called the shift parameter. The function set $(\psi_{a,b}(t))$ is known as a wavelet family. As the parameters (a, b) are continuous-

valued parameters, the transform is called continuous wavelet transform. Classical wavelets as dilates of one function are defined as high-frequency wavelets with a width corresponding to $a < \mathrm{b}$ or narrower, while low-frequency wavelets have a width of $a > 1$ or wider. The wavelet transform *f*(*t*) is defined as a linear combination of wavelet and scaling wavelet functions. Both the wavelet and scaling functions are complete sets (Rioul and Vetterli, 1991). Generally, the shift and scale parameters of the discreet wavelet family are given by

$$a = a_0^j,\ b = kb_0a_0^j \qquad 5.12$$

where k and j are integers. The function family with discretised parameters is given as

$$\psi_{j,k}(t) = a_0^{\frac{-j}{2}}\psi\left(a^{-j}t - kb_0\right) \qquad 5.13$$

$\psi_{j,k}(t)$ is known as the DWT basis. Even though it is known as DWT, the time variable of the transform is still continuous. The DWT coefficients of a continuous-time function are expressed as

$$d_{j,k} = \left\langle f_w(t), \psi_{j,k}(t)\right\rangle = \frac{1}{a_0^{j/2}}\int f_w\,(t)\psi(a_0^{-j}t - kb_0)dt. \qquad 5.14$$

When the DWT set $(\psi_{j,k}(t))$ is complete, the wavelet representation of a function $f_w(t)$ is defined as

$$f_w(t) = \ \Sigma_j\,\Sigma_k\left\langle f_w(t), \psi_{j,k}(t)\right\rangle\,\psi_{j,k}(t) \qquad 5.15$$

Generally, a function can be represented by using *L*-finite resolutions of the wavelet and the scaling function with a parameter value of $a_0 = 2$ *and* $b_0 = 1$ as

$$f_w(t) = \sum_{k=-\infty}^{\infty} C_{L,k}\ 2^{-\frac{L}{2}}\varphi\left(2^{\frac{t}{L}} - k\right) + \sum_{j=1}^{L}\sum_{k=-\infty}^{\infty} d_{j,k}\ 2^{-\frac{j}{2}}\varphi\left(2^{\frac{t}{j}} - k\right) \qquad 5.16$$

where scaling coefficients $[C_{L,k}]$ are expressed as

$$C_{L,k} = \left\langle f_w(t), \psi_{L,k}(t)\right\rangle = \int f_w\,(t)2^{-\frac{L}{2}}\varphi(2^{\frac{t}{L}} - k)dt \qquad 5.17$$

and

$$\varphi_{L,k}(t) = 2^{-\frac{L}{2}}\varphi(2^{-L}t - k) \quad 5.18$$

$$\psi = 2\sum_k h_1\,(\mathrm{k})\varphi(2t - k) \quad 5.19$$

$$\varphi = 2\sum_k h_0\,(\mathrm{k})\varphi(2t - k). \quad 5.20$$

5.5.4 **Multi-resolution decomposition of Doppler ultrasound signals**

Discrete wavelet transform analyses the Doppler signal at different frequency bands and with different resolutions by decomposing the Doppler signal into a coarse approximation and detailed information. It uses two sets of functions called wavelet functions and scaling functions, which are associated with high-pass and low-pass filters, respectively. The decomposition of the signal into the different frequency bands is obtained by successive low-pass and high-pass filtering of the time-domain signal.

The original signal (*S*) is first passed through a half-band high-pass filter and a low-pass filter. After the signal filtering, half of the signal samples can be removed as indicated by the Nyquist criteria, as the signal at this point has the highest frequency of π/2 radians, instead of π (Saric, Bilicic and Dujmic, 2005). The signal can, therefore, be divided into two sub-samples by simply discarding every other sample. This process is called the multi-resolution decomposition of a signal and is schematically shown in Figure 5-5: Sub-band decomposition of Each stage in this scheme consists of two digital filters and two factor-of-two down-samplers. The discrete mother wavelet is the first filter, which is high-pass in nature, and the second is its mirror version, which is low-pass in nature. The down-sampled outputs of the first high-pass and low-pass filters provide the detail D_1 and the approximation A_1, respectively. The first approximation, A_1, is further decomposed and this process is continued as shown in Figure 5-5.

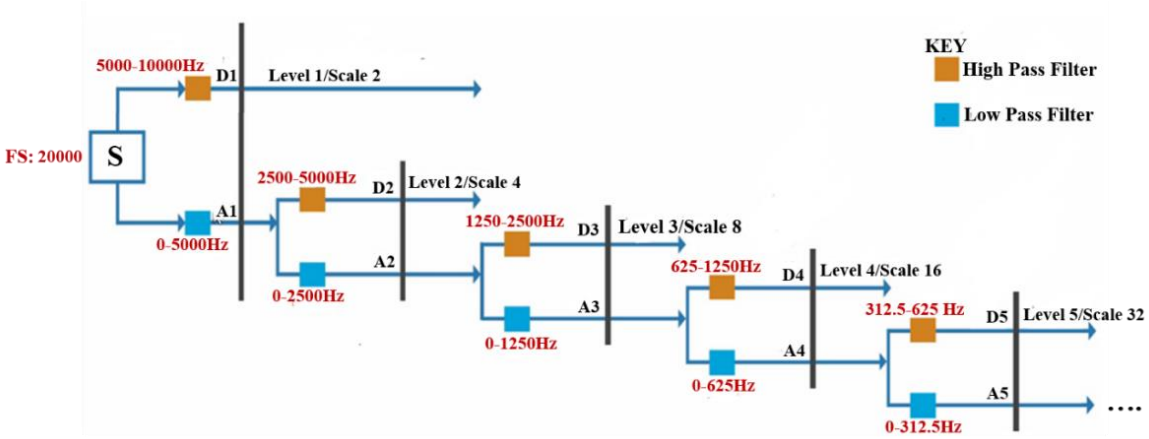

Figure 5-5: Sub-band decomposition of DWT

The signals decomposition provides detail and approximation levels, with different frequency bands employing successive high-pass and low-pass filtering. In the time domain, these detail levels do not lose their information (Bendjama et al., 2015). However, valuable information can be acquired from the sub-bands of the dominant frequencies. Hence, the statistical measurements of the sub-bands represent these detail levels. The flow signals were decomposed continuously until all the dominant frequency ranges were viewed. The Doppler ultrasound signal was decomposed into the detail coefficients of D_1–D_{10}, where 1–10 is the detailed wavelet coefficients levels (Abbagoni and Hoi, 2016).

In this chapter, the Doppler ultrasonic signal was decomposed into the detail coefficients of D_1–D_{10}, where 1–10 refers to the detail wavelet coefficient levels: the first to the seventh and the last approximations is A_{10}. The frequency sub-band ranges are given in Table 5-3. The fourth-order Daubechies wavelet (db4) was deployed to compute the signal's wavelet coefficients (Abbagoni and Hoi, 2016). The coefficient's DWT was computed using the MATLAB software package. For each of the datasets, detail wavelet coefficients at the first level, second level and up to the tenth level were computed. Primarily, in order to reduce the size of the feature extracted from the coefficients, statistical

measurements were applied to the values of D_1 to D_{10}, as in Übeyli and Güler (2005):

a. The wavelet coefficients' maximum in each sub-band.
b. The wavelet coefficients' mean in each sub-band.
c. The wavelet coefficients' minimum in each sub-band.
d. The wavelet coefficients' standard deviation in each sub-band.

The features (a-c) represent the signal's frequency distribution and the feature (d) represents the number of changes in a frequency distribution. These are the statistical measures used to extract a unique feature from the ultrasonic measurements and were also the inputs into the neural net for flow monitoring (Lee, Ishii and Kim, 2008; Übeyli and Güler, 2005). For each of the 125 ultrasonic datasets, the maximum, minimum, mean and standard deviation of the wavelet coefficients were derived.

Table 5-3: Frequency band range in the different wavelet decomposition levels

Wavelet decomposition ranges of frequency bands		
Decomposed signals	Number of samples	Frequency range (Hz)
D_1	600,000	2,500–5,000
D_2	300,000	1,250–2,500
D_3	150,000	625–1,250
D_4	75,000	312.5–625
D_5	37,500	156.25–312.5
D_6	18,750	75.125–156.25
D_7	9,375	39.0625–78.125
D_8	4,687.50	19.53125–39.0625
D_9	2,343.75	9.765625–19.53125
D_{10}	1171.88	4.88280 - 9.765625

5.6 **Flow regimes classification with neural network**

The extracted features from DWT and PSD were fed as input into a feedforward neural network for the two-phase gas-liquid flow regimes' classification. The classified flow regimes, which are the network output, are slug

flow, bubbly flow, churn flow, and annular flow. The feature extracted from the 125 datasets is randomly divided into training, validation and testing datasets in the ratio of 0.60:0.15:0.25, as shown in Figure 5-6 and Figure 5-7, where the x-axis labelled 1–4 represents the four flow regimes: 1. slug flow, 2. bubbly flow, 3. churn flow and 4. annular flow. The all-data subplot shows the number of samples collected for each flow regime. The data distribution used in a neural network with features extracted from DWT and PSD is Figure 5-6 and Figure 5-7.

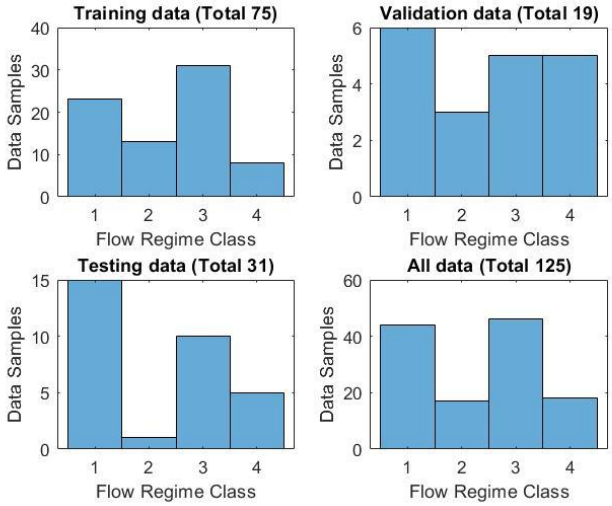

Figure 5-6: Distribution of experimental, testing and training datasets for DWT

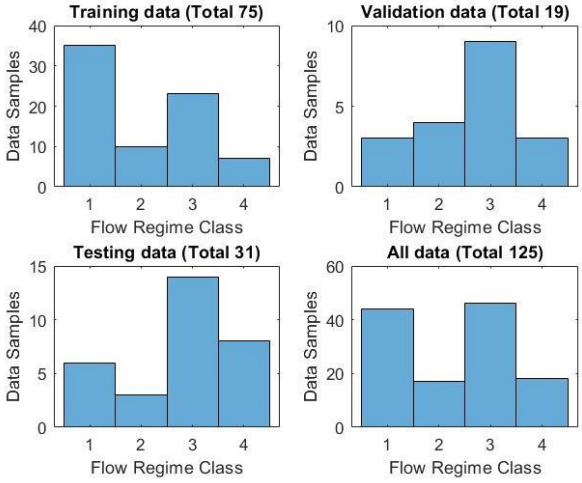

Figure 5-7: Distribution of experimental, testing and training datasets for PSD

The neural network applied for flow regime classification in this work is comprised of a feedforward network with 20 hidden neurons. The 20 hidden neurons were determined using an iterative process. A sigmoid activation function is applied in the hidden layer and a softmax activation function is applied in the output layer. The network has four output neurons, which correspond to the element number in the target vector, as shown in Figure 5-8. When features from PSD are applied, the network has 13 inputs, as shown in Figure 5-8. However, when DWT features are applied, the network has 40 inputs, as shown in Figure 5-9.

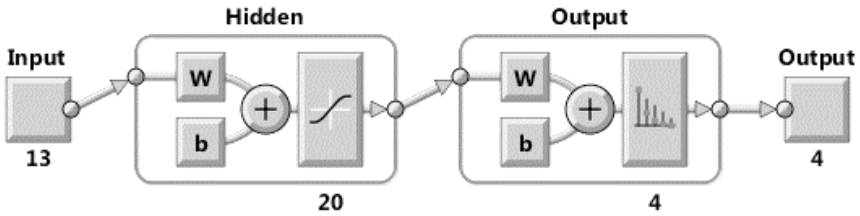

Figure 5-8: Feedforward neural network with 13 input features from PSD

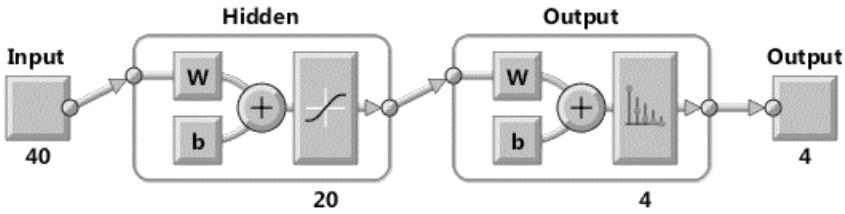

Figure 5-9: Feedforward neural network with 40 input features from DWT

During training, the network is adjusted according to the error, and the validation dataset is used to measure the network's generalisation. Unlike the validation datasets, the test dataset does not affect the training but provides the performance of the network during and after training (Ferentinou and Fakir, 2018). Training is aborted when the generalisation stops improving, as indicated by an increase in the cross-entropy error of the validation samples for up to six consecutive iterations. The classification is improved as the cross-entropy error is minimised and the percentage error indicates the number of misclassified samples. In addition to an increase in cross-entropy error, overfitting is also

observed when the performance of the training set is good but that of the test set is significantly worse.

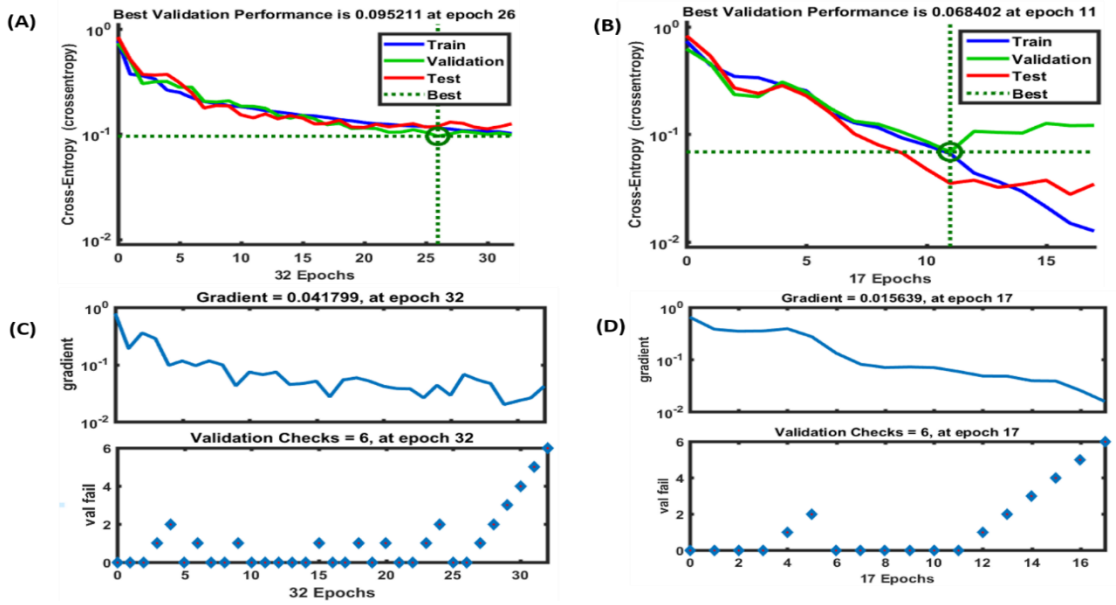

Figure 5-10: The best validation performance of the network using PSD- and DWT-extracted features is represented in Plots A and B, respectively

Figure 5-10 describes the best validation performance of the network using PSD- and DWT-extracted features, which are represented in Plots A and B, respectively. The validation performance for DWT features (Plot B: 68.4 x 10^{-3}) shows improvement compared to that for PSD features (Plot A: 95.2 x 10^{-3}). Discrete wavelet transform was observed to have a lower cross-entropy error and gradient. The classification is improved as the cross-entropy error is minimised. This information is further explained in Figure 5-11 using the Receiver Operating Characteristic (ROC) plot. In each axis, the coloured lines represent the ROC curve, which is the false positive rate (1 - specificity) against the true positive rate (sensitivity) plot as the threshold is varied. An accurate test would show points in the upper-left corner, with 100% specificity and 100% sensitivity. For this case study, the network performance was quite good. Subplots A and B show the result obtained using features from PSD and DWT, respectively. Again, the improvement from using the feature from DWT instead of PSD is seen. Discrete wavelet transform features give a minimal false positive rate, showing

points in the upper-left corner, with higher specificity and sensitivity percentages. The test data ROC of B gives 100% specificity and sensitivity for all classes except class 1 (slug flow), with 98.6% specificity and 98.6% sensitivity.

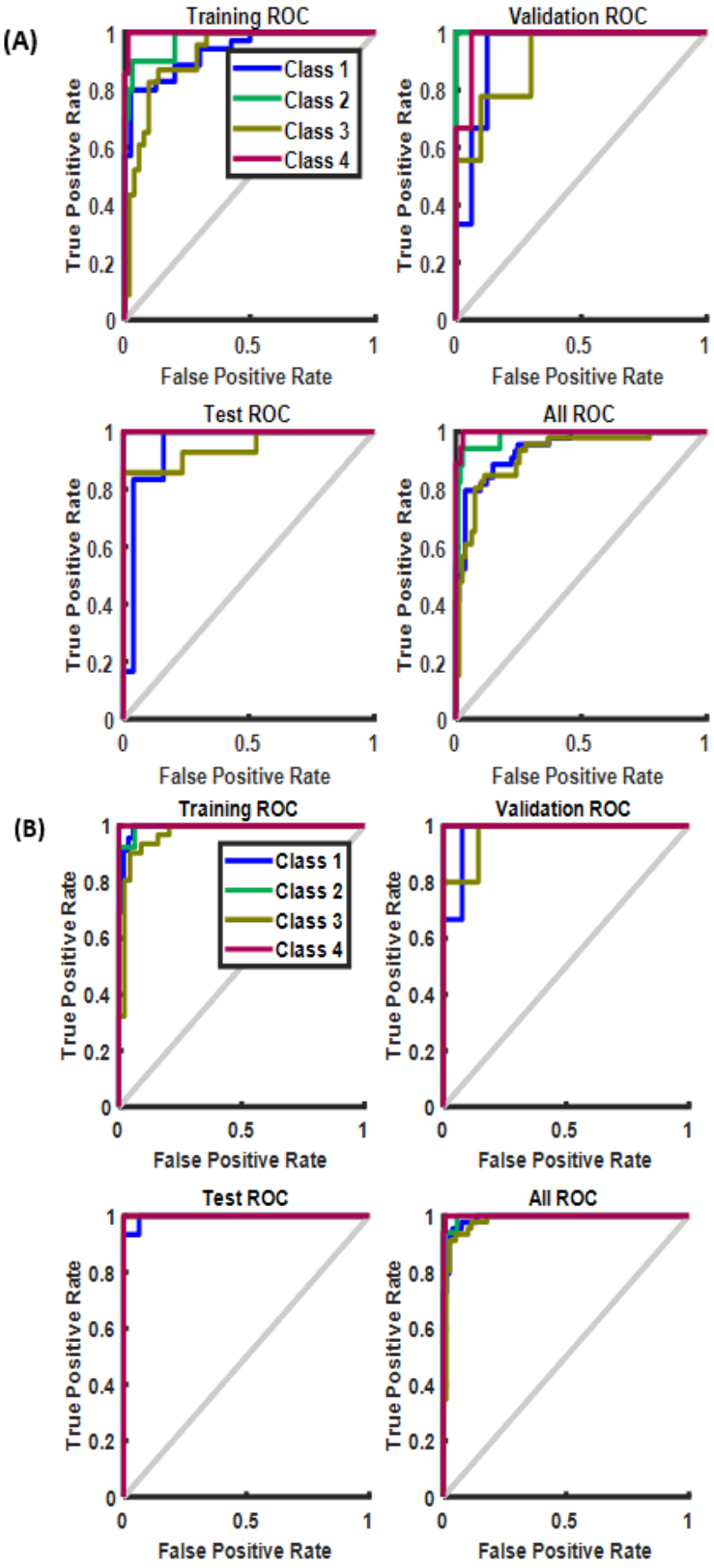

Figure 5-11: The receiver operating characteristic curve for PSD and DWT

Various neural network algorithms available in MATLAB were applied during training, including BFGS quasi-Newton, Levenberg-Marquardt (LM), conjugate gradient with Powell/Beale restarts, Fletcher-Powell conjugate gradient, Polak-Ribiére conjugate gradient, one step secant, resilient backpropagation, Variable learning rate backpropagation and scaled conjugate gradient. The Scaled Conjugate Gradient (SCG) produced a superior performance for the flow regime classification compared to other algorithms.

The conjugate gradient (SCG) algorithms and SCG, in particular, seem to perform well over a wide variety of problems, especially for networks with a large number of weights. The SCG algorithm is virtually as fast as Resilient Backpropagation (Rprop) on pattern recognition problems and function approximation problems, while SCG is as fast as the Levenberg-Marquardt (LM) algorithm. The SCG performance does not decrease (degrade) as quickly as the Rprop performance when the error is reduced. The SCG algorithms have relatively low memory requirements (Møller, 1993).

Generally, based on function approximation problems, for networks that contain roughly a few hundredweights, the LM algorithm has the fastest convergence (Sugihara, 2011). This advantage of LM is usually noticeable if very accurate training is needed. In most cases, LM can provide lower Mean Square Errors (MSE) than any of the other tested algorithms. However, as the network weight number increases, the LM advantage decreases. Moreover, the performance of LM is relatively poor on pattern recognition problems. The LM storage requirements are more significant than those of the other algorithms tested.

Resilient Backpropagation (Rprop) is the fastest algorithm for pattern recognition problems. However, it does not have a good performance on function approximation problems. Its performance decreases as the error goal decreases. The Rprop algorithm's memory requirements are relatively small compared to those of the other algorithms considered (Riedmiller and Braun, 1993; Zhang and Roberts, 1992).

The BFG performance is similar to LM performance. It does not require as much storage as LM, but the computation requirement geometrically increases with the network size because the matrix inverse equivalent must be estimated at each iteration (Ramesh, Vanathi and Gunavathi, 2008).

The GDX variable's learning rate algorithm is far slower than that of the other methods and its storage requirements are almost equivalent to those of the Rprop, but it can still be useful for certain problems. In several specific situations, it is better to converge more slowly. For instance, in using early stopping, the results can be inconsistent if an algorithm that converges too quickly is used, as the point at which the error on the validation set is minimised might be overshot (Ramesh, Vanathi and Gunavathi, 2008).

Table 5-4: Different neural network algorithms used

Description	Symbols
Levenberg-Marquardt	LM
BFGS quasi-Newton	BFGS
Resilient backpropagation	Rprop
Scaled conjugate gradient	SCG
Conjugate gradient with Powell/Beale restarts	CGB
Fletcher-Powell conjugate gradient	CGF
Polak-Ribiére conjugate gradient	CGP
One step secant	OSS
Variable learning rate backpropagation	GDX

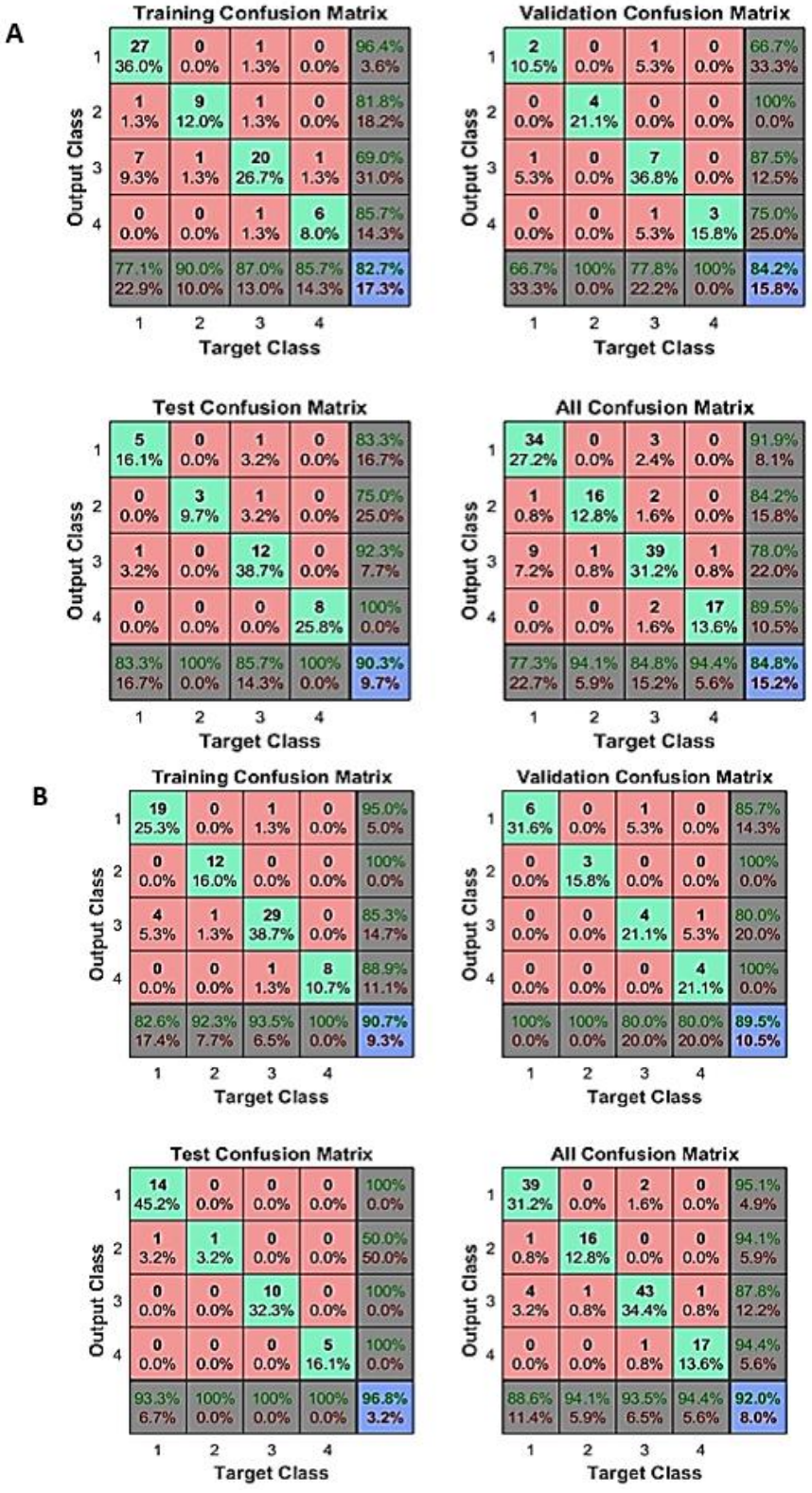

Figure 5-12: A confusion plot of the PSD (A) and DWT (B) features used in the combined neural network for flow regimes classification

The Confusion matrix is a table that is used to illustrate the performance of a classifier (classification model) on a test data set for which the true values are known. It allows the visualisation of the algorithm performance. The confusion matrix in Figure 5-12 A and B is used to further compare the neural network results obtained by applying features extracted using PSD and DWT, respectively. The diagonal cells show the correctly classified dataset's number and the misclassified datasets are shown in the off-diagonal cells. The total percentage of the correctly classified cases in green and the misclassified cases in red is shown in the blue cell at the bottom right. The confusion matrix shows that in using PSD during testing, 90.7% of datasets (28 out of 31) were classified correctly and 9.7% were misclassified (3 out of 31), while in using DWT features, 98.6% were classified correctly (30 out of 31) and 3.2% were misclassified (1 out of 31). The information also reveals the flow regime for the misclassified testing data. For instance, from subplot A it can be observed that one dataset from class 1 (slug flow) and two datasets from class 3 (churn flow) were misclassified. Similarly, from subplot B it can be observed that the only misclassified data came from class 1 (slug flow). The trained network misclassified three datasets, while the DWT-trained network misclassified only one data point.

Table 5-5 presents a summary of the accuracies of the flow regime classification and the classification method used according to the test confusion matrix in Figure 5-12.

Table 5-5: Accuracies of each of the flow regime classification and overall accuracies of the classifiers.

Classifiers	Flow regimes	Classification accuracies (%)
ANN with PSD features	Slug flow	83.3
	Bubbly flow	100
	Churn flow	85.7
	Annular flow	100
	Total accuracy	90.3
ANN with DWT features	Slug flow	93.3
	Bubbly flow	100
	Churn flow	100
	Annular flow	100
	Total accuracy	98.6

5.7 Results and Discussions

A trial was made to classify gas-liquid two-phase flow using an ANN with Doppler ultrasonic signals. The features acquired from the PSD and DWT frequency bands were fed into the neural network as the input, as shown in Figure 5-2. Using a neural network, the extracted features were classified into one of the four flow regime categories: the bubbly, slug, churn and annular flow regimes. To improve the neural network flow regime classifier's performance, the number of features or inputs and the number of hidden neurons were increased with caution to avoid overfitting. In addition, the initial network weights and biases of the network were tuned accordingly.

5.7.1 Feature extractions

Doppler ultrasonic signal features of the flow were extracted using PSD and DWT. The spectral analysis frequency domain of Doppler ultrasonic signals was deployed using PSD based on Fourier transform. The average PSD spectrum was then taken and fed into the neural network as input. It is essential to extract the spectra statistical moments (Xie, Ghiaasiaan and Karrila, 2004). Ten frequency bands were extracted from the DWT coefficients and 40 features from the 10 DWT coefficient levels were obtained for each of the datasets using the statistical measures deployed to the wavelet levels.

5.7.2 Flow regime identification

The feature extracted from the 125 datasets was randomly divided into training, validation and testing datasets in the ratio of 0.60:0.15:0.25, as shown in Figure 5-6 and Figure 5-7. The flow regimes classifier testing was done using 31 datasets (comprised of the four flow regimes), as shown in Figure 5-6 and Figure 5-7. After training and validation using training and validation datasets, the network was tested with the testing datasets that were yet unseen by the network. The result was analysed, after which the testing dataset's classification errors were evaluated using the best validation performance, the ROC plot and a confusion matrix. The neural network results obtained from the features extracted

using DWT and PSD were compared. The result obtained from the features extracted using the DWT feedforward neural network showed improvement compared to those obtained using PSD.

5.7.3 Comparison of classification results in chapter four and chapter five

Table 4-3 presents the classification results gotten using the SVM classifier with extracted PSD features for gas-liquid two-phase flow regime classification. Using the SVM classifier, 33 datasets were correctly classified out of 39 test data samples while 6 datasets were misclassified out of 39 test data samples used. The overall accuracy using the SVM classifier was 84.6 %.

On the other hand, Table 5-5 shows the classification results using ANN with extracted features from PSD and DWT. Using the extracted features from the PSD, the neural network misclassified three out of 31 test datasets and correctly classified 28 out of 31 datasets used giving 90.3 % in classification accuracy. But, using DWT features, the neural network classified 30 datasets correctly out of 31 datasets and misclassified only one dataset and gave 95.8 % in classification accuracy. Hence, showing the superiority of the DWT in feature extraction.

5.8 Summary

5.8.1 Summary

In this work, an ANN that uses a Doppler ultrasonic sensor was developed for the objective classification of gas-liquid two-phase flow regimes. The Doppler ultrasonic signal was processed using PSD and DWT features' extraction methods for the extraction of input features in the neural network models. Using a neural network, the features extracted were classified into one of the four flow regime categories: the bubbly, slug, churn and annular flow regimes. To improve the performance of the neural network flow regime classifier, the number of inputs or features and hidden neurons was increased with caution to avoid overfitting. Also, the initial network biases and weights of the network were tuned accordingly. Using PSD features, the neural network classifier misclassified three

out of 31 test datasets in the classification and gave 90.3% accuracy, while with the DWT features only one dataset was misclassified, yielding an accuracy of 95.8% and thereby showing the superiority of the DWT in feature extraction of flow regime classification. This approach demonstrates the application of a neural network and DWT for flow regime classification in industrial applications, using a clamp-on non-intrusive ultrasonic sensor. It is considered superior to other techniques as it uses a clamp-on non-intrusive and non-radioactive sensor.

CHAPTER SIX

6 Venturi Multiphase Flow Measurement for Active Slug Control

Riser slug flow poses a significant challenge to offshore oil production systems, most especially for oil fields in their later life. Active control of slugging through choking has been proven a practical approach in eliminating riser slug flow in oil production pipeline-riser systems. However, existing conventional active slug control systems may reduce oil production significantly due to excessive over choking. Again, some of the existing active slug flow control systems rely on seabed measurements, which are difficult to maintain, costly to install, unreliable, and seldom readily available. This study is an experimental investigation of the feasibility of active riser slug control by taking topside differential pressure measurement from the inlet of the venturi flow meter to the throat. Experimental results indicate that under active slug flow control, the system was able to eliminate slug flow at a higher valve opening compared to manual choking. A valve opening of 24% with riser base pressure at 2.85 bar from open-loop unstable of 23% was recorded, which is superior to manual choking which maintained flow stability up to 21% valve opening with riser base pressure of 3.8 bar.

6.1 Introduction

Riser-induced severe slug flow is one of the most challenging flow regimes due to its potential to cause riser-pipeline system instability. During the later stage of oil field production life when reservoir pressure and production are low, riser-induced severe slug flows form in the pipeline-riser system because of low liquid and gas flow rates. Riser-induced severe slug flow consists of four cyclic

processes which include the liquid slug buildup/formation, slug production, gas penetration and gas blowout/liquid fallback (Schmidt, Brill and Beggs, 1980); (Taitel, 1986).

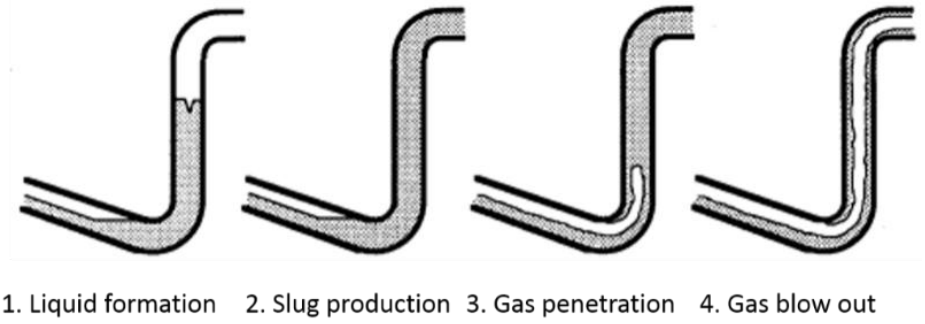

Figure 6-1: Cycles of riser-induced severe slug flow (Fabre et al., 1990)**.**

This transient four-cycle process causes large fluctuations in pressure and flow rate of the system, creating problems in downstream facilities such as compressors, pumps, and separators, which have been designed to operate under steady-state operating conditions.

Riser-induced severe slug flow is an undesirable flow regime and has caused several operational problems such as:

- Overpressurisation of the separator: The peak flow rates during gas and liquid surges might induce flooding and separator overpressurisation, which may lead to complete plant shutdown (Malekzadeh, Henkes and Mudde, 2012).
- Increased back pressure: Increased back pressure at the wellhead may cause production termination and well abandonment (Malekzadeh, Henkes and Mudde, 2012).
- Unstable flow: high liquid flow, followed by a large volume of gas delivery and then a period of no-flow. This causes unnecessary gas flaring, high-level trips and overpressurisation in the separator (Montgomery and Yeung, 2002).

- Increased mechanical stresses: High liquid flow velocities during the period of blowdown and a highly varying liquid inventory in the riser cause stress and decrease the riser operating life (Shotbolt, 1986).

Riser-induced severe slug flow could be problematic in oil production systems offshore especially for oil fields in their later life. Considering different slug flow elimination methods proposed in the literature, active slug flow control has numerous benefits; it is less expensive than the implementation of new equipment, it requires less modification to the existing production systems, and also it eliminates slug flow thereby eliminating the strain on the system. Hence, much money can be saved on system maintenance.

The first implementation of active slug flow control can be found in the Ph.D. work of Schmidt in the 1970s, where severe slug flow was eliminated by choking the riser outlet flow. However, choking the riser outlet increases the backpressure, which reduces overall oil production. However, Jansen et al. (1996) report that using an automatic control valve at the riser outlet to regulate (control) the pressure at the riser base would reduce the backpressure needed to eliminate slug flow instead of choking the riser outlet flow manually. In reference to this principle, ASEA Brown Boveri (ABB) developed an active slug controller using upstream riser pressure as the measurement (Havre, Stornes and Stray, 2000; Havre and Dalsmo, 2002).

The control solution in Havre et al. (2000) and Havre and Dalsmo (2002) requires riser base pressure measurement, which is difficult to maintain, unreliable and expensive. However, to avoid the use of riser base pressure, an idea was proposed to maintain outlet riser flow at the steady condition to reduce the fluctuation induced by slug flow. To facilitate the multiphase flow measurement at the outlet riser, a small pre-separator was introduced between the first stage separator and the riser to provide both gas and liquid flow rates. This resulted in the development of Shell's Slug Suppression System (S^3) (Kovalev, Cruickshank and Purvis, 2003) and Shell's Vessel-less S^3 system (Kovalev, Seelen and Haandrikman, 2004). The major disadvantage of this

control solution is that it requires the retrofit of the existing system for new devices installation.

While the S^3 and the Vessel-less S^3 are robust solutions for controlling gas surges and mitigating liquid slugs, they require the pre-separation of liquid and gas phases in each pipeline where slug flow could be a problem. The system requires two control valves which in combination with the separator may not be cost-effective for some slug flow problems that only appear in a field's later life. Again, for some situations where multiple risers/pipelines have to be on-boarded to a single production facility, the S^3 is not a feasible option. A slug flow mitigation solution based on a single valve that can effectively control gas surges and mitigate liquid slugs is then a preferred option. Based on this principle, the Shell Smart Choke was developed, where the S^3 control algorithm is implemented on a single control valve. However, this solution was also based on controlling the flow rates (Eken, Haandrikman and Seelen, 2007).

Some other contributions on active slug flow control can be found in the following work: Godhavn et al. (2005), Sivertsen et al. (2010), Pedersen et al. (2015), Sivertsen et al. (2010), Henriot et al. (1999), Sivertsen and Skogestad (2005), and Tandoh et al. (2016).

In summary, the main contribution of the chapter is to investigate the feasibility of active control of riser-induced severe slug flow by taking the differential pressure measurement from the venturi inlet to the throat. This meets objective 4 given in Section 1.6 which is to control slug using differential pressure and throat pressure measurement from venturi metre.

This chapter is organised as follows. Section 6.2 presents the experimental setup for the work. Section 6.3 described the Inferential Slug Control method used for the work. In Section 6.4, the experimental results and discussion are presented, and finally, the summary is drawn in Section 6.5.

6.2 **Experimental setup**

6.2.1 **The multiphase flow test facility**

The test facility is the same as described in Chapter 3. However, for the benefit of this present work, venturi metre was installed to aid the investigation. The schematic diagram of the test rig section with the venturi meter is presented in Figure 6-2.

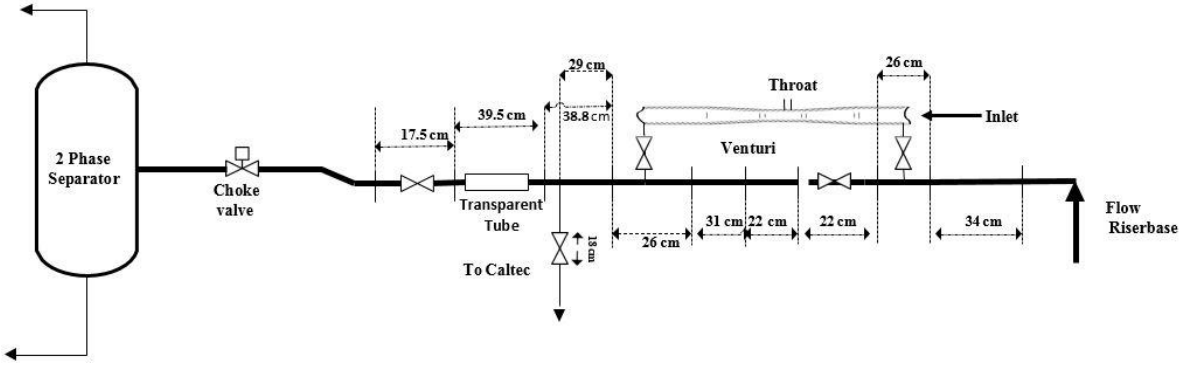

Figure 6-2: Schematic diagram of the flow facility section showing the venturi meter.

Table 6-1: Experimental process and instrumentation list

Sensor tags	Description	Unit
DPT409	Differential pressure (Venturi inlet–throat)	bar
PT312	Air delivery pressure	bar
PT403	Top separator pressure	bar
PT408	Riser top pressure	bar
PT417	Riser base pressure	bar
PT501	3-phase separator pressure	bar
PIC501	3-phase separator outlet air valve	%
FT102	Inlet water temperature	^{o}C
FT102	Inlet water density	Kg/m^3
FT102/104	Inlet water flow rate	Kg/s
FT305	Inlet air temperature	^{o}C
FT305/302	Inlet air flow rate	Sm^3/hr
FT404	Top separator gas outlet	M^3/hr
FT406	Top separator liquid outlet	Kg/s
LI101	Liquid tank level	m
LI502	Three-phase separator water-oil level	%
LI503	Liquid coalescer level	%
LVC502-SR	Outer valve liquid coalescer level	%

6.3 **Inferential Slug Controller**

The Inferential Slug Controller (ISC) works based on a single control variable acquired through a combination of various available multiphase flow measurements using algebraic calculations. The ISC system determines the choke valve opening by adopting the following control law:

$$V = V_0 + k(W^T Y - R) \quad 6\text{-}1$$

where V_0 is the choke valve setpoint, V is the estimated choked valve opening, k is the controller gain, Y is the measurement vector, W is measurement weight vector and R is the controlled variable set point.

The measurement weight vector W can be expressed mathematically as

$$W = [k_1, k_2, k_3, \ldots\ldots, k_{n-1}, k_n]^T \quad 6\text{-}2$$

where $k_i, i = 1, 2, 3, \ldots, n$ is the ith measurement weight and the number of control measurements used is n.

Moreso, the vector Y is expressed as

$$Y = [Y_1, Y_2, Y_3, \ldots\ldots, Y_{n-1}, Y_n]^T \quad 6\text{-}3$$

where $Y_i, i = 1, 2, 3, \ldots, n$ is the ith measurement weight and the number of control measurements used is n.

Mathematically, combining equations 6-1, 6-2, and 6-3, the control law becomes

$$V = V_0 + k(\sum_{i=1}^{n} k_i y_i - R) \quad 6\text{-}4$$

In this chapter, the ISC controller was used but only the venturi measurement was used as the controlled variable.

6.4 **Experimental results and discussion**

6.4.1 **Experimental test matrix**

The test matrix for the two-phase 2-inch S-shape riser tests is presented in Table 6-2. The test matrix covers different flow regimes such as slug, churn, bubbly and

annular flow but concentrated more on collecting data under the severe slugging regions.

Table 6-2: Experimental test matrix

Water flowrate kg/s				0.1	0.5	1	1.5	2	3	3.5	5
water volumetric flowrate				0.00010	0.00050	0.00100	0.00150	0.00200	0.00301	0.00351	0.00501
Superficial water velocity per second (volumetric / area)				0.05	0.25	0.49	0.74	0.99	1.48	1.73	2.47
Air Flowrate sm3/h	Air Flowrate nm3/h	Superficial air velocity per hour	Superficial air velocity per second								
5.00	2.42	1191.93	0.33	0.26	0.24	0.23	0.22	0.22	0.20	0.19	0.18
10.00	4.83	2383.86	0.66	0.56	0.52	0.49	0.46	0.45	0.40	0.37	0.35
20.00	9.66	4767.72	1.32	1.14	1.12	0.99	0.95	0.89	0.79	0.74	0.69
30.00	14.50	7151.58	1.99	1.73	1.64	1.51	1.47	1.34	1.17	1.09	1.01
50.00	24.16	11919.30	3.31	2.94	2.65	2.50	2.36	2.18	1.88	1.75	1.62
70.00	33.83	16687.02	4.64	4.14	3.69	3.42	3.25	2.88	2.42	2.23	2.06
100.00	48.32	23838.60	6.62	5.92	5.12	4.69	4.26	3.98	3.33	3.06	3.00
120.00	57.99	28606.32	7.95	7.10	6.09	5.46	4.95	4.46	3.69	3.38	3.11
150.00	72.48	35757.90	9.93	8.82	7.49	6.66	5.82	5.21	4.28	4.01	3.62
200.00	96.65	47677.20	13.24	9.77	9.29	9.05	8.87	8.10	7.42	7.14	6.77
250.00	120.81	59596.49	16.55	12.21	11.37	10.61	10.20	9.33	9.06	8.78	8.28
300.00	144.97	71515.79	19.87	14.66	12.78	12.25	11.50	10.88	10.71	9.90	8.89

Table 6-2 presents various air-water flow rates tested to ascertain the flow conditions under the severe slugging flow regime. The area of the pipe is 0.0020271 and it is constant.

6.4.2 **Description of Observed Flow Regimes**

Flow regime maps are vital tools for obtaining an overview of flow patterns that can be expected for a particular fluid condition. These maps depict the geometrical distribution of the flow moving through a pipeline. Different flow regimes such as bubbly, slug, churn and annular are used to depict this distribution. Two-phase flow regimes have often been illustrated as maps, or plots, with the superficial phase velocities on each axis.

The flow pattern map showing all the test points is presented in Table 6-3.The area of the pipe is 0.0020271

Table 6-3: Experimental flow regime observations

Water flowrate kg/s				0.1	0.5	1	1.5	2	3	3.5	5
water volumetric flowrate				0.00010	0.00050	0.00100	0.00150	0.00200	0.00301	0.00351	0.00501
Superficial water velocity per second (volumetric / area)				**0.05**	**0.25**	**0.49**	**0.74**	**0.99**	**1.48**	**1.73**	**2.47**
Air Flowrate sm3/h	Air Flowrate nm3/h	Superficial air velocity per hour	Superficial air velocity per second	**Observed Flow Regimes**							
5.00	2.42	1191.93	0.33	slug	slug	slug	Slug	bubbly	bubbly	bubbly	bubbly
10.00	4.83	2383.86	0.66	slug	slug	slug	slug	slug	slug	slug	bubbly
20.00	9.66	4767.72	1.32	slug	slug	slug	slug	slug	slug	slug	slug
30.00	14.50	7151.58	1.99	slug	slug	slug	slug	slug	slug	slug	slug
50.00	24.16	11919.30	3.31	churn	slug	slug	slug	slug	slug	slug	slug
70.00	33.83	16687.02	4.64	churn	slug	slug	slug	slug	slug	slug	slug
100.00	48.32	23838.60	6.62	churn	slug	slug	slug	slug	slug	slug	slug
120.00	57.99	28606.32	7.95	churn	slug	slug	slug	slug	slug	slug	slug
150.00	72.48	35757.90	9.93	annular	slug	slug	slug	slug	slug	slug	slug
200.00	96.65	47677.20	13.24	annular	slug	slug	slug	slug	slug	slug	slug
250.00	120.81	59596.49	16.55	annular	annular	slug	slug	slug	slug	slug	slug
300.00	144.97	71515.79	19.87	annular	annular	slug	slug	slug	slug	slug	slug

Table 6-3 presents the air-water flow conditions under various flow regimes ranging from annular, bubbly, churn and slug flow.

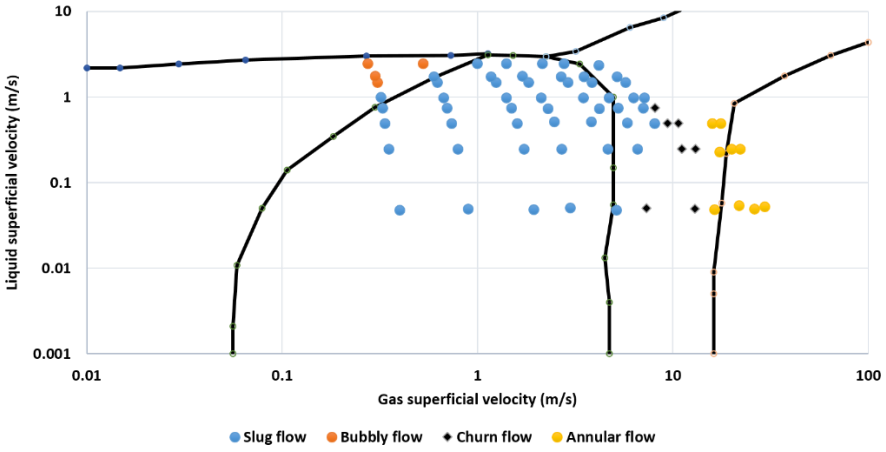

Figure 6-3: Experimental flow regime map for the 2" S-shaped riser with venturi

The flow regime map was examined to estimate the operating conditions under severe slugging conditions. The selected operating points that fall into the slugging regime are the gas flow rate of 10 Sm^3/h and liquid flow rate of 1 kg/s with superficial velocities of 0.6941 m/s and 0.4952 m/s, respectively.

6.4.3 **S-shape pressure trend**

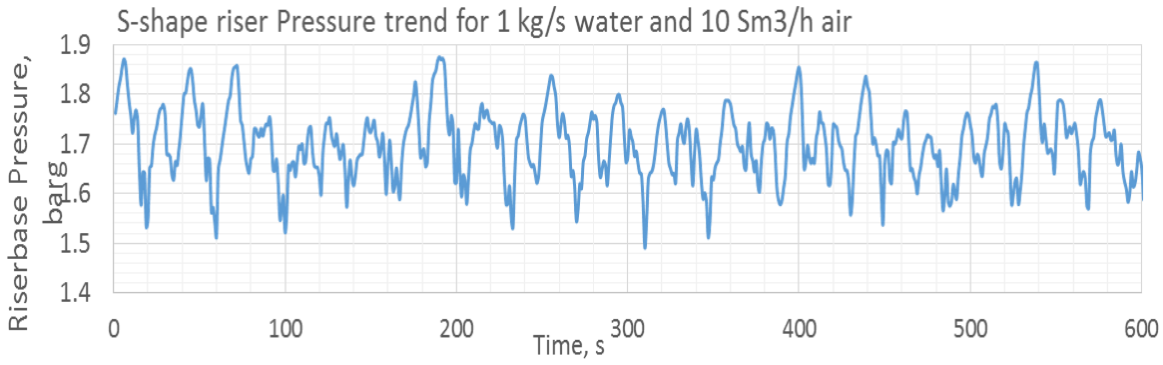

Figure 6-4: S-shape riser pressure trend for 1 kg/s water and 10 Sm^3/h air

At the flow condition of 10 Sm^3/h and liquid flow rate of 1 kg/s with superficial velocities of 0.6941 m/s and 0.4952 m/s, respectively, a severe slug flow was observed as illustrated in Figure 6-4. At this flow condition, the maximum and minimum pressure was 1.89 barg and 1.49 barg respectively. Hence, the magnitude of oscillation is 0.40 barg. The period of oscillation which is the time taken to complete one full oscillation or cycle was observed to be 20 seconds. All these observations indicated that the system is under severe slugging.

6.4.4 **System Stability (Bifurcation map)**

Bifurcation map analysis is a study of assessing the stability of a system at a constant flow rate. The bifurcation can be obtained by keeping the flow rate constant and varying the choke valve openings (1% - 100%). This study aims to achieve the bifurcation point which is the maximum valve opening at which the flow in the pipeline system becomes stable in an open loop. This translates to a point at which the system loses its stability as a result of an increase in the valve opening. The stability loss of the system is a resultant of a pair of complex poles crossing the imaginary axis on the s-plane which however changes the sign of

the real part of the pole from negative to positive. In the controller design process the first step is to establish the system bifurcation point, that is, the maximum valve opening for which the flow becomes stable in an open-loop condition. This serves as the reference point for the controller to stabilize flow in an open-loop unstable region as illustrated in Figure 6-5.

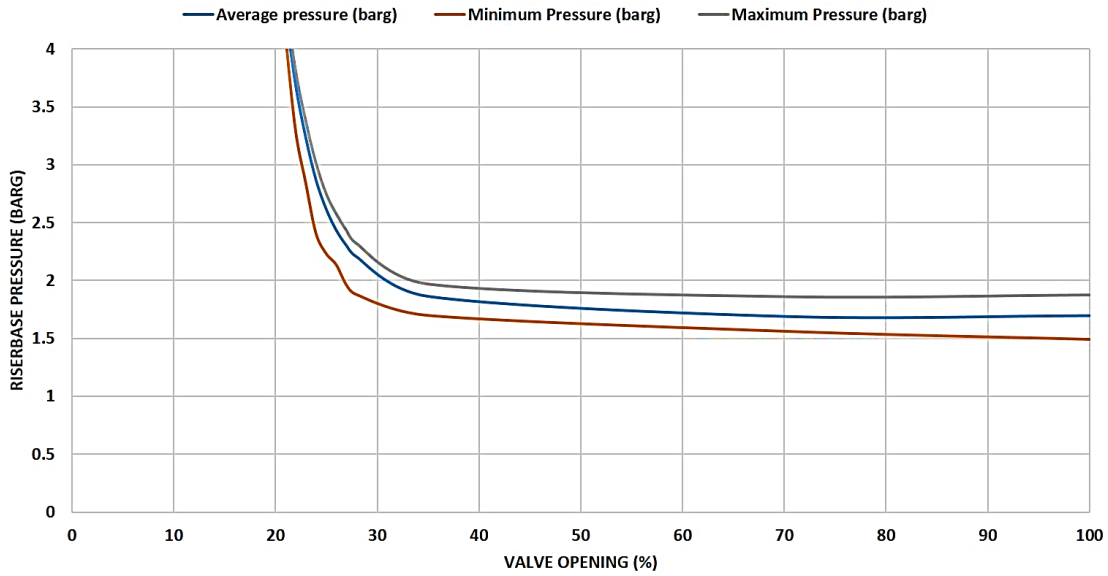

Figure 6-5: Bifurcation Map of 1 kg/s of Water and 10 Sm3/h of Air

Figure 6-5 presents the bifurcation map for the boundary condition of 2" S-shaped riser, where system stability was obtained at a valve opening of 21%, which corresponds to a pressure of 3.8 bars from the result of the bifurcation map. This is the highest choke valve opening for stable operations when no active slug control is applied, stabilizing the system at the open-loop unstable region where u >21 % will be aimed for to obtain a desired stable non-oscillatory flow regime.

6.4.5 Slug control using differential pressure from the venturi inlet to the venturi throat

The performance of the venturi measurement used for slug flow control is as shown in Figure 6-6.

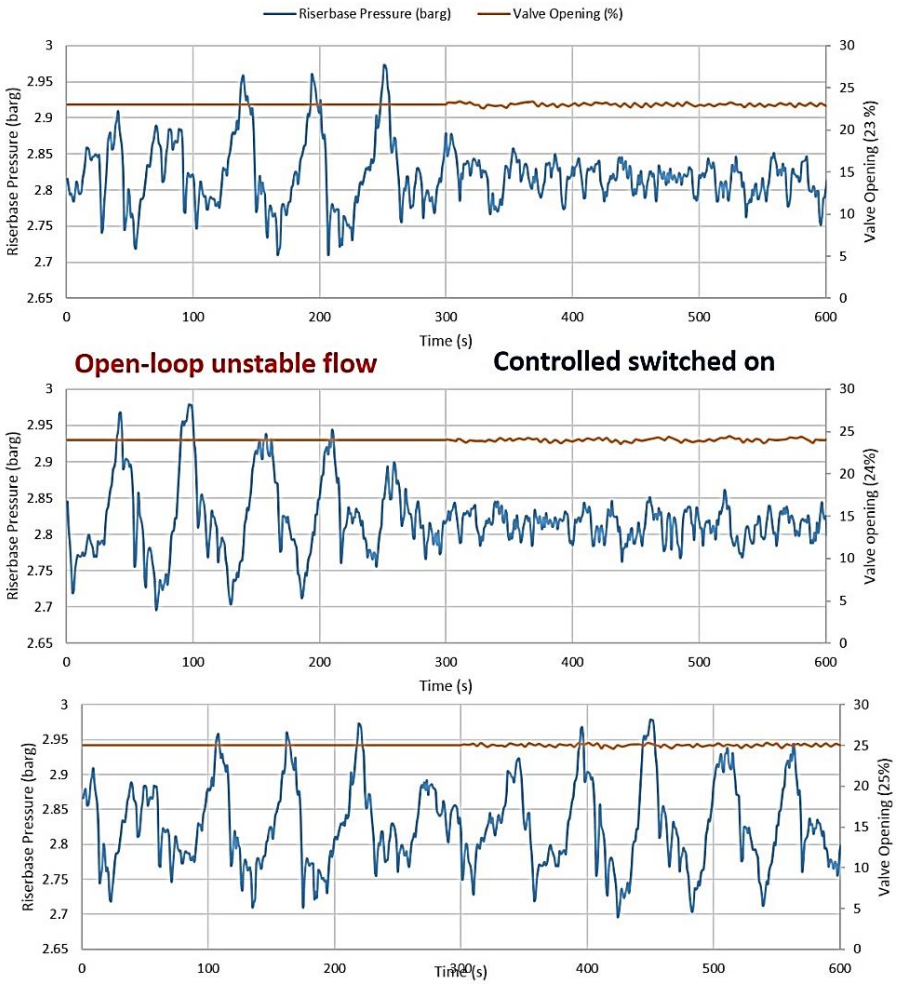

Figure 6-6: Riser base pressure response with the equivalent valve opening using the differential pressure measurement from the venturi inlet–throat

Figure 6-6 demonstrates that slug flow stability using differential pressure from the venturi inlet to the venturi throat stabilised the flow from valve opening of 23% open-loop unstable to 24%. Figure 6-6a indicates that the riser system was unstable at valve opening of 23 % from 0 seconds to 300 seconds until the controller was switched on, which stabilised the system. The same process happened in Figure 6-6b, but in Figure 6-6c, the system was unstable even when the controller was switched on. A benefit of a 4 % reduction in the riser base pressure from 2.95 barg to 2.85 barg was recorded with a 14 % increase in production. Hence, this demonstrates a superior control performance given that with manual choking the flow was stabilised at 21% valve opening.

6.4.6 **Comparisons of Venturi measurement to Riserbase pressure measurement**

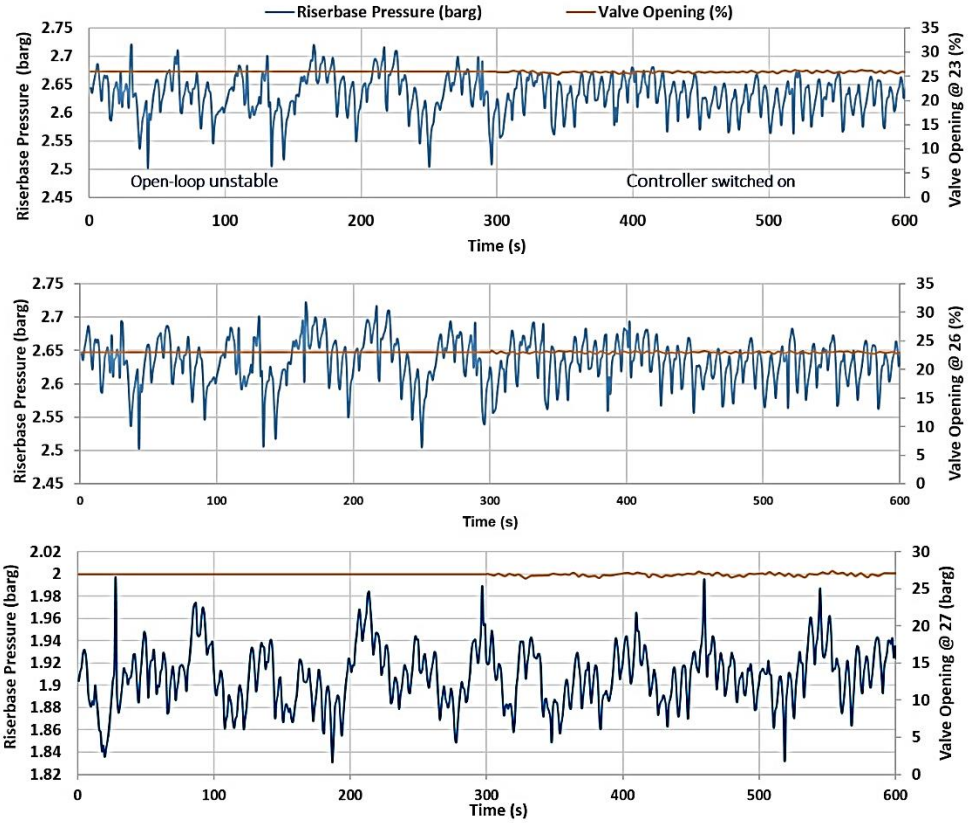

Figure 6-7: Riser base pressure response with the equivalent valve opening using subsea pressure measurement for slug control

Figure 6-7 demonstrates that slug flow stability using only riserbase pressure stabilised the flow from valve opening of 23% open-loop unstable to 26%. Figure 6-7a indicates that the riser system was unstable at valve opening of 23 % from 0 seconds to 299 seconds until the controller was switched on at 300 seconds, which stabilised the system. The same process repeated in Figure 6-7b, but in Figure 6-7c, the system was unstable even when the controller was switched on. A benefit of 3% reduction in the riser base pressure from 2.74 barg to 2.65 barg was recorded with a 23% increase in production rate. Hence, this demonstrates a superior control performance given that with differential pressure from the venturi inlet to the venturi throat the flow was stabilised at 24% valve opening.

6.5 Summary

Riser slug flow poses a significant challenge to offshore oil production systems, most especially for oil fields in their later life. Active control of slugging through choking has been proven a practical approach in eliminating riser slug flow in oil production pipeline-riser systems. However, existing conventional active slug control systems may reduce oil production significantly due to excessive over choking. Again, some of the existing active slug flow control systems rely on seabed measurements, which are difficult to maintain, costly to install, unreliable, and seldom readily available. This study is an experimental investigation of the feasibility of active riser slug control by taking topside differential pressure measurement from the inlet of the venturi flow meter to the throat.

Experimental results indicate that under active slug flow control, the system was able to eliminate slug flow at a higher valve opening compared to manual choking. A valve opening of 24% with riser base pressure at 2.85 bar from open-loop unstable of 23% was recorded, which is superior to manual choking which maintained flow stability up to 21% valve opening with riser base pressure of 3.8 bar.

CHAPTER SEVEN

7 Active Slug Control using an Ultrasonic Sensor

An approach for active slug flow control using a non-intrusive ultrasonic sensor is proposed. Active slug control in the oil production pipeline-riser system using manual choking is an effective technique for slug control but this approach still undergoes the risk of limiting hydrocarbon production due to inappropriate over choking. Moreso, some active slug control relies on subsea measurements such as riser base pressure and most of these subsea measurements are expensive, difficult to maintain, and unreliable. Hence, in order to achieve an efficient slugging control performance, the need to find a reliable, robust, and efficient measurements which is more sensitive to slugging is important. The riser slug flow control using Continuous Wave Doppler Ultrasound (CWDU) has been carried out experimentally and it gives a good control performance. Achieving a valve opening of 26% from open-loop unstable of 23% which is more superior to the manual choking which maintained its stability up to 21% valve opening.

7.1 Introduction

Slugging flow is a challenge faced by offshore oil and gas production systems. Active slug control is a widely accepted solution to tackle this challenge. However, like any other control system, the efficiency of a slug control solution depends on which variable is adopted for control. Due to the difficulty of multiphase flow measurement, in an offshore oil production system, measurements suitable for slug control are very limited. Among many solutions, riser base pressure has been proven as the best slug control variable. However, this solution requires a subsea installation, which is expensive and unreliable. The gamma densitometer has also been demonstrated to be suitable for slug control. It is a clamp-on measurement, hence the installation cost is low. Nevertheless, due to its radioactive nature, it has not been well adopted in offshore systems. In this chapter, another clamp-on instrument, the Doppler ultrasonic sensor, is studied

for slug control. The sensor as a single-phase flow meter is based on the Doppler Effect, namely that the frequency of an ultrasonic wave reflected from the scatterers of a moving medium is shifted in proportion to the velocity of the medium. However, directly applying such a sensor to measure multiphase flows does not work well, resulting in uncertainties and measurement errors, hence it is still an open challenge. Due to this deficiency, ultrasonic sensors have never been used in any slug control system. Through our study on inferential slug control, we concluded that a reliable slug control variable does not need to relate to a physical flow parameter. The Doppler ultrasonic sensor can produce signals sensitive to slugging fluctuations. Hence, it is suitable for slug control. This chapter summarises results obtained in the preliminary study which demonstrate the effectiveness of the Doppler ultrasonic sensor for slug control. This meets objectives 1 and 3 given in Section 1.6 which are to develop a continuous wave Doppler ultrasound (CWDU) system for multiphase flow slug control and also to determine the applicability of CWDU for riser slug control.

The aim of this chapter is to investigate the applicability of continuous-wave Doppler ultrasound (CWDU) for slug control. This chapter is structured as follows: Section 7.2 gives a brief literature survey, section 7.3 describes the ultrasonic sensor used in this investigation, Section 7.4, describes the slug control structure, Section 7.5, presents the results acquired, and Section 7.6 summarised the findings of the chapter.

7.2 Literature survey

In recent years, offshore oil and gas production and exploration facility production optimization have been vigorously investigated, as any promising enhanced hydrocarbon recovery can result in great economic benefits (Havre, Stornes and Stray, 2000). Hence, in offshore oil and gas industries, multiphase flow behaviour in pipelines is of great interest. A lot of effort and investments have been made investigating this slugging phenomenon, this is because any alteration in operating conditions can vary the pipeline flow behaviour drastically. This has a large impact on significant factors such as safety, maintenance, and productivity.

An undesirable flow regime that may induce severe problems at topside processing facilities occurs at some certain operating conditions due to pressure and flow rate fluctuations in the system (Payne, Huff and Ogren, 1996). This normally occurs during the late-life of a well when the flow rates in the system are much lower than what the system was designed for. These pressure and flow rate fluctuations are instigated by a flow regime known as slugging flow.

Avoiding slugging flow in pipelines creates significant economic benefits. Hence, it is imperative to predict or detect the flow regime before starting production in order to tackle problems as soon as possible. Conventionally, flow regime maps are developed to predict the flow regime that will occur in a pipeline (Hewitt and Roberts, 1969; Taitel, 1986; Barnea, 1987). The flow regime is estimated by the quantities such as gas/liquid densities, pipe diameter, gas/liquid viscosities, gas/liquid surface tension, pipe incline and gas/liquid superficial velocities (Griffith and I, 1961). As these quantities may vary along the pipeline, the flow regime can vary as well (Hewitt and Roberts, 1969). The reliance of the flow regime on the aforementioned parameters describes the flow regime map.

Slugging flow has negative effects on the topside processing facilities during the production of oil and gas offshore due to large variations in pressure and flow rates (Taitel et al., 1990). Some of the common problems caused by slugging are operating capacity reduction and unwanted flaring. The pressure variations also cause strains on some parts of the system such as bends and valves. In most cases, the burden in the compressors and separators at the top side becomes so great that it causes a lot of damage and shuts down the plant, which is a great disadvantage to oil-producing companies.

Slugging flow prevention or control has great economic benefits, which is the main reason why a lot of effort and money have been invested in search of a robust remedy for the problems caused by slugging flow. There are many possible ways of preventing/controlling slugging such as design changes, for instance, increasing the separators' size, gas lift or slug catcher installation, or changing the topology of the pipeline. Hence, the installation and maintenance of

this new equipment are capital intensive. The next method is changing the system operating conditions, which is done by choking the valve at the topside. The major disadvantage of this method is production rate reduction due to a pressure increase in the pipeline.

For the past few decades, a lot of studies have been carried out on the use of active control as a tool for flow stabilization. Schmidt et al. (1979) implemented an automatic control system successfully on a pipeline-riser system with a topside choke valve as an actuator. Hedne and Linga (1990) proved that it is possible to stabilise the flow by applying a PI controller and a pressure sensor estimating the difference in pressure over the riser. Recently, different control techniques have also been utilised on offshore production systems with great success (Courbot, 1996; Havre, Stornes and Stray, 2000; Godhavn, Fard and Fuchs, 2005). An active control system alters the boundaries of the flow regime map, preventing the slugging regime in an area where slugging is predicted. Hence, it is feasible to operate with the exact average flow rate as in the early days of an oil field without the great fluctuations in pressure and the flow rates.

The benefits of applying active control are significant. It is more economically efficient and effective than the deployment of new equipment, and it can also eliminate slugging flow in the system effectively, thereby relieving the system from the strain. Hence, system maintenance issues will be reduced and money will be saved. A high production rate is more feasible with active control than with the conventional choking of the topside valve.

The subsea multiphase measurements are normally included during control structures; pressure measurements at the riser base or further upstream are some of the measurements. In slugging mitigation/control, subsea measurements have been proven to be effective in slugging mitigation/control (Taitel et al., 1990). In the absence of these measurements, slug mitigation/control gets tougher.

However, subsea measurements are often not readily available and are expensive to implement and less reliable than the topside measurements. It is

imperative to ascertain the possibility of slug control using solely the topside measurements, hence, the introduction of topside measurements. However, questions have been raised about the possibility of improving system performance by using a single topside measurement or combination of topside measurements and whether the results will be similar or comparable to when a controller based on subsea measurements is deployed. To answer these questions, new multiphase flow topside measurements that will provide reliable control performance are investigated in this work.

Describing the features of multiphase flows using techniques that are non-radioactive, non-invasive, fast and appropriate for opaque systems has been of great interest for several industrial applications. Ultrasonic techniques meet all these requirements.

There are many advantages of using ultrasonic techniques for measurements such as rapidity, high accuracy, greater sensitivity, safety, and simplicity compared to existing techniques like X-ray and Gamma-ray.

7.3 Continuous-Wave (CW) ultrasonic Doppler sensor

Doppler shift (or Doppler Effect) is the frequency variation of acoustic waves when movement exists between the acoustic receiver and the source, and the shift in frequency is in proportion to the acoustic source velocity (Weinstein 1982). Thus, the velocity of the acoustic source can be obtained by calculating the frequency shift between the acoustic receiver and the source. In the CW ultrasonic Doppler technique, a fixed frequency acoustic beam is released continuously from the transducer (ultrasonic) into the flow, and the sound wave is reflected by moving the scatterers. The scattered acoustic beam is received by another ultrasonic transducer so that the velocity of the flow can be estimated with the frequency shift based on the Doppler Effect.

The Continuous Wave Ultrasound Doppler (CWUD) used in this work is a non-invasive flowmeter manufactured by United Automation Ltd. based in the Southport United Kingdom. The CWUD is suitable for the measurement of the

ultrasonic reflective fluid of any flow. It calculates the shifts in frequency, processes the ultrasonic signals, and evaluates the velocity of the flow. The CWUD calculates the shift in the frequency of the signals reflected from the discontinuities or scatterers like bubbles in the flowing fluid. For a suitable bond between the external conduit surface and the sensor, a glycerin gel was applied to avoid air cavities trapped between the sensor and the conduit surface.

The CWUD has two separate crystal transducers embedded in one probe which transmit and receive ultrasonic signals continuously at 500 kHz. The transducer is electrified by the electronic circuit of the meter in a continual mode; one of the transducers emits an ultrasonic signal, and the other receiving transducer provides the output signals. The received output signals are then emitted and amplified by the flowmeter electronics. The Doppler frequency shift signal is the processed output signal obtained using a data acquisition card (NI-PCI-6040E) and a LabVIEW program which controlled the 10kHz sampling frequency for every 0.1s for each dataset.

The relationship between the Doppler shift Fd and the velocity of the scatters is described as (Sanderson & Yeung 2002):

$$Fd=2ft\ v/c\ \cos\Theta$$

where Fd is the Doppler frequency shift, ft is the transmitted ultrasound frequency, v is the flow velocity average, and Θ is the angle between the flow velocity and the ultrasound beam.

7.4 Slug control configuration

The experiment was conducted at Cranfield University Oil and Gas Centre on a 2-inch two-phase flow S-shaped riser. A clamp-on non-invasive Doppler ultrasound transducer with an excitation voltage of ± 10V operating at the 500 kHz frequency was attached at the topside of the S-shaped riser. The ultrasound beam incident angle was 58^0 with respect to the flow direction of the S-shaped riser. A coupling agent (gel) was applied between the pipe wall and the Doppler transducer for ease of ultrasound energy transmission. The electronics of the

Doppler ultrasound flow meter (DFM-2, United Automation Ltd, Southport, UK) were adapted to record the voltage signals of the Doppler frequency shift for further analysis. The LabVIEW data acquisition system at 10 kHz sampling frequency was used to acquire the Doppler frequency shift voltage signals which were further analysed using spectral analysis. The air used was supplied from a bank of two compressors connected in parallel. When both compressors are run in parallel, a maximum air flow rate of 1410m^3/hr Free Air Delivery (FAD) at 7 bar can be supplied. The air from the two compressors accumulates in an 8m^3 capacity receiver to reduce the pressure fluctuation from the compressor. Air from the receiver passes through a bank of three filters (coarse, medium, fine) and then through a cooler where debris and condensates present in the air are stripped from the air before it enters the flow meters. The air flow rate was metered by a bank of two Rosemount mass probar flow meters of 1⁄2'' and 1'' diameter respectively. The water flow rate was supplied from a 12.5m^3 capacity water tank. The water was supplied into the flow loop by two multistage Grundfos CR90-5 pumps. The water pump has a duty of 100m^3/hr at 10 barg. The speed control is achieved using frequency variables inverters. The water pumps are operated remotely using DeltaV. The water flow rate was metered by a 1'' Rosemount 8742 magnetic flow meter (up to 7.36 l/s) and 3'' Foxboro CFT50 Coriolis meter (up to 30kg/s).

After the experiment, air and water were gravity separated in an 11.12m^3 horizontal three-phase separator. After the separation in the three-phase separator and cleaning, the air is exhausted into the atmosphere while water from the three-phase separator enters its 1.6m^3 coalescers, where the water is further cleaned before returning to the storage tank.

The 2-inch flow loop test facility used in this experiment has 54.8mm internal diameter, 40m length, and 00 inclinations. The 2-inch flow loop test section has a transparent pipe for flow regime observation. The continuous wave ultrasonic Doppler measurement system was mounted on the test section at the topside facility.

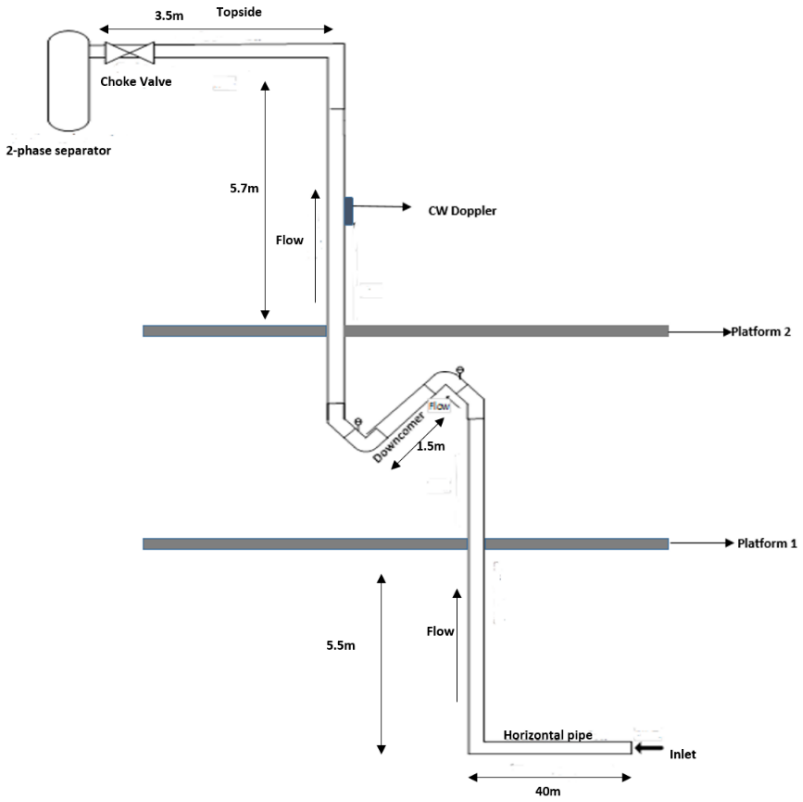

Figure 7-1: Schematic diagram of 2" S-shaped riser

7.5 Results and discussions

7.5.1 Experimental test matrix

The test matrix for the two-phase 2-inch S-shaped riser tests is the same as Chapter 6 using the riser test facility described in Chapter 3. The test matrix covered a wide range of flow regimes such as slug, churn, bubbly and annular flow but concentrated more on collecting data under the severe slugging regions.

7.5.2 Description of different flow regimes observed

The flow regime map depicting all the points tested is presented in Figure 6-3. Different types of flow regimes were observed.

7.5.3 **Slug control using ultrasonic measurements**

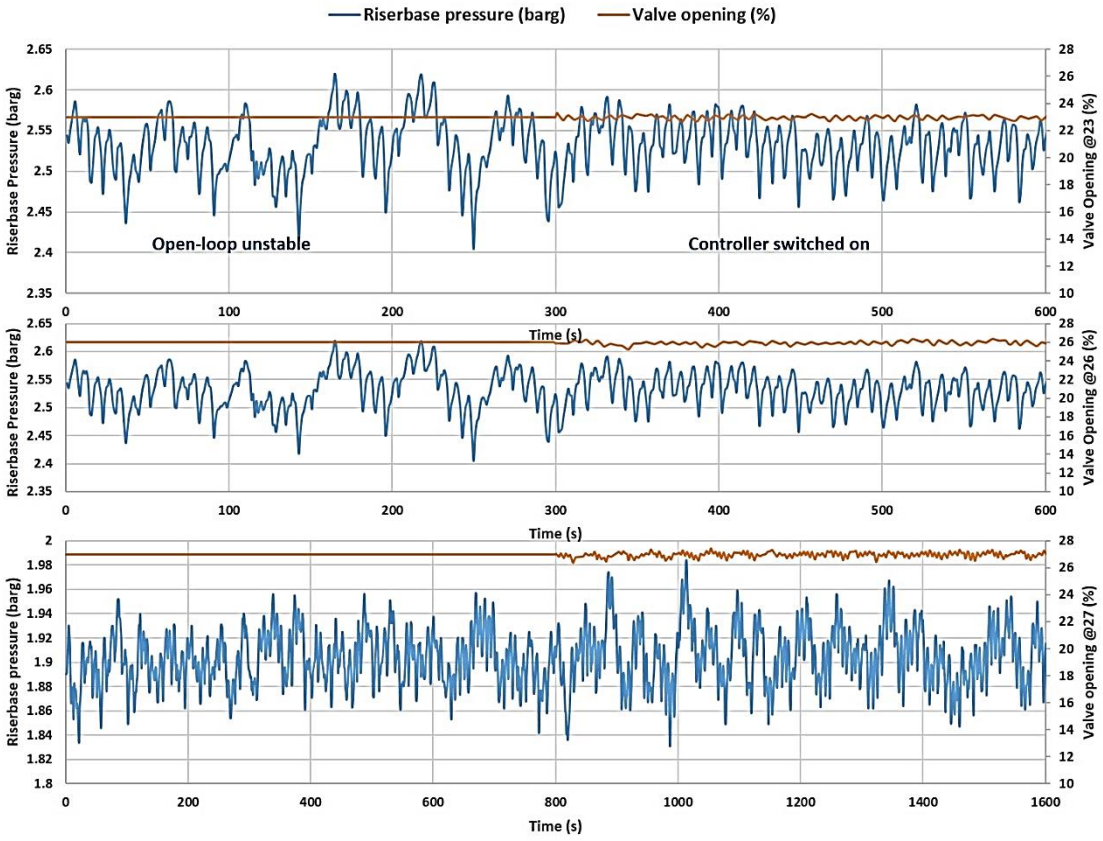

Figure 7-2: Riserbase pressure response with their equivalent valve opening using velocity measurements from CW Doppler ultrasound

As illustrated in Figure 7-2, slug flow stability using the velocity measured from CW Doppler was able to stabilise the flow from a valve opening of 23% (top plot) to 26% (middle plot). This indicates successful control performance given that using manual choking, the flow was stabilised at a 21% valve opening.

It is noteworthy to know that the work in this chapter also adopted the same control method used in chapter six. The only difference is that ultrasonic signals were used as the only control variable to control the choke valve opening.

7.5.4 Comparison of slug control using riserbase pressure to control using ultrasonic measurement

The slug control systems using CWDU measurements can achieve the same performance as using the riser base pressure, this is illustrated in Figure 7-3.

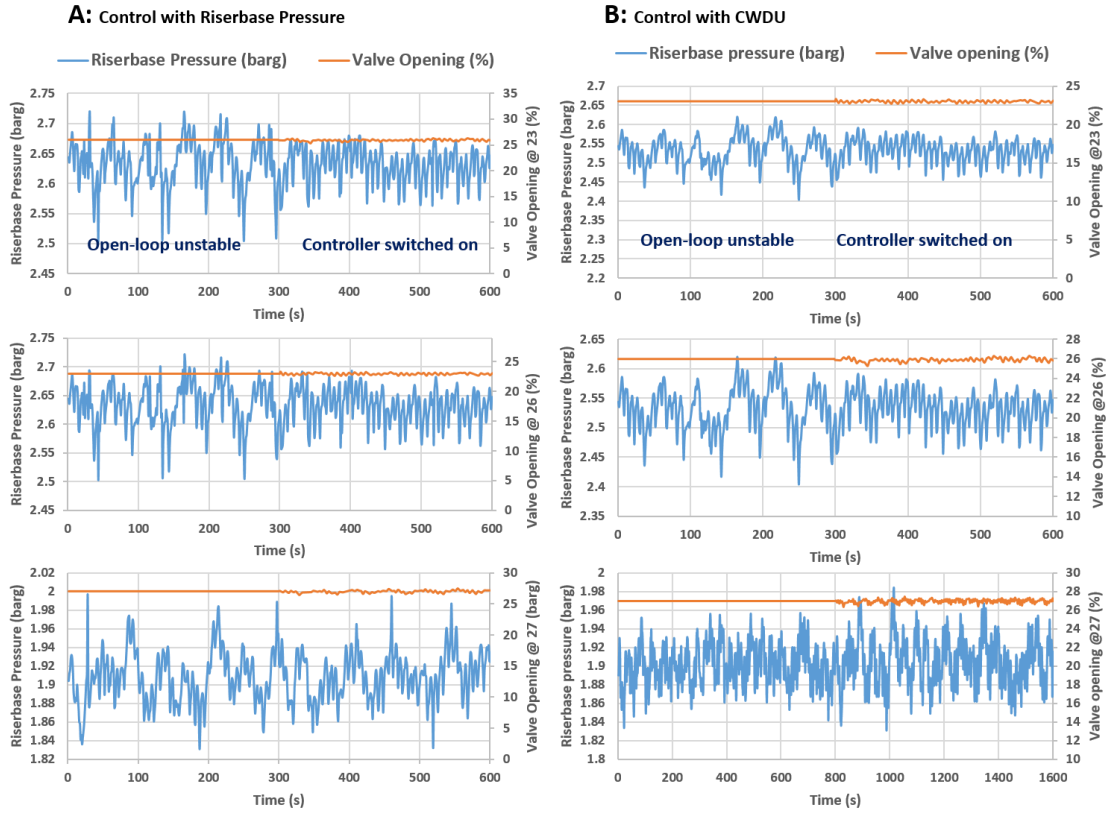

Figure 7-3: Comparisons of slug control using riser base pressure to control using CWDU

Figure 7-3 demonstrates that slug flow stability using either riser base pressure or CWDU measurement stabilised the flow from valve opening of 23% open loop unstable to 26%. Figure 7-3a (top plot) indicates that the riser system for both systems (either the system using riser base pressure measurement or CWDU measurement) was unstable at valve opening of 23 % from 0 seconds to 299 seconds until the controller was switched on at 300 seconds, which stabilised the system. The same process happened in Figure 7-3b (middle plot), but in Figure 7-3c (bottom plot), the system was unstable for the two slug control system (slug control system using riser base pressure and the one using CWDU) even when

the controller was switched on. The two slug control system recorded a 3% reduction in the riser base pressure with a 23% increase in hydrocarbon production rate. Hence, this demonstrates a great potential of using CWDU measurement in industrial practice. The lower pressure and larger choke valve opening is beneficial for larger hydrocarbon production.

7.6 **Summary**

The offshore multiphase flow pipeline-riser platforms are facing severe challenges instigated by slugging flow, an uneven flow regime condition where the pressure, temperature, and flow rate fluctuates in the pipelines. One of the regular severe slugging conditions is incited by vertical risers or wells causing the build-up of pressure, and initiating flow and pressure fluctuations. There are several negative effects of severe slugging which have triggered so much research, investments, and effort towards minimising or eliminating the riser slugging flow. Several active slugging control techniques have been examined for decades in the oil and gas industries, but many of these techniques still carry the risk of limiting hydrocarbon production due to inappropriate over choking. Additional challenges facing active slug control is that some systems depend on subsea measurements such as riser base pressure, and most of these subsea measurements are expensive and difficult to maintain, are seldom available, and can be unreliable. To efficiently control slugging, there is the need to find reliable, robust, and efficient measurements which are more sensitive to slugging flow for control, which motivates this work. Although slugging control is a well-defined phenomenon that has been examined for many decades, some of the existing techniques still have issues. It is also predicted that slugging flow problems will still be on the rise for years due to the use of longer risers in deep-water productions and explorations. Hence, slug control and mitigation is still an ongoing research topic.

A non-intrusive and non-radioactive topside measurement, the CW ultrasonic Doppler sensor was studied for active slug control. Preliminary results indicate that the control system can eliminate slug flow for up to a 26% valve opening with

riser base pressure at 2.6 bar, which is much lower than the critical pressure of 3.8 bar under manual choking. Similar technology has never been reported in the open literature. Hence, it is patentable.

CHAPTER EIGHT

8 Taming Severe Slug Flow in a U-shaped Riser System

8.1 Introduction

Severe slug flow is an operational problem associated with offshore gas and oil production systems, especially for brown oil fields or aging oil fields. The irregular or varying liquid and gas flow in pipeline-riser systems is a serious problem for the gas and oil industry. An efficient and effective way to mitigate or control slug flow is important (Zhou et al., 2018).

Unstable slug flow behaviour in multiphase flow pipelines has had a significant negative operational impact on offshore production platforms. Slug flow can cause the shutdown of a plant. The rapid and large flow fluctuations can reduce the compression and separation unit's operating capacity and can cause undesired flaring (Havre, Stornes and Stray, 2000).

Pipeline choking is one of the most effective approaches to eliminate severe slugging in oil and gas production systems. However, due to the restriction caused by choking, oil production can be significantly reduced (Havre, Stornes and Stray, 2000).

Active control has proven to be an efficient technique to mitigate slug flow problems (Godhavn, Strand and Gunleiv, 2005). In the active control, a topside choke valve is usually the manipulated variable which controls the riser-base pressure at a stipulated set point. The drawback of this method is the ready availability of the measurement at the riser-base and the rapid increase in capital and operational cost because of its application on the seabed.

Sivertsen et al. (2010), designed a controller-based only on topside pressure measurement for slug flow. During the experiment conducted in a medium-scale rig riser, it was observed that achieving stability with this type of controller is not

possible. Another approach was the use of measurement of topside density, which was observed to be noisy if applied directly to the control (Storkaas, 2005).

Cao et al. (2010) invented a novel severe slug suppression technique called Inferential Slug Control (ISC). The ISC address the associated slugging issues using topside measurement signals as the only input parameters applied for the controller owing to the fact that a specific measurement may not be available on all systems and the fact that a single measurement may not be sensitive enough to adjust the choke valve accurately. This novel technique suppressed severe slug flow conditions for a certain set of operating conditions in an unstable region. The drawback with this technique is the implementation of gamma measurement, which is radioactive and hazardous to health. However, to improve the performance of ISC, new measurements that will be more sensitive to slugging flow are sought. In this work, the feasibility of using differential pressure from the venturi inlet to the throat and liquid velocity measurement for slug control is studied. These measurements are implemented in the ISC cascade controller for slug flow control. This contributes to objectives 3 and 4 given in Section 1.6.

This chapter is organised as follows. Section 8.2 presents the methodology for the work. Section 8.3 described the controller design used for the work. In Section 8.4, the simulation results and discussion are presented, and finally, the summary of the chapter is drawn in Section 8.5.

8.2 Methodology

8.2.1 Case study for slug control carried out using OLGA

8.2.1.1 Pipeline riser configuration

The pipeline profile used in this model to investigate the slugging system is a U-shape riser, which is typically sectioned into three sections namely: a down-comer pipeline with an inlet source, a horizontal section, and a vertical riser pipeline system beyond which the topside test section is located.

The pipeline model is from the Chevron Energy Technology Company; the pipeline model is a satellite field that is made up of two different U-shaped risers combined at their outlets by a horizontal pipe before reaching the topside section. For privacy, the field is called B-J1. This field is equipped with a venturi device, separator, and a choke valve to aid this investigation.

Based on the OLGA regulations about the ratio between two pipelines, pipes were sectioned to avoid a ratio higher than 2 or lower than 0.5. That is, the section was such that two pipes adjacent to each other are not shorter than the other or more than two times longer. A single branch model (two nodes and a flowpath) was developed for the case under investigation.

Table 8-1 presents the U-shape riser pipeline geometry data used in this work (Tandoh, Cao and Avila, 2016). The geometry is shown in Figure 8-1.

Table 8-1: B-J1 U-shape pipeline geometry data

Pipe	X (m)	Y (m)	#Sections	Length of section (m)	Diameter	Roughness
1	45.108	0	7	7(6.44403)	0.2032	0.00019
2	56.674	2.74307	2	2(5.94331)	0.2032	0.00019
3	92.334	50.2895	10	10(5.94331)	0.2794	0.00019
4	1924.09	48.7658	17	9.8, 17.5, 32, 60, 115, 210, 128, 136, 150, 2:290, 190, 100, 52, 28, 15, 8.45859	0.2794	0.00019
5	1939.11	3.04785	5	5(5.99411)	0.2032	0.00019
6	2011.35	3.04785	12	12(6.01951)	0.2032	0.00019

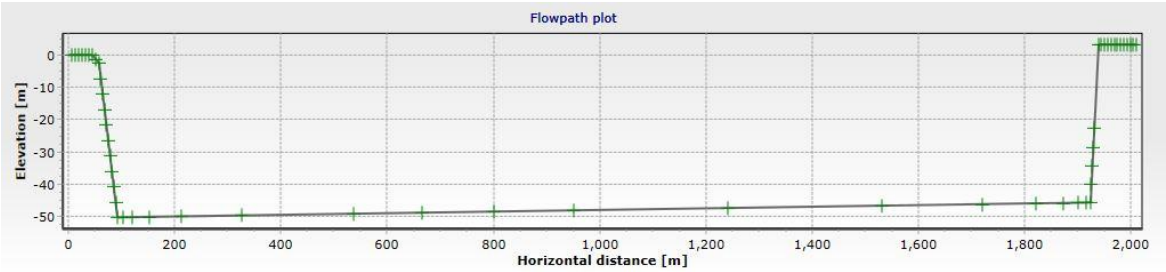

Figure 8-1: B-J1 U-Shaped riser flow-path plot

The inlet down-comer is 50.29 m long, and the riser section is 51.81m long. It has a horizontal section, which is 2011.35 m in length. The pipeline system has a uniformly distributed diameter (0.288951 m) across.

8.2.2 **Flow Conditions and Parameters**

The U-shape riser model developed was operated under the flow conditions as indicated in Table 8-2. This is because, at the operating conditions indicated in Table 8-2, the flow is unstable with large pressure and flow variations. This instability is because of the flow of gravity and the compressibility of the gas. The compressibility of gas in a system can either have a negative effect (instability) or positive effect (stability) because of these factors.

Table 8-2: the Case study of a typical slug flow operating condition

Operating Parameters (Initial Condition)						
Source Temp. (^{O}C)	Ambient Temp. (^{O}C)	U-value (Wat/(m*K))	Inlet Temp. (^{O}C)	Outlet Temp. (^{O}C)	Inlet Pressure (bar)	Outlet Pressure (bar)
44.44	23.89	69.18	47.22	47.22	12.41	12.41
Operating Conditions						
Total Mass Flow, kg/s	Gas Mass Fraction	Oil Mass Fraction	Water Mass Fraction	Inlet Temp. (^{O}C)	Outlet Temp. (^{O}C)	Outlet Pressure (bar)
11	0.02	0.49	0.49	44.4	23.89	10.687

8.3 **The Controller Design**

An active control system as a technique for slug mitigation operates at a higher valve opening than manual choking. After the establishment of the stability point in the open-loop system, the next objective is to control the system at a higher choke valve opening relative to that in an open-loop system. This would serve as a base case to establish the effects of each measurement on the system. Riser base pressure shows the pipeline system throughput while the pressure gradient connotes the stability of the system. Stability is estimated by $DP/dQ > 0$ whereas $DP/dQ < 0$ is an unstable flow.

The inferential slug controller (ISC) was designed to suppress the system at a choke valve opening of 5%. The controller parameters were designed based on a methodology described in Tandoh et al., (2016). From the work of Tandoh et al., (2016), the minimum gain K of the ISC for any preferred pressure drop gradient at a particular choke valve opening could be estimated using the mathematical expression below in the quest to suppress the slug flow at a higher choke valve opening.

$$\frac{d\Delta P_v}{dQ_g} = \frac{2aQ_g}{u^2} + \frac{2aQ^2{}_g}{u^3} K\ [W^T \frac{dY}{dQ_g}] \qquad 8\text{-}1$$

where '*a'* is a constant associated with valve coefficient, mixture density, and the given reference liquid flow rate; Q_g is the gas flow rate, and u is the valve opening ranging from 0 to 1; $K = du/dc$ is the controller gain to be designed, and $W^T\, dY/dQ_g$ is estimated from the weighted deviations in measurements resulting from the perturbation of Q_g.

Since the ISC can employ various signals from the topside of the riser system, for this investigation, three measurement signals were deployed. The measurements investigated are riser top pressure (PT), liquid velocity (UL), and differential pressure from the venturi (DPV) due to the ready availability of these signals, the signal sensitivity to noise, and accuracy. For the inferential slug controller (ISC), the measurement signal weights were deployed to estimate the

controller gains in a cascade configuration. Data from a simulation run on OLGA were analysed using various expressions for designing an ISC discussed in Cao et al. (2010).

8.4 Simulation results and discussion

8.4.1 U-shaped riser simulation results

8.4.1.1 Manual choking (System stability)

Bifurcation analysis is a study of assessing the stability of a system at a constant flow rate, Q for varying choke valve openings. This study aims to determine the bifurcation point which is the maximum valve opening at which the flow in the pipeline system becomes stable in an open loop. This translates to a situation for which a system loses its stability as a result of an increase in the independent variable (valve opening). In the controller design process, the first step is to establish the system bifurcation point. This serves as the reference point for the controller to stabilise flow in an open-loop unstable region.

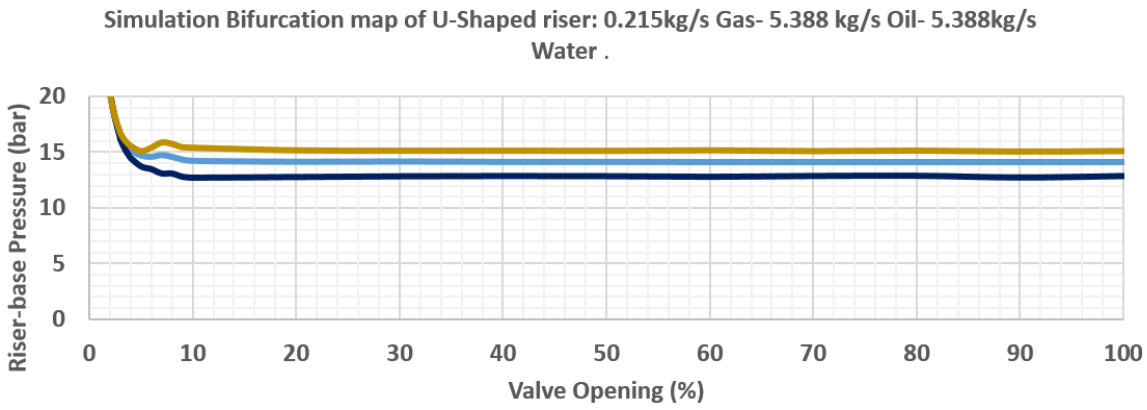

Figure 8-2: Simulation Bifurcation map of U-Shaped riser: 0.215kg/s Gas- 5.388 kg/s Oil- 5.388kg/s Water

Figure 8-2 presents the bifurcation map for the boundary condition presented in Table 8-2 from which the system stability was obtained at a valve opening of 3%, which corresponds to a pressure of 17.8 bar. From the results of the bifurcation

map, stabilising the system at the open-loop unstable region where u >3% will be targeted to obtain the desired stable non-oscillatory flow regime.

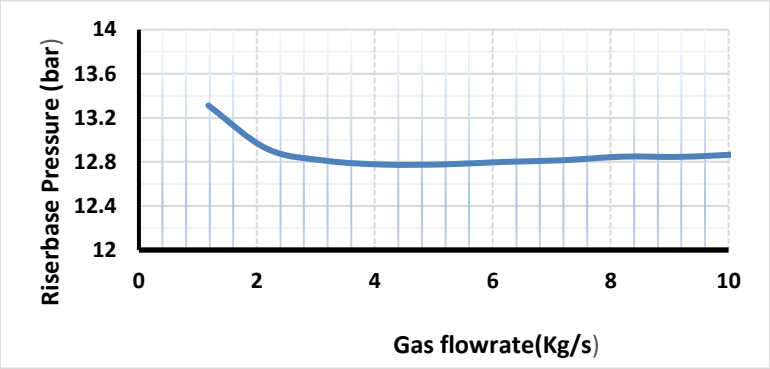

Figure 8-3: Riser-base pressure as a function of gas flow rate

Figure 8-3 describes the overall relationship that governs riser-base pressure and the gas flow rate for the constant liquid flow rate of 10.78kg/s. If the flow rate of the gas is low, which entails low friction loss, any upsurge in the flow rate of gas will cause an increase in the gas/liquid ratio (GLR) in the riser and a decrease in riser-base pressure. On the contrary, as indicated in Figure 8-3 by the vertical line on the right-hand side, if the flow rate of the gas is great enough, the friction loss will become dominant; thus, an upsurge in the flow rate of gas will give rise to friction loss, which results in an increase in the riser-based pressure.

The riser-base pressure states the throughput of the pipeline whereas system stability is dictated by the pressure gradient.

The lowest point on the curve in Figure 8-3 is the minimum flow rate of gas that could be used to stabilise the system for the given flow conditions.

After 1% gas flow rate perturbation at a constant liquid flow rate of 10.78kg/s, the slope of the riser-base pressure against the gas flow rate is -6 bar/kg/s^{-1}. This demonstrates that the system is unstable because of the negative slope obtained, and therefore a minimum slope of 6 bar/kg/s^{-1} is needed to stabilise the system.

In this work, we targeted system stability at a 5% choke valve opening. In an open-loop unstable system, this gives a gradient of -3.35 bar/kgs^{-1} after 1% gas flow-rate perturbation. However, the gradient obtained is less than that required

for system stability; 6 bar/kg/s^{-1} is estimated from the slope needed for the system stability at 100% valve opening at the same flow condition. The extra gradient is required via a control to achieve this and thereby compensate for the gradient loss because of the valve opening increment.

8.4.2 **Inferential Slug Controller**

Cao, et al, (2010) invented and patented Inferential Slug Control (ISC) in 2010. Inferential slug controller uses the combination of all the available topside measurements through algebraic scheming. ISC is superior to other standard controllers that use subsea pressure measurements for control because ISC uses only the topside measurements for control purposes, making it cost effective.

In 2014, Kadulski applied proportional controllers to design a cascade configuration of ISC to allow its easy implementation in an OLGA simulator. The simple algebraic calculation was applied to acquire a single variable from all the available topside measurements to make it more sensitive to slugging flow. The control law for the determination of ISC valve opening is given as

$$V = V_o + K(W^T Y - R) \qquad 8\text{-}2$$

where V_o is the valve set point which is predetermined and manually set to a position where the flow becomes stable or within an acceptable range, K is the control gain, $W = [k_1, k_{2,\ldots\ldots,} k_{n-1,} k_n]T$ is the measurement weights, $Y = [y_1, y_{2,\ldots\ldots,} y_{n-1,} y_n]$ is the vector of measurements, $W^T Y$ is the control variable, n is the number of measurements, and R is the control variable set point.

The modelled ISC in a cascade configuration is presented in Figure 8-4.

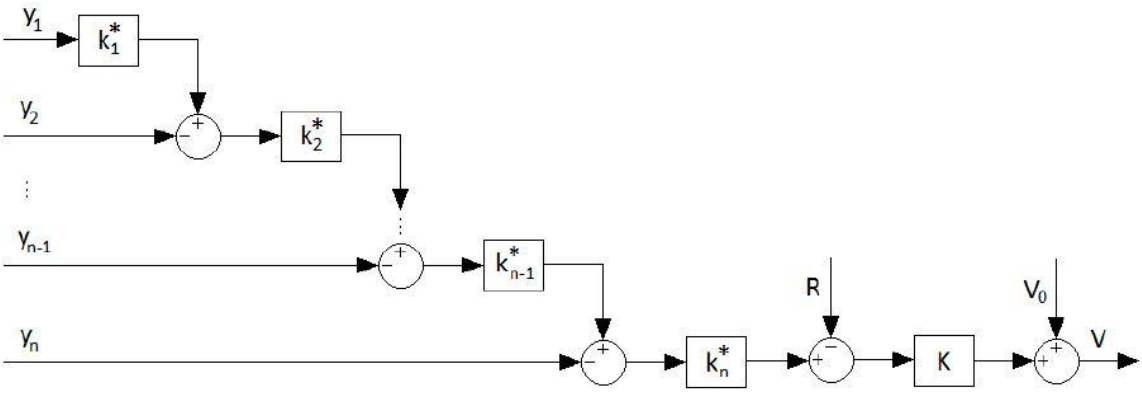

Figure 8-4: Block Diagram of the Inferential Slug Control System in a cascade configuration

In order to properly deploy ISC in a cascade form, control law derivation is needed. In this work, three measurements are used.

From Figure 8-4, using equation 8-2, we have

$$\mathrm{V} = \mathrm{V}_0 + \mathrm{k}\left[\left(-\mathrm{k}_{n+1}\left(\frac{\mathrm{k}_n}{\mathrm{k}_{n+1}}\left(\frac{\mathrm{k}_{n-1}}{\mathrm{k}_n}\ (\ldots\left(-\frac{\mathrm{k}_1}{\mathrm{k}_2}\mathrm{y}_1 - \mathrm{y}_2\right)\ldots\right) - \mathrm{y}_{n-1}\right) - \mathrm{y}_n\right) - \mathrm{y}_{n+1}\right) - \mathrm{R}\right].$$

8-3

Using three signals, equation 8-3 becomes

$$V = V_0 + k\ [(k_1 y_1 + k_2 y_2 + k_3 y_3) - R]\ . \qquad 8\text{-}4$$

$$V = V_0 + k\ [(\ -k_3\ (\frac{k_2}{k_3}(-\ \frac{k_1}{k_2} y_1 - y_2) - y_3 - R]\ . \qquad 8\text{-}5$$

$$V = V_0 + k\ [(k_C\ (k_B\ (k_A y_1 - y_2) - y_3) - R]. \qquad 8\text{-}6$$

$$k_A = -\frac{k_1}{k_2}, = -\frac{k_2}{k_3}\ , k_C = -k_3 \qquad 8\text{-}7$$

Equation 8-6, which is the new control law, is applied to calculate the cascade controller gains using weights from the ISC simulation under standard conditions. The three measurement signals used in this work are riser top pressure (PT), liquid velocity (UL), and the differential pressure (DPV).

The MAX-CHANGE, MAX-INPUT, and MIN-INPUT under the PID controller except for the one operating the valve directly were set at 100000, -100000 and

100000, respectively and 1, 0, and 0.05 for the one controlling the valve directly. Similarly, the keyword STROKE-TIME was set as 0 and 20 s for the controller controlling the valve directly. Figure 8-5 presents the OLGA interface pictorial view of the ISC implemented on a U-shape riser.

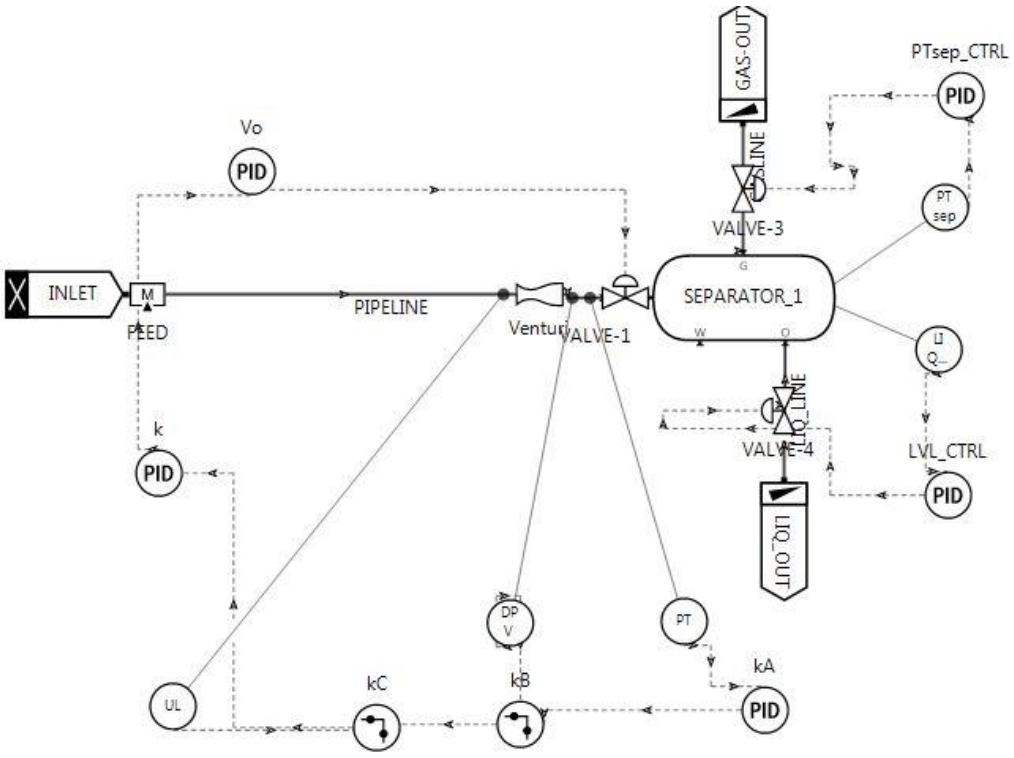

Figure 8-5: The OLGA interface pictorial view of the ISC implemented on a U-shaped riser

8.4.3 Controller Gains

The instability in the U-shaped riser was examined numerically with the OLGA simulator. The three measurements used for this study are riser outlet pressure (PT), Liquid velocity (UL), and venturi differential pressure measurement (DPV).

To get the cascade controller gain of k_A ,k_B, and k_C, it is important to first calculate the weight of the variables measured. Cao et al. (2011) proposed the use of Principal Component Analysis (PCA) as a possible method to achieve it.

To acquire the measurement signals from the simulated model, the valve position was adjusted to a 5% choke valve opening where the pipeline-riser system is operating under the severe slugging regime. The trends of liquid velocity, venturi differential pressure, and topside riser pressure consisting of the slug cycles were obtained and sent to MATLAB for further analysis.

The MATLAB script was developed to perform the following:

I. To normalise the measurement signals.
II. To perform the PCA of the measurement signals using the princomp MATLAB function.
III. To extract the PC1 from the analysis and then divide measurement coefficients by the corresponding signal's amplitude. The measurement weight vector is the obtained vector of the coefficient.

When the PCA is applied to the slugging data set containing all the topside measurements being considered, the First Principal Component (PC1) can be obtained as the linear combination of all the topside measurements that is more sensitive to severe slugging flow. However, PC1 is a suitable control variable for severe slug flow control (Cao, Lao and Yeung, 2013).

MATLAB code developed Figure 8-5 to extract the features of principal components from the input parameters is listed in Appendix C. It normalises the input variables and determines the appropriate eigenvector.

The coefficients of the ISC measurement weights for PT, UL, and DPV correspond to -0.5601, 0.5884, and 0.9519, respectively.

The deviation in the vector of measurement signals mathematically represented by dY/dQ_g for various measurement signals from a slight perturbation in the gas flow rate of 0.22kg/s, for Figure 8-5, PT, UL, and DPV correspond to 0.00824, 0.134, and 0.0045.

The weighted deviations in the measurements as a result of a 1% increment in gas flow rate, Q_g gives 0.0785.

The cascade controller gain calculated using PCA is presented in Table 8-3.

Table 8-3: The cascade controller gains

Cascade Controller gain (PCA)	
Cascade_1, kA=k_1/k_2	0.9519
Cascade_2, kB = k_2/k_3	1.0090
Cascade_3, kC = $-k_4$	-0.5832
K	0.0459

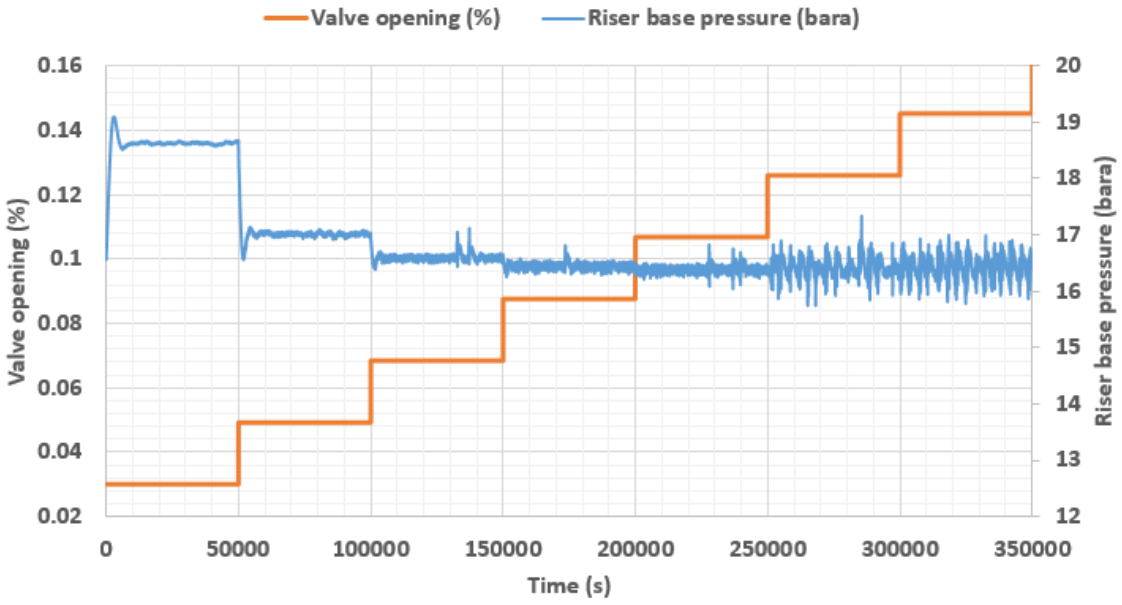

Figure 8-6: Riser base pressure response with their corresponding valve opening

The performance of the controller was assessed by the measure of valve opening at which the flow stability can no longer be maintained. This is because producing hydrocarbon at an increased valve opening entails increased production and less

friction loss. Being able to increase the choke valve opening while still maintaining flow stability leads to great economic gains. Having deployed the ISC in action with a 1% stepwise increment in the valve opening resulted in the riser-base pressure response presented in Figure 8-6. Figure 8-6 indicates that the ISC using PT, UL, and DPV was able to stabilise the flow at an 8.41% increase in choke valve opening, thus from a 3% to approximately 11.41% choke valve opening. The backpressure was further reduced by 1 bar.

8.5 Summary

The simulation results using the new multiphase measurements implemented in cascade ISC were successful. The controller stabilised the flow far into an unstable region. The flow was stabilised at an 8.55% increase in a choke valve opening from 3% to approximately 11.55% choke valve opening. This leads to an increase in oil production rate compared with riser based pressure control or with standard manual choking. However, the negative impact of slugging control on production is minimised.

CHAPTER NINE

9 Conclusion and further work

9.1 Conclusion

The conclusion from this research work is given in this section. This work has introduced new multiphase flow measurements for slug flow control with a focus on achieving stability while maximising production rate.

In chapter two, a literature review of all the relevant slug flow control methods ranging from its applications, benefits, and limitations is discussed. The lack of appropriate knowledge of the performance of existing slug flow control systems is considered a challenge to its further improvement or development. Further research is still needed for more exposure, understanding, and knowledge of slug flow mitigation and control.

The accurate prediction of flow regimes is vital for the analysis of behaviour and operation of gas/liquid two-phase systems in industrial processes. Chapter four and chapter five investigate the feasibility of a non-radioactive and non-intrusive method for the objective identification of two-phase gas/liquid flow regimes using a Doppler ultrasonic sensor and machine learning approaches. The two approaches adopted in Chapter 4 and Chapter 5 fulfill the thesis's second objective which aims to determine the applicability of CWDU for flow regime identification. The experimental data is acquired from a 16.2-m long S-shaped riser connected to a 40-m horizontal pipe with an internal diameter of 50.4 mm. The tests cover the bubbly, slug, churn and annular flow regimes.

In chapter four, the power spectral density (PSD) method is applied to the flow modulated ultrasound signals in order to extract the frequency-domain features of the two-phase flow. Principal Component Analysis (PCA) is then used to

reduce the dimensionality of the data to enable visualisation in the form of a virtual flow regime map. Finally, a support vector machine (SVM) is deployed to develop an objective classifier in the reduced space. The classifier attained 85.7% accuracy on training samples and 84.6% accuracy on test samples. The approach has demonstrated the success of the ultrasound sensor, PCA-SVM, and virtual flow regime maps for objective two-phase flow regime classification on pipeline-riser systems, which is beneficial to operators in industrial practice. The use of a non-radioactive and non-intrusive sensor also makes it more favourable than other existing techniques.

In chapter five, an approach that classifies the flow regime by means of a neural net operating on extracted features from the Doppler ultrasonic signals of the flow using either Power Spectral Density (PSD) or Discrete Wavelet Transform (DWT) is proposed. The features extracted are categorised into one of the four flow regime classes: the annular, churn, slug and bubbly flow regimes. The scheme is tested on signals from an experimental facility. The neural network used in this work is a feedforward network with 20 hidden neurons. The network has four output neurons, which correspond to the element number in the target vector. When PSD features are applied, the network has 13 inputs. However, when features from DWT are applied, the network has 40 inputs. Using the PSD features, the neural network classifier misclassified three out of 31 test datasets and was 90.3% accurate, while only one dataset was misclassified with the DWT features, yielding an accuracy of 95.8%, thereby establishing the superiority of the DWT in feature extraction of flow regime classification. This approach demonstrates the application of a neural network and DWT for flow regime classification in industrial applications, using a clamp-on Doppler ultrasonic sensor. The scheme has significant advantages over other techniques in that it uses a non-radioactive and non-intrusive sensor. This appears to be the first known successful attempt for the objective identification of gas-liquid flow regimes in an S-shaped riser using CWDU and a neural network.

Riser slug flow poses a significant challenge to offshore oil production systems, most especially for oil fields in their later life. Active control of slugging through

choking has been proven a practical approach in eliminating riser slug flow in oil production pipeline-riser systems. However, existing conventional active slug control systems may reduce oil production significantly due to excessive over choking. Again, some of the existing active slug flow control systems rely on seabed measurements, which are difficult to maintain, costly to install, unreliable, and seldom readily available. New measurements for slug control were investigated in chapter six and chapter seven.

Chapter six is an experimental investigation of the feasibility of active riser slug control by taking topside differential pressure measurements from the inlet of the venturi flow meter to the throat. Experimental results indicate that under active slug flow control, the system was able to eliminate slug flow at a higher valve opening compared to manual choking. A valve opening of 24% with riser base pressure at 2.85 bar from open-loop unstable of 23% was recorded, which is superior to manual choking, which maintained flow stability up to 21% valve opening with riser base pressure of 3.8 bar. Chapter six fulfilled the thesis's fourth objective which aims to control slug flow while maximizing hydrocarbon production through venturi measurements based active slug control. This slug control approach was successful and very promising for industrial applications.

Chapter seven discusses the effort to control the riser slug flow using ultrasonic measurements. The CWDU system was developed and used for active slug flow control in order to phase out the use of Gamma densitometry which is radioactive and hazardous to human health. Moreso, it can replace the use of subsea riser base pressure which is not reliable and expensive to maintain. Hence, this fulfills the thesis's first and third objective which was to develop the CWDU system for active slug flow control. The controller was able to stabilise the flow with acceptable control performance while maximising oil production. This technique has never been reported in the open literature and hence is patentable.

Finally, the work done using the new multiphase flow measurements in a cascade controller configuration was successful as presented in chapter eight. Chapter eight contributes to the actualisation of the thesis's fourth objective by deploying

venturi measurements in a cascade controller for active control of severe slug flow in a U-shaped pipeline-riser system. Many control methods use several measurement combinations for active slug flow control without considering the fact that each measurement has its own uncertainty and also contributes to the control systems' overall performance. Hence, the fewer the number of multiphase flow measurements used the better the control system performance.

9.2 **Further work**

This section introduces areas for possible further research work based on the findings from this work. Although this work has presented some specific methods for flow recognition and slug flow control using new approaches, there is still the need for further research and improvement.

Currently, the CWDU has been developed and used experimentally for riser slug flow control in a 2-inch S-shaped riser system; more CWDU approaches to slug flow control can be further investigated using other types of riser configurations such as U-shaped risers, horizontal risers, vertical risers, and catenary risers.

Since CWDU and venturi measurement for slug control were only tested experimentally on two-phase air-water flow, further work is needed to test this approach on a three-phase air-oil-water flow on different pipeline-riser configurations. This is just to further validate the proposed active slug control method.

Continuous Wave Doppler Ultrasound (CWDU) techniques for slug control can also be tested using theoretical models for further improvement.
The CWDU and venturi measurements can be linked for slug control and tested experimentally or by using the OLGA simulator. One of the reasons why the combination of the CWDU and venturi measurements could be a good approach for active control of slug flow is because no measurement is 100% reliable.

Further work is required in the deployment of non-intrusive Doppler ultrasonic sensors for the objective classification of oil-water two-phase flow regimes. Furthermore, a study is required to investigate the feasibility of combining a neural network with fuzzy logic for online flow monitoring and control. The neural net will be used to classify the different flow regimes in the pipeline and then feed the output into the fuzzy logic control system. Basically, the perception is that slug flow control is a mature and unchanging technological area of research. There are still industrial applications, for example, deep waters or oil brownfields that desire faster response to unwanted flow disturbance with minimal undershoot and overshoot when the setpoint varies. The conventional PID control approach cannot meet all these requirements.

Of the possible approaches for developing highly advanced active slug flow controllers, two seem promising. One approach is improving the standard PID controllers by adding extra features that will make the PID tuning easier and more reliable and the second approach is the application of a fuzzy logic control system.

Implementation of the enhanced PID control system could be very challenging especially a situation where the auto-tuning method is desired to aid in finding the PID optimal control constants. Moreover, the PID control theory is already known and widely applied in many industrial control applications.

On the contrary, the Fuzzy Logic (FL) control system can achieve the same quality control performance with lesser complexity. The fuzzy logic control system is relatively new and it gives room for more improvements. The schematic diagram of the idea is shown in Appendix D.

References

Abbagoni, B.M. and Hoi, Y. (2016) ‘Non-invasive classification of gas – liquid two-phase horizontal flow regimes using ultrasonic Doppler sensor and neural network’, *Measurement Science and Technology*, 27(8), pp. 1–38.

Adedigba, A.G. (2007) *Two-phase flow of gas-liquid mixtures in horizontal helical pipes*. Cranfield University.

Al-naser, M., Elshafei, M. and Al-sarkhi, A. (2016) ‘Artificial neural network application for multiphase flow patterns detection : A new approach’, *Journal of Petroleum Science and Engineering*, 145, pp. 548–564.

Almeida, A., G. (1999a) ‘Venturi for severe slugging elimination’, *The 9th International Conference on Multiphase Production*. Cannes, France, pp. 149–158.

Almeida, A., G. (1999b) *Device and method for eliminating severe slugging in multiphase-stream flow lines*.

Alssayh, M., Addali, A., Mba, D. and Dao, T. (2013) ‘Identification of two phase flow regime using acoustic emission technology’, *International Journal of Mechanical and Production Engineering*, 1(6), pp. 27–31.

Arrieta, O., Vilanova, R. and Balaguer, P. (2008) ‘Procedure for cascade control systems design: Choice of suitable PID tunings’, *International Journal of Computers, Communications and Control*, 3(3), pp. 235–248.

Awadalla, M., Yousef, H., Al-hinai, A. and Al-shidani, A. (2016) ‘Prediction of oil well flowing bottom-hole pressure in petroleum fields’, *6th International Conference on Industrial Engineering and Operations Management*. Kuala Lumpur, Malaysia, pp. 3007–3017.

Baghernejad, Y., Hajidavalloo, E., Hashem Zadeh, S.M. and Behbahani-Nejad, M. (2019) ‘Effect of pipe rotation on flow pattern and pressure drop of horizontal two-phase flow’, *International Journal of Multiphase Flow*, 111, pp. 101–111.

Barnea, D. (1987) ‘A unified model for predicting flow-pattern transitions for the whole range of pipe inclinations’, *International Journal of Multiphase Flow*, 13(I), pp. 1–12.

Barnea, D., Shoham, O. and Taitel, Y. (1980) ‘Flow pattern characterization in two phase flow by electrical conductance probe’, *International Journal of Multiphase Flow*, 6(5), pp. 387–397.

Bendiksen, K.H., Maines, D., Moe, R. and Nuland, S. (2007) ‘The dynamic two-fluid model OLGA: Theory and application’, *SPE Production Engineering*, 6(02), pp. 171–180.

Bendjama, H., Idiou, D., Gherfi, K. and Laib, Y. (2015) ‘Selection of wavelet decomposition levels for vibration monitoring of rotating machinery’, *The Ninth International Conference on Advanced Engineering Computing and Applications in Sciences*. Nice, France, pp. 96–100.

Bin, S., Zhang, H., Cheng, L. and Zhao, Y. (2006) ‘Flow regime identification of gas-liquid two-phase flow based on HHT’, *Chinese J. Chem. Eng.*, 14(1), pp. 24–30.

Bisoyi, N., Gupta, H., Padhy, N.P. and Chakrapani, G.J. (2019) ‘Prediction of daily sediment discharge using a back propagation neural network training algorithm: A case study of the Narmada River, India’, *International Journal of Sediment Research*, 34(2), pp. 125–135.

Blaney, S. and Yeung, H. (2008) ‘Investigation of the exploitation of a fast-sampling single gamma densitometer and pattern recognition to resolve the superficial phase velocities and liquid phase water cut of vertically upward multiphase flows’, *Flow Measurement and Instrumentation*, 19(2), pp. 57–66.

Boe, A. (1981) ‘Severeslugging characteristics, part 1, flow regime for severe slugging’, *Presented at Special Topics in Two Phase Flow*. Trondheim, Norway.

Bordalo, S.N. and Morooka, C.K. (2018) ‘Slug flow induced oscillations on subsea petroleum pipelines’, *Journal of Petroleum Science and Engineering*, 165(August

2017), pp. 535–549.

Brasjen, B.J., Veltin, J., Delft, T.N.O. and Hansen, J.H. (2014) ‘Mitigation of terrain induced slugging using mixer devices’, *SPE Annual Technical Conference and Exhibition*. Amsterdam, The Netherlands: Society of Petroleum Engineers, p. SPE-170946-MS.

Brill, J.P., Schmidt, Z., Coberly, W.A., Herring, J.D. and Moore, D.W. (1981) ‘Analysis of two-phase tests in large-diameter flow lines in prudhoe bay field’, *Society of Petroleum Engineers Journal*, 21(03), pp. 363–378.

Cai, S., Toral, H., Qiu, J. and Archer, J. (1994) ‘Neural network based objective flow regime identification in air-water two phase flow’, *The Canadian Journal of Chemical Engineering*, 72(3), pp. 440–445.

Cao, Y., Lao, L. and Yeung, H. (2013) *Method, controller and system for controlling the slug flow of a multiphase liquid*. p., pp. 1–49.

Carvalho, T.P., Soares, F.A.A.M.N., Vita, R., Francisco, R. da P., Basto, J.P. and Alcalá, S.G.S. (2019) ‘A systematic literature review of machine learning methods applied to predictive maintenance’, *Computers & Industrial Engineering*, 137(August), p. 106024.

Chakraborty, S., Keller, E., Talley, J., Srivastav, A., Ray, A. and Kim, S. (2009) ‘Void fraction measurement in two-phase flow processes via symbolic dynamic filtering of ultrasonic signals’, *Measurement Science and Technology*, 20(2), p. 023001.

Chan, A.M.C. and Banerjee, S. (1981) ‘Design aspects of gamma densitometers for void fraction measurements in small scale two-phase flows’, *Nuclear Instruments and Methods*, 190(1), pp. 135–148.

Chan, A.M.C. and Bzovey, D. (1990) ‘Measurement of mass flux in high temperature high pressure steam-water two-phase flow using a combination of Pitot tubes and a gamma densitometer’, *Nuclear Engineering and Design*, 122(1–3), pp. 95–104.

Chaouki, J., Larachi, F. and Dudukovic, M. (1997) *Non-invasive monitoring of multiphase flows*.

Cheng, L., Ribatski, G. and Thome, J.R. (2008) 'Two-phase flow patterns and flow-pattern maps: fundamentals and applications', *Applied Mechanics Reviews*, 61(5), p. 050802.

Chivers, R.C. and Hill, C.R. (1975) 'A spectral approach to ultrasonic scattering from human tissue: methods, objectives and backscattering measurements.', *Physics in Medicine and Biology*, 20(3), pp. 799–815.

Choi, J., Pereyra, E., Sarica, C., Lee, H., Jang, I.S. and Kang, J.M. (2013) 'Development of a fast transient simulator for gas-liquid two-phase flow in pipes', *Journal of Petroleum Science and Engineering*, 102(1) Elsevier, pp. 27–35.

Cobbold, R. (1989) 'Doppler ultrasound: Physics, instrumentation, and clinical applications', *Journal of Biomedical Engineering*, 11, p. 528.

Cohen, A. and Kovačević, A.J. (1996) 'Wavelets: The mathematical background', *Proceedings of the IEEE*, 84(4), pp. 514–522.

Cortes, C. and Vapnik, V. (1995) 'Support-vector networks', *Machine Learning*, 20(3), pp. 273–297.

Courbot, A. (1996) 'Prevention of severe slugging in the Dunbar 16' multiphase pipeline', *Offshore Technology Conference*. Houston, Texas, pp. 445–452.

Cristianini, N. and Shawe-Taylor, J. (2014) *Support vector machines and other kernel-based learning methods*. Cambridge University Press.

Drahoš, J. and Čermák, J. (1989) 'Diagnostics of gas—liquid flow patterns in chemical engineering systems', *Chemical Engineering and Processing: Process Intensification*, 26(2), pp. 147–164.

Dyakowski, T. (1996) 'Process tomography applied to multi-phase flow measurement', *Measurement Science and Technology*, 7(3), pp. 343–353.

Ehinmowo, A.B. and Cao, Y. (2016) 'Stability analysis of slug flow control',

Systems Science and Control Engineering, 4(1), pp. 183–191.

Ehinmowo, A.B. and Cao, Y. (2015) 'Stabilizing slug flow at large valve opening using active feedback control', *2015 21st International Conference on Automation and Computing (ICAC)*. Glasgow, UK, pp. 1–6.

Eikrem, G.O. (2006) *Stabilization of gas-lift wells by feedback control*. Norwegian Univeristy of Science and Technology.

Eikrem, G.O., Foss, B., Imsland, L., Hu, B. and Golan, M. (2004) 'Stabilization of gas lifted wells', *IFAC Proceedings Volumes (IFAC-PapersOnline)*, 15(1), pp. 139–144.

Eken, N.A., Haandrikman, G. and Seelen, W.M.G.M. (2007) *Method, system, controller and computer program product for controlling the flow of a multiphase fluid*. 1 (19).

Elgsæter, S.M. (2006) 'Modelling and control of growing slugs in horizontal multiphase pipe flows', *Modeling, Identification and Control*, 27(3), pp. 157–169.

Enilari, B.T. and Kara, F. (2015) 'Slug flow and it's mitigation techniques in the oil and gas Industry', *SPE Nigeria Annual International Conference and Exhibition*. Lagos, Nigeria, p. 19.

Enrique, J., Yang, L., Sidharth, P. and Ishii, M. (2008) 'Upward vertical two-phase flow local flow regime identification', *Nuclear Engineering and Design*, 238, pp. 156–169.

Esmaeilpour, M. (2013) *Robust control solutions for stabilizing flow from the reservoir : S-Riser experiments*. Norwegian University of Science and Technology.

Evans, D.H. and McDicken, W.N. (2000) *Doppler ultrasound: physics, instrumentation, and signal processing*. 2nd edn. Chichester, New york: John Wiley & Sons, Inc.

Fabre, J., Peresson, L.L., Corteville, J., Odello, R. and Bourgeois, T. (1990)

‘Severe slugging in pipeline/riser systems’, *SPE Production Engineering*, 5(03), pp. 299–305.

Fairhurst, H. and P. (1998a) ‘Challenges in the mechanical and hydraulic aspects of riser design for deep water developments’, *IBC Offshore Pipeline Technology Conference*. Oslo, Norway.

Falcone, G., Hewitt, G.F., Alimonti, C. and Harrison, B. (2002) ‘Multiphase flow metering : current trends and future developments’, *SPE Annual Technical Conference and Exhibition*. New Orleans, Louisiana, pp. 77–84.

Faluomi, V., Bonizzi, M., Ghetti, L. and Andreussi, P. (2017) ‘Development and validation of a multiphase flow simulator’, *13th Offshore Mediterranean Conference and Exhibition*. Ravenna, Italy, pp. 1–14.

Fard, M.P., Godhavn, J.-M. and Sagatun, S.I. (2006) ‘Modeling of severe slug and slug control with OLGA’, *SPE Production & Operations*, 21(03), pp. 381–387.

Farghaly, M.. (1987) ‘Study of severe slugging in real offshore pipeline riser-pipe system’, *Middle East Oil Show*. Bahrain, p. SPE-15726-MS.

Ferentinou, M. and Fakir, M. (2018) ‘Integrating rock engineering systems device and artificial neural networks to predict stability conditions in an open pit’, *Engineering Geology*, 246(1), pp. 293–309.

Fernandes Junior, F.E. and Yen, G.G. (2019) ‘Particle swarm optimization of deep neural networks architectures for image classification’, *Swarm and Evolutionary Computation*, 49(June), pp. 62–74.

Firouzi, M. and Hashemabadi, S. (2009) ‘Analytical solution for newtonian laminar flow through the concave and convex ducts’, *Journal of Fluids Engineering*, 131, pp. 1–6.

Gao, X., Xie, Y., Wang, S., Wu, M., Wang, Y., Tan, C., Zuo, X. and Chen, T. (2020) ‘Offshore oil production planning optimization: An MINLP model considering well operation and flow assurance’, *Computers and Chemical Engineering*, 133, p. 106674.

Gioia Falcone, Geoffrey Hewitt, C.A. (2009) *Multiphase flow metering: principles and applications*.

Godhavn, J.-M., Strand, S. and Gunleiv, S. (2005) 'Increased oil production by advanced control of receiving facilities', *IFAC Proceedings Volumes*, 38(1), pp. 567–572.

Godhavn, J.M., Fard, M.P. and Fuchs, P.H. (2005) 'New slug control strategies, tuning rules and experimental results', *Journal of Process Control*, 15(5), pp. 547–557.

Goncalves, J.L., Paiva, T.A., Abud Jr, J.R., Carvalho, R.D.M. and Venturini, O.J. (2011) 'Development of a multiphase flow metering procedure based on the ultrasonic technique', *15th International Conference on Multiphase Production Technology*. Cannes, France: BHR Group, pp. 101–115.

Griffith, P. and I, G.B.W. (1961) 'Two-phase slug flow', *Heat transfer*, 83, pp. 307–318.

Hanus, R., Zych, M., Kusy, M., Jaszczur, M. and Petryka, L. (2018) 'Identification of liquid-gas flow regime in a pipeline using gamma-ray absorption technique and computational intelligence methods', *Flow Measurement and Instrumentation*, 60(September 2017), pp. 17–23.

Hanus, R., Zych, M., Petryka, L., Świsulski, D. and Strzępowicz, A. (2017) 'Application of ANN and PCA to two-phase flow evaluation using radioisotopes', *EPJ Web of Conferences*, 143(1), pp. 2–5.

Harun, A.F., Cochran, S.W. and Choate, T.G.A. (2002) 'Optimization of ramp-up operations in a dual large diameter long-distance subsea wet gas pipeline system', *SPE Annual Technical Conference and Exhibition, 29 September-2 October*. San Antonio, Texas: Society of Petroleum Engineers, pp. 1–9.

Havre, K. (2007) *Method, computer program product and use of a computer program for stabilizing a multiphase flow*.

Havre, K. and Dalsmo, M. (2002) 'Active feedback control as a solution to severe

slugging', *SPE Production & Facilities*, 17(03), pp. 138–148.

Havre, K., Stornes, K.O. and Stray, H. (2000) 'Taming slug flow in pipelines', *ABB Review*, 2000(4)(4), pp. 55–63.

Hedne Pal and Linga Harald (1990) 'Suppression of terrain slugging with automatic and manual riser choking', *Winter Annual Meeting ASME*. Dallas, Texas, pp. 453–460.

Helgesen, A.H. (2010) *Antislug control of two-phase flow in risers with: Controlability analysis using alternative measurements*. Norwegian University of Science and Technology.

Henriot, V., Courbot, A., Henintzé, E. and Moyeux, L. (1999) 'Simulation of process to control severe slugging: application to the dunbar pipeline', *SPE Annual Technical Conference and Exhibilion*. Houston, Texas: Society of Petroleum Engineers, pp. 171–179.

Henríquez, P.A. and Ruz, G.A. (2018) 'A non-iterative method for pruning hidden neurons in neural networks with random weights', *Applied Soft Computing Journal*, 70, pp. 1109–1121.

Hewitt, G.F. and Roberts, D.N. (1969) *Studies of two-phase flow patterns by simultaneous X-ray and flash photography*. Harwell, Berkshire.

Hill, T.J. and Wood, D.G. (1994) 'Slug flow : occurrence , consequences , and prediction', *Society of Petroleum Engineers*. Tulsa, Oklahoma, p. SPE-27960-MS.

Hoffmann, A., Hirsch, T. and Pitz-Paal, R. (2016) 'Numerical investigation of severe slugging under conditions of a parabolic trough power plant with direct steam generation', *Solar Energy*, 133, pp. 567–585.

Hou, Q., Liu, L., Zhen, L. and Jing, L. (2018) 'A novel projection nonparallel support vector machine for pattern classification', *Engineering Applications of Artificial Intelligence*, 75(January 2017), pp. 64–75.

Issa, R.I. and Kempf, M.H.W. (2003) ‘Simulation of slug flow in horizontal and nearly horizontal pipes with the two-fluid model’, *International Journal of Multiphase Flow*, 29(1), pp. 69–95.

Jahanshahi, E. (2013) *Control solutions for multiphase flow: Linear and nonlinear approaches to anti-slug control*. Norwegian University of Science and Technology.

Jahanshahi, E., De Oliveira, V., Grimholt, C. and Skogestad, S. (2014) ‘A comparison between internal model control, optimal PIDF and robust controllers for unstable flow in risers’, *IFAC Proceedings Volumes*, 47(3), pp. 5752–5759.

Jahanshahi, E., Skogestad, S. and Grøtli, E.I. (2013) ‘Nonlinear model-based control of two-phase flow in risers by feedback linearization’, *IFAC Proceedings Volumes*, 9(1), pp. 301–306.

Jahanshahi, E., Skogestad, S. and Helgesen, A.H. (2012) ‘Controllability analysis of severe slugging in well-pipeline-riser systems’, *IFAC Proceedings Volumes*, 1(1), pp. 101–108.

Jansen, F.E., Shoham, O. and Taitel, Y. (1996a) ‘The elimination of severe slugging - experiments and modeling’, *International Journal of Multiphase Flow*, 22(6), pp. 1055–1072.

Jha, D.K., Ray, A., Mukherjee, K. and Chakraborty, S. (2012) ‘Classification of two-phase flow patterns by ultrasonic sensing’, *Journal of Dynamic Systems Measurement and Control*, 135(2), p. 024503.

Johal, K.S., Teh, C.E. and Cousins, A.R. (1997) ‘An alternative economic method to riserbase gas lift for deep water subsea oil/gas field developments’, *Offshore Europe Conference*. Aberdeen, UK, p. SPE-38541-MS.

Jones, O.C. and Delhaye, J.M. (1976) ‘Transient and statistical measurement techniques for two-phase flows: A critical review’, *International Journal of Multiphase Flow*, 3(2), pp. 89–116.

Jones, O.C. and Zuber, N. (1975) ‘The interrelation between void fraction

fluctuations and flow patterns in two-phase flow', *International Journal of Multiphase Flow*, 2(3), pp. 273–306.

Julia, J.E. and Hibiki, T. (2011) 'Flow regime transition criteria for two-phase flow in a vertical annulus', *International Journal of Heat and Fluid Flow*, 32(5), pp. 993–1004.

Juliá, J.E., Liu, Y., Paranjape, S. and Ishii, M. (2008) 'Upward vertical two-phase flow local flow regime identification using neural network techniques', *Nuclear Engineering and Design*, 238(1), pp. 156–169.

Julia, J.E., Ozar, B., Jeong, J.J., Hibiki, T. and Ishii, M. (2011) 'Flow regime development analysis in adiabatic upward two-phase flow in a vertical annulus', *International Journal of Heat and Fluid Flow*, 32(1), pp. 164–175.

K.Bendiksen and M.Espedal (1992) 'Onset of slugging in horizontal gas-liquid pipe flow', *International Journal of Multiphase Flow*, 18(2), pp. 237–247.

Kelessidis, V.C. and Dukler, A.E. (1989) 'Modeling flow pattern transitions for upward gas-liquid flow in vertical concentric and eccentric annuli', *International Journal of Multiphase Flow*, 15(2), pp. 173–191.

De Kerret, F., Béguin, C. and Etienne, S. (2017) 'Two-phase flow pattern identification in a tube bundle based on void fraction and pressure measurements, with emphasis on churn flow', *International Journal of Multiphase Flow*, 94, pp. 94–106.

Kjeldby, T.K., Henkes, R.A.W.M. and Nydal, O.J. (2013) 'Lagrangian slug flow modeling and sensitivity on hydrodynamic slug initiation methods in a severe slugging case', *International Journal of Multiphase Flow*, 53(July) Elsevier Ltd, pp. 29–39.

Kolasa, M., Długosz, R., Talaśka, T. and Pedrycz, W. (2018) 'Efficient methods of initializing neuron weights in self-organizing networks implemented in hardware', *Applied Mathematics and Computation*, 319, pp. 31–47.

Kouam, D., Girault, J. and Remenieras, J. (2003) 'High resolution processing

techniques for ultrasound doppler velocimetry in the presence of colored noise . Part II : Multiplephase pipe-flow velocity measurement', *IEEE Trans. on Ultrason. Ferroelec. and Frequ. Control*, 50(3), pp. 267–278.

Kovalev, K., Cruickshank, A. and Purvis, J. (2003) 'The slug suppression system in operation', *Offshore Europe*. Aberdeen, United Kingdom: Society of Petroleum Engineers, p. SPE 84947.

Kovalev, K., Seelen, M.G.W.M. and Haandrikman, G. (2004) 'Vessel-Less S3: advanced solution to slugging pipelines', *SPE Asia Pacific Oil and Gas Conference and Exhibition*. Perth, Australia: Society of Petroleum Engineers, p. SPE-88569-MS.

Kremkau, F.W. (1975) 'Physical principles of ultrasound', *Seminars in Roentgenology*, 10(4), pp. 259–263.

Krima, H., Cao, Y. and Lao, L. (2012) 'Gas injection for hydrodynamic slug control', *IFAC Proceedings Volumes (IFAC-PapersOnline)*, 1(PART 1) IFAC, pp. 116–121.

Kulkarni, S.R. and Rajendran, B. (2018) 'Spiking neural networks for handwritten digit recognition—Supervised learning and network optimization', *Neural Networks*, 103, pp. 118–127.

Lao, L. (2014) *Three-phase rig description manual*.

Lee, A.. H., Sun, J.-Y. and Jepson, W.P. (1993) 'Study of flow regime transitions of oil- water-gas mixtures in horizontal pipelines', *Proceedings of the Third International Offsore and Polar Engineering Conference*, II(June), pp. 6–11.

Lee, J.Y., Ishii, M. and Kim, N.S. (2008) 'Instantaneous and objective flow regime identification method for the vertical upward and downward co-current two-phase flow', *International Journal of Heat and Mass Transfer*, 51(13–14), pp. 3442–3459.

Lee, K.M., Yoo, J., Kim, S.W., Lee, J.H. and Hong, J. (2019) 'Autonomic machine learning platform', *International Journal of Information Management*, 49(June),

pp. 491–501.

Lee, M., Lee, J. and Chang, J.H. (2019) ‘Ensemble of jointly trained deep neural network-based acoustic models for reverberant speech recognition’, *Digital Signal Processing: A Review Journal*, 85, pp. 1–9.

Li, W., Guo, L. and Xie, X. (2017) ‘Effects of a long pipeline on severe slugging in an S-shaped riser’, *Chemical Engineering Science*, 171, pp. 379–390.

Lin, C., Wang, H., Yuan, J., Yu, D. and Li, C. (2019) ‘An improved recurrent neural network for unmanned underwater vehicle online obstacle avoidance’, *Ocean Engineering*, 189(August), p. 106327.

Liu, H., Pan, L. ming, Hibiki, T., Zhou, W. xiong, Ren, Q. yao and Li, S. song (2018) ‘Axial development of gas-liquid flow regime maps in a vertical 5 × 5 rod bundle with prototypic spacer grids’, *Nuclear Engineering and Design*, 339(November 2017), pp. 1–10.

Liu, J., Gong, M. and He, H. (2019) ‘Deep associative neural network for associative memory based on unsupervised representation learning’, *Neural Networks*, 113, pp. 41–53.

Livieris, I.E. and Pintelas, P. (2019) ‘An adaptive nonmonotone active set – weight constrained – neural network training algorithm’, *Neurocomputing*, 360, pp. 294–303.

Van Der Maaten, L.J.P., Postma, E.O. and Van Den Herik, H.J. (2009) ‘Dimensionality reduction: a comparative review’, *Journal of Machine Learning Research*, 10, pp. 1–41.

Malekzadeh, R., Henkes, R.A.W.M. and Mudde, R.F. (2012) ‘Severe slugging in a long pipeline-riser system: Experiments and predictions’, *International Journal of Multiphase Flow*, 46(November), pp. 9–21.

Masella, J.M., Tran, Q.H., Ferre, D. and Pauchon, C. (1998) ‘Transient simulation of two-phase flows in pipes’, *International Journal of Multiphase Flow*, 24(5), pp. 739–755.

McGuinness, M. and Cooke, D. (1993) ‘Partial stabilisation at st. Joseph’, *Proceedings of the Third International Offshore and Polar Engineering Conference*. Singapore, Vol.2, pp. 235–241.

Di Meglio, F., Kaasa, G., Petit, N. and Alstad, V. (2010) ‘Model-based control of slugging flow : an experimental case study’, *American Control Conference (ACC)*, 1, pp. 2995–3002.

Di Meglio, F., Petit, N., Alstad, V. and Kaasa, G.O. (2012) ‘Stabilization of slugging in oil production facilities with or without upstream pressure sensors’, *Journal of Process Control*, 22(4) Elsevier Ltd, pp. 809–822.

Meire, H.B. and Farrant, P. (1995) ‘*Basic ultrasound*’, in , p. 234.

Meribout, M., Al-Rawahi, N.Z., Al-Naamany, A.M., Al-Bimani, A., Al-Busaidi, K. and Meribout, A. (2010) ‘A multisensor intelligent device for real-time multiphase flow metering in oil fields’, *IEEE Transactions on Instrumentation and Measurement*, 59(6), pp. 1507–1519.

Mi, Y., Ishii, M. and Tsoukalas, L.H. (1998) ‘Vertical two-phase flow identification using advanced instrumentation and neural networks’, *Nuclear Engineering and Design*, 184(2–3), pp. 409–420.

Mi, Y., Ishii, M. and Tsoukalas, L.H. (2001) ‘Flow regime identification methodology with neural networks and two-phase flow models’, *Nuclear Engineering and Design*, 204(1–3), pp. 87–100.

Mohmmed, A.O., Al-Kayiem, H.H., Nasif, M.S. and Time, R.W. (2019) ‘Effect of slug flow frequency on the mechanical stress behavior of pipelines’, *International Journal of Pressure Vessels and Piping*, 172(July 2018), pp. 1–9.

Mokhatab, S. and Towler, B.F. (2007) ‘Severe slugging in flexible risers: Review of experimental investigations and OLGA predictions’, *Petroleum Science and Technology*, 25(7), pp. 1091–6466.

Mokhatab, S., Towler, B.F. and Purewal, S. (2007) ‘A review of current technologies for severe slugging remediation’, *Petroleum Science and*

Technology, 25(10), pp. 1235–1245.

Møller, M.F. (1993) 'A scaled conjugate gradient algorithm for fast supervised learning', *Neural Networks*, 6(4), pp. 525–533.

Molyneux, P. D., Kinvig, J.P. (2000) *Method and apparatus for eliminating severe slugging in a riser of a pipeline includes measuring pipeline pressuree and operating a valve*.

Montgomery, J.A. and Yeung, H.C. (2002) 'The stability of fluid production from a flexible riser', *Journal of Energy Resources Technology*, 124(2), p. 83.

Morchid, M. (2018) 'Parsimonious memory unit for recurrent neural networks with application to natural language processing', *Neurocomputing*, 314, pp. 48–64.

Muvvala, K., Kumar, V., Meikap, B.C. and Chakraborty, S. (2010) 'Development of soft sensor to identify flow regimes in horizontal pipe using digital signal processing technique', *Industrial and Engineering Chemistry Research*, 49(6), pp. 3001–3010.

Nicola, W. and Clopath, C. (2017) 'Supervised learning in spiking neural networks with FORCE training', *Nature Communications*, 8(1), pp. 333–349.

Ogazi, A.I. (2011) *Multiphase severe slug flow control*. Cranfield University.

Ogazi, A.I., Cao, Y., Yeung, H. and Lao, L. (2009) 'Slug control with large valve opening to maximise oil production', *Offshore Europe Oil and Gas Conference and Exhibition*. Aberdeen, UK: Society of Petroleum Engineers, Vol.2, pp. 8–11.

Ogazi, A.I., Cao, Y., Yeung, H. and Lao, L. (2010) 'Slug control with large valve openings to maximize oil production', *SPE Journal*, 15(3), pp. 812–821.

Okereke, N.U. and Omotara, O.O. (2018b) 'Combining self-lift and gas-lift: A new approach to slug mitigation in deepwater pipeline-riser systems', *Journal of Petroleum Science and Engineering*, 168(October 2017), pp. 59–71.

Omebere-Iyari, N.K. and Azzopardi, B.J. (2007) 'A study of flow patterns for gas/liquid flow in small diameter tubes', *Chemical Engineering Research and*

Design, 85(2 A), pp. 180–192.

Pan, L.M., Zhang, M., Ju, P., He, H. and Ishii, M. (2016) 'Vertical co-current two-phase flow regime identification using fuzzy C-means clustering algorithm and Relief attribute weighting technique', *International Journal of Heat and Mass Transfer*, 95(2016) Elsevier Ltd, pp. 393–404.

Payne, R.L., Huff, R.E. and Ogren, W.E. (1996) *Slug flow mitigation control system and method*. p., p. 08/139391.

Peddu, A., Chakraborty, S. and Kr. Das, P. (2017) 'Visualization and flow regime identification of downward air-water flow through a 12 mm diameter vertical tube using image analysis', *International Journal of Multiphase Flow*, 100(March), pp. 1–15.

Pedersen, S., Durdevic, P. and Yang, Z. (2017) 'Challenges in slug modeling and control for offshore oil and gas productions: A review study', *International Journal of Multiphase Flow*, 88, pp. 270–284.

Pedersen, S., Durdevic, P. and Yang, Z. (2015) 'Review of slug detection, modeling and control techniques for offshore oil & amp; gas production processes', *IFAC-PapersOnLine*, 48(6), pp. 89–96.

Pierro, A., Spadoni, S., Chiappetta, F. and Ferrini, F. (2019) 'Slug catcher finger-type CFD simulator for two-phase flow separation', *Petroleum*, 5(2), pp. 133–140.

Pilario, K.E. (2018) *Binary and multi-class SVM.*, *MATLAB Central File Exchange*

Platt, J., Cristianini, N. and Shawe-Taylor, J. (2000) 'Large margin DAGs for multiclass classification', *International Conference on Neural Information Processing Systems*, 12(3), pp. 547–553.

Postlethwaite, S.S. and I. (2005) 'Multivariable feedback control analysis and design', *International Journal of Robust and Nonlinear Control*, 8(14), pp. 1237–1238.

Ramesh, J., Vanathi, P.T. and Gunavathi, K. (2008) 'Fault classification in phase-

locked loops using back propagation neural networks', *Electronics and Telecommunications Research Institute*, 30(4), pp. 546–554.

Rezzónico, R. and Carp, A. (2007) 'Transient analysis of flowlines and slug catcher level control', *Latin American & Caribbean Petroleum Engineering Conference*. Buenos Aires, Argentina: Society of Petroleum Engineers, p. SPE-108181-MS.

Riedmiller, M. and Braun, H. (1993) 'A direct adaptive method for faster backpropagation learning: The Rprop algorithm', *IEEE International Conference On Neural Networks*. San Francisco, CA, USA, pp. 586–591.

Rioul, O. and Vetterli, M. (1991) 'Wavelets and signal processing', *IEEE Signal Processing Magazine*, 8(4), pp. 14–38.

Rosa, E.S., Salgado, R.M., Ohishi, T. and Mastelari, N. (2010) 'Performance comparison of artificial neural networks and expert systems applied to flow pattern identification in vertical ascendant gas-liquid flows', *International Journal of Multiphase Flow*, 36(9), pp. 738–754.

Rossi, L., De Fayard, R. and Kassab, S. (2018) 'Measurements using X-ray attenuation vertical distribution of the void fraction for different flow regimes in a horizontal pipe', *Nuclear Engineering and Design*, 336(August 2017), pp. 129–140.

Rouhani, S.Z. and Sohal, M.S. (1983) 'Two-phase flow patterns: A review of research results', *Progress in Nuclear Energy*, 11(3), pp. 219–259.

Salgado, C.M., Pereira, C.M.N.A., Schirru, R. and Brandão, L.E.B. (2010) 'Flow regime identification and volume fraction prediction in multiphase flows by means of gamma-ray attenuation and artificial neural networks', *Progress in Nuclear Energy*, 52(6), pp. 555–562.

Sanderson, M.L. and Yeung, H. (2002) 'Guidelines for the use of ultrasonic non-invasive metering techniques', *Flow Measurement and Instrumentation*, 13(4), pp. 125–142.

Santoso, B., Indarto, Deendarlianto and Thomas, S.W. (2012) 'The identification of gas-liquid co-current two phase flow pattern in a horizontal pipe using the power spectral density and the artificial neural network (ANN)', *Modern Applied Science*, 6(9), pp. 56–67.

Saric, M., Bilicic, L. and Dujmic, H. (2005) 'White noise reduction of audio signal using wavelets transform with modified universal threshold', *4th WSEAS Transactions on Information Science and Applications*, 2(2), pp. 279–283.

Sarica, C. and Tengesdal, J.Ã. (2000) 'A new technique to eliminate severe slugging in pipeline/riser systems', *SPE Annual Technical Conference and Exhibition*. Dallas, Texas, p. SPE 63185.

Schmidt, Z., Brill, J.P. and Beggs, H.D. (1980) 'Experimental study of severe slugging in a two-phase-flow pipeline - riser pipe system', *Society of Petroleum Engineers Journal*, 20(5), p. SPE-8306-PA.

Schroeder, P.W., John, V., Lederer, P.L., Lehrenfeld, C., Lube, G. and Schöberl, J. (2019) 'On reference solutions and the sensitivity of the 2D Kelvin–Helmholtz instability problem', *Computers and Mathematics with Applications*, 77(4), pp. 1010–1028.

Shang, Z., Yang, R., Cao, X. and Yang, Y. (2004) 'An investigation of two-phase flow instability using wavelet signal extraction technique', *Nuclear Engineering and Design*, 232(2), pp. 157–163.

Shotbolt, T. (1986) 'Methods for the alleviation of slug flow problems and their influence on field development planning', *European Petroleum Conference*. London, United Kingdom: Society of Petroleum Engineers, p. SPE-15891-MS.

Sivertsen, H. (2008) *Stabilization of desired flow regimes using active control*. Norwegian University of Science and Technology.

Sivertsen, H., Alstad, V. and Skogestad, S. (2009) 'Medium-scale experiments on stabilizing riser-slug flow', *SPE Projects, Facilities & Construction*, 4(4), pp. 156–170.

Sivertsen, H. and Skogestad, S. (2005a) ‘Cascade control experiments of riser slug flow using topside measurements’, *IFAC Proceedings Volumes*, 38(1) Prague, Czech Republic, pp. 129–134.

Sivertsen, H. and Skogestad, S. (2005b) ‘Anti-slug control experiments on a small-scale two-phase loop’, *Computer Aided Chemical Engineering*, 20(C), pp. 1021–1026.

Sivertsen, H. and Skogestad, S. (2005c) ‘Cascade control experiments of riser slug flow using topside measurements’, *IFAC Proceedings Volumes Volume*, 38(1), pp. 129–134.

Sivertsen, H., Storkaas, E. and Skogestad, S. (2010) ‘Small-scale experiments on stabilizing riser slug flow’, *Chemical Engineering Research and Design*, 88(2), pp. 213–228.

Spedding, P.L., Woods, G.S., Raghunathan, R.S. and Watterson, J.K. (1998) ‘Vertical two-phase flow Part I: Flow regimes’, *Oil and Natural Gas Production*, 76(5), pp. 612–619.

Van Spronsen, G., Entaban, A., Mohamad Amin, K., Sarkar, S. and Henkes, R. (2013) ‘Field experience with by-pass pigging to mitigate liquid surge’, *16th International Conference on Multiphase Production Technology*. Cannes, France, pp. 299–308.

Srinivas, J., Ramana Murthy, J. V. and Sai, K.S. (2015) ‘Entropy generation analysis of the flow of twoimmiscible couple stress fluids between two porous beds’, *Computational Thermal Sciences*, 7(2), pp. 123–137.

Stasiak, M.E., Pagano, D.J. and Plucenio, A. (2012) ‘A new discrete slug-flow controller for production pipeline risers’, *IFAC Workshop on Automatic Control in Offshore Oil and Gas Production*. Trondheim, Norway, pp. 122–127.

Storkaas, E. (2005) *Stabilizing control and controllability: Control solutions to avoid slug flow in pipeline-riser systems*. Norwegian University of Science and Technology.

Storkaas, E. and Godhavn, J.-M. (2005) ‘Extended slug control for pipeline-riser systems’, *12th International Conference on Multiphase Production Technology*. Barcelona, Spain, pp. 297–311.

Storkaas, E. and Skogestad, S. (2007) ‘Controllability analysis of two-phase pipeline-riser systems at riser slugging conditions’, *Control Engineering Practice*, 15(5), pp. 567–581.

Subasi, A. (2005) ‘Automatic recognition of alertness level from EEG by using neural network and wavelet coefficients’, *Expert Systems with Applications*, 28(4), pp. 701–711.

Sugihara, T. (2011) ‘Solvability-unconcerned inverse kinematics by the levenberg-marquardt method’, *IEEE Transactions on Robotics*, 27(5), pp. 984–991.

Sun, Z. and Zhang, H. (2008) ‘Neural networks approach for prediction of gas-liquid two-phase flow pattern based on frequency domain analysis of vortex flowmeter signals’, *Measurement Science and Technology*, 19(1), p. 015401.

Sunde, C., Avdic, S. and Pázsit, I. (2005) ‘Classification of two-phase flow regimes via image analysis and a neuro-wavelet approach’, *Progress in Nuclear Energy*, 46(3–4), pp. 348–358.

Taitel, Y. (1986) ‘Stability of severe slugging’, *International Journal of Multiphase Flow*, 12(2), pp. 203–217.

Taitel, Y., Lee, N. and Dukler, A.. (1976) ‘Transient gas-liquid flow in horizontal pipes: Modeling the flow pattern transitions’, *American Institute of Chemical Engineers*, 22(1), pp. 47–55.

Taitel, Y., Vierkandt, S., Shoham, O. and Brill, J.. (1990) ‘Severe slugging in a riser system : experiments and modeling’, *International Journal of Multiphase Flow*, 16(I), pp. 57–68.

Tambouratzis, T. and Pázsit, I. (2009) ‘Non-invasive on-line two-phase flow regime identification employing artificial neural networks’, *Annals of Nuclear*

Energy, 36(4), pp. 464–469.

Tandoh, H., Cao, Y. and Avila, C. (2016) 'Stability of severe slug flow in U-shape riser', *22nd International Conference on Automation and Computing, (ICAC 2016)*. Colchester, United Kingdom: IEEE, pp. 372–377.

Taras, Makogon, Y. and Brook, G.J. (2013) *Device for controlling slugging*.

Tengesdal, J.O., Sarica, C. and Thompson, L. (2003) 'Severe slugging attenuation for deepwater multiphase pipeline and riser systems', *Spe Production & Facilities*, 18(4), pp. 269–279.

Thorn, R., Johansen, G.A. and Hjertaker, B.T. (2013) 'Three-phase flow measurement in the petroleum industry', *Measurement Science and Technology*, 24(1), p. 17.

Trafalis, T.B., Oladunni, O. and Papavassiliou, D. V. (2005) 'Two-phase flow regime identification with a multiclassification support vector machine (SVM) model', *Industrial & Engineering Chemistry Research*, 44(12), pp. 4414–4426.

Troniewski, L. and Ulbrich, R. (1984) 'The analysis of flow regime maps of two-phase gas-liquid flow in pipes', *Chemical Engineering Science*, 39(7–8), pp. 1213–1224.

Übeyli, E.D. and Güler, I. (2005) 'Improving medical diagnostic accuracy of ultrasound Doppler signals by combining neural network models', *Computers in Biology and Medicine*, 35(6), pp. 533–554.

Wang, H.X. and Zhang, L.F. (2009) 'Identification of two-phase flow regimes based on support vector machine and electrical capacitance tomography', *Measurement Science and Technology*, 20(11), p. 4007.

Weinstein, E. (1982) 'Measurement of the differential doppler shift', *IEEE Transactions on Acoustics, Speech, and Signal Processing*, 30(1), pp. 112–117.

Winters, K. B. and Rouseff, D. (1993) 'Tomographic reconstruction of stratified fluid flow', *IEEE Trans. on Ultrason. Ferroelec. and Frequ. Control, UFFC-40*,

40(1), pp. 26–33.

Wu, B., Firouzi, M., Mitchell, T., Rufford, T.E., Leonardi, C. and Towler, B. (2017) ‘A critical review of flow maps for gas-liquid flows in vertical pipes and annuli’, *Chemical Engineering Journal*, 326(15), pp. 350–377.

Xiao, J. and Hrnjak, P. (2019) ‘A flow regime map for condensation in macro and micro tubes with non-equilibrium effects taken into account’, *International Journal of Heat and Mass Transfer*, 130, pp. 893–900.

Xie, T., Ghiaasiaan, S.M. and Karrila, S. (2004) ‘Artificial neural network approach for flow regime classification in gas-liquid-fiber flows based on frequency domain analysis of pressure signals’, *Chemical Engineering Science*, 59(11), pp. 2241–2251.

Xing, L., Yeung, H., Shen, J. and Cao, Y. (2013a) ‘A new flow conditioner for mitigating severe slugging in pipeline/riser system’, *International Journal of Multiphase Flow*, 53, pp. 1–10.

Xing, L., Yeung, H., Shen, J. and Cao, Y. (2013b) ‘Numerical study on mitigating severe slugging in pipeline/riser system with wavy pipe’, *International Journal of Multiphase Flow*, 53(7), pp. 1–10.

Xing, L., Yeung, H., Shen, J. and Cao, Y. (2013c) ‘Experimental study on severe slugging mitigation by applying wavy pipes’, *Chemical Engineering Research and Design*, 91(1), pp. 18–28.

Yan, Y., Wang, L., Wang, T., Wang, X., Hu, Y. and Duan, Q. (2018) ‘Application of soft computing techniques to multiphase flow measurement: A review’, *Flow Measurement and Instrumentation*, 60, pp. 30–43.

Yaw, S.Y., Lee, C.Y., Haandrikman, G., Groote, G., Asokan, S. and Malonzo, M.E. (2014) ‘Smart choke - a simple and effective slug control technology to extend field life’, *International Petroleum Technology Conference*. Kuala Lumpur Malaysia: International Petroleum Technology Conference, p. IPTC-17825-MS.

Yocum, B.T. (1973) ‘Offshore riser slug flow avoidance: mathematical models for

design and optimization', *SPE European Meeting*. London, United Kingdom, p. SPE-4312-MS.

Yue, J., Xu, K.J., Liu, W., Zhang, J.G., Fang, Z.Y., Zhang, L. and Xu, H.R. (2019) 'SVM based measurement method and implementation of gas-liquid two-phase flow for CMF', *Measurement: Journal of the International Measurement Confederation*, 145, pp. 160–171.

Zhang, J. (2006) 'Improved on-line process fault diagnosis through information fusion in multiple neural networks', *Computers and Chemical Engineering*, 30(3), pp. 558–571.

Zhang, J. and Roberts, P.D. (1992) 'On-line process fault diagnosis using neural network techniques', *Transactions of the Institute of Measurement & Control*, 14(4), pp. 179–188.

Zhou, H., Guo, L., Yan, H. and Kuang, S. (2018) 'Investigation and prediction of severe slugging frequency in pipeline-riser systems', *Chemical Engineering Science*, 184, pp. 72–84.

Zhu, H., Gao, Y. and Zhao, H. (2018) 'Experimental investigation on the flow-induced vibration of a free-hanging flexible riser by internal unstable hydrodynamic slug flow', *Ocean Engineering*, 164(July), pp. 488–507.

Appendices

Appendix A: The characteristics of severe slug flow

A.1 Severe slug flow number derivation

The upstream pipeline of the riser dip has a cross-section (*A)* and length (L_F). Assume that the flow is stratified in this part of the pipeline with a liquid holdup fraction (α_F). Considering the time the liquid blocked the riser dip, the increase in pressure at the back of the liquid blockage can be stated mathematically as:

$$(dp/dt)_{flowline} = \quad RT\ \frac{d\rho_G}{dt}. \tag{0-1}$$

The ideal gas law is assumed to hold, with gas density (ρ_G), temperature (*T*) and gas constant (*R*). The gas density is equal to the ratio of the gas volume and gas mass (M_G) in the upstream pipeline:

$$\rho_G = \frac{M_G}{(1-\alpha_F)L_F A}. \tag{0-2}$$

Substitution gives

$$(dp/dt)_{flowline} = \frac{RT}{(1-\alpha_F)L_F A}\frac{dM_G}{dt}. \tag{0-3}$$

When the liquid blocked the riser, the gas mass change is simply because of the gas inflow at the inlet of the pipeline, which gives:

$$(dp/dt)_{flowline} = \frac{P_s}{(1-\alpha_F)L_F}V_{SGs}. \tag{0-4}$$

where P_s , is the pressure at standard condition V_{SGs} is the superficial gas velocity at standard condition.

The pressure downstream of the blockage of liquid is due to the hydrostatic head increase, which can be presented mathematically as:

$$(dp/dt)_{riser} = (\rho_L - \rho_G)V_{SL,R}\ g\ sin\ \varphi. \tag{0-5}$$

Where $V_{SL,R}$ is the riser superficial liquid velocity while φ is the riser angle with respect to the horizontal (for the vertical riser, φ =90^0). The riser's superficial velocity follows from the pipeline's superficial velocity as stated below:

$$V_{SL,R} = (D_F/D_R)^2 V_{SL}. \quad \text{0-6}$$

Here, D_R is the riser diameter while D_F is the pipeline diameter.

The severe slugging number Πss is the ratio of upstream pressure increase and downstream of the liquid blockage as given mathematically below:

$$\Pi ss = \frac{(dp/dt)flowline}{(dp/dt)riser} = \frac{Ps}{(1-\alpha_F)(\rho_L-\rho_G)(D_F/D_R)^2 g \sin\varphi L_F} GLR. \quad \text{0-7}$$

Where the gas-liquid ratio at standard condition is GLR (in unit, m^3/m^3) ($GLR = V_{SGs}/V_{SL}$). This is simplified to give

$$\Pi ss = \frac{(dp/dt)flowline}{(dp/dt)riser} = \frac{Ps}{(1-\alpha_F)\rho_L g L_F} GLR, \quad \text{0-8}$$

assuming (a) $\rho_{G \ll} \rho_L$, (b) the riser is vertical, (c) the riser and the pipeline have an equal diameter.

A.2 Slug length and period

The severe slug flow cycle period can be deduced from the time (Δt) it takes the gas in the pipeline to accumulate enough pressure to push the liquid out of the riser. It starts at the time the slug was cleared (blown out) and at minimum rise-base pressure ($\Delta t\ level\ 1$) and ends at the time the liquid filled the riser, and at the maximum riser-base pressure ($\Delta t\ level\ 2$). Hence, the mass balance of the gas upstream of the riser base of the pipeline can be stated mathematically as:

$$\dot{m}_G \Delta t = (\rho_2 - \rho_1)(1-\alpha_F) L_F A, \quad \text{0-9}$$

where $\dot{m}_G$ is the inlet gas mass flowrate, which is equal to ($\rho_{Gs} V_{SGs} A$) with the gas superficial velocity and gas density taken at the standard condition. Applying the ideal gas law, we can rewrite the mass balance to give:

$$\Delta t = \frac{\Delta P}{Ps} \frac{(1-\alpha_F) L_F}{V_{SGs}}, \quad \text{0-10}$$

with $P_2 - P_1 = \Delta P$. The ΔP can be taken to be equal to hydrostatic head of the riser when filled with liquid ($i.e\ \Delta P = L_R \rho_L g$).

$$\Delta t = \frac{L_R}{V_{SLs}} \frac{1}{\Pi_{ss}}. \quad \text{0-11}$$

where: $\frac{L_R}{\Pi_{ss}}$ is the liquid slug body length.

The pipeline superficial liquid velocity at standard condition is denoted as V_{SLs}. (The relation for Δt solely denotes the severe slugging cycle part where there is production starvation. The liquid blow out time is excluded. However, the liquid blow out time is lower than that of production starvation time).

Appendix B : The experimental operations

B.1 Precautions for safe rig operation

A thorough walk-around check of the entire test facility before and after each operating session is a requirement the facility users must observe. Before starting the loop, facility users are required to make sure that the facility is not already in use by another operator. External operations are prohibited except if the facility manager gives a go-ahead order. Facility users are also required to check and dispose of the liquid residues in the air-discharging pipe (U-bend) before and after operations, and they must report the amount of liquid to the lab manager, the rig administrator, or the technician. Any the health and safety issues observed must be reported immediately to any available lab staff.

The manual valves are correctly and cautiously positioned for the chosen riser (vertical, horizontal, s-shaped, catenary, U-shaped) for the experiment. The compressors are then switched on, and the liquid pump is switched on from the DeltaV control panel after starting the DeltaV. The appropriate flowrates (liquid and gas flowrates) are then introduced into the system through the DeltaV metering section.

B.1.1 Linking the LabVIEW to MATLAB

To establish steady communication between the LabVIEW model and the Simulink model designed for slug flow control, the following steps were followed.

1. First step: The LabVIEW programme was installed on the topside computer with a Matlab algorithm that will process the raw Doppler ultrasound signals and relate it to an appropriate parameter, which will be transmitted continuously for slug control. Another LabVIEW programme was installed in the computer in the control room tagged APP1 with an appropriate algorithm developed in Matlab to receive the transmitted signals from the topside computer. So that researchers could avoid running back and forth from the topside facility to the control room, the topside computer was remotely controlled using another computer in the control room.
2. Second step: For convenience, the topside computer and the computer in the control room had to be linked to avoid the researcher running to and from the test loop facility. For remote control of the topside system, the following steps were followed:

a) From the desktop, click on the start button and then type *remote desktop connection*. The remote desktop connection will pop-up.
b) Click on the remote desktop to display a window with *remote connection*. On the remote desktop, type in the computer name to be controlled remotely, and click connect. When the remote control is established, the next step is to link the two computers so that stable communication will exist between the two systems.

3. Third step: To establish communication between the LabVIEW model and the Simulink model designed for slug flow control, the following steps are required:
    a) On the Matlab command window, type *workspace*. This ensures that the shared variable in the LabVIEW is already established in Matlab.
    b) In the same Matlab command window, type *opctool*. A window will be displayed. In that window, click on *add host* (to add the computer

with the shared variable's IP address). Click on *add client* and add the IP address as well. After establishing the connection, on OPC toolbox object, add the items (variable).

Another approach to link the LabVIEW model to Simulink model designed for slug flow control is through the following steps.

a) From the Simulink model developed for slug flow control, go to the OPC configuration block and click on it. A display window will pop-up titled *Block parameters*: *OPC configuration*.
b) Click on *configure OPC clients* from the displayed window. Another display window will come up titled *OPC client Manager*.
c) On the OPC client manager, click the *add* button. Another display window will come up titled *OPC server properties*.
d) Add the Host (the appropriate computer IP address as above), select the server required for the experiment, and then connect.

Appendix C : Principal Component Analysis MATLAB code

```
% This is a PCA (Principal Component Analysis) code for controller gain
calculation
%Inputs:
%data:     5% opening of choke valve data for pipeline B-J1. Rows represent
observations, columns represent variables.
%data1:    GG: B-J1 riser outlet, ROL: B-J1 riser outlet, PT: Section after choke,
QG: B-JI outlet.
%a:        Confidence level

data = load ('pca.txt');
% Normalization of Simulation data
m1 = size(data,1);
```

```
% Compute mean of simulation data(i.e. mean of each column)
mx=mean(data);
% Compute standard deviation of simulation data(i.e standard %deviation
%of each column)
stdx=std(data);
% subtract the mean from each column entry and divide by the standard
% deviation to standardise data
X=(data-mx(ones(m1,1),:))./stdx(ones(m1,1),:);
% Compute the covariance matrix (cov)
cov=X'*X/(m1-1);
% Compute eigen values and eigenvectors of the covariance matrix
%[eigvec,eigval]=eig(cov);
[U,D,~]=svd(cov);
U=U(:,1);
k1=U(1);
k2=U(2);
k3=U(3);
kA=-k1/k2
kB=k2/k3
kC=-k3
```

Appendix D : ANN and Fuzzy logic proposed work

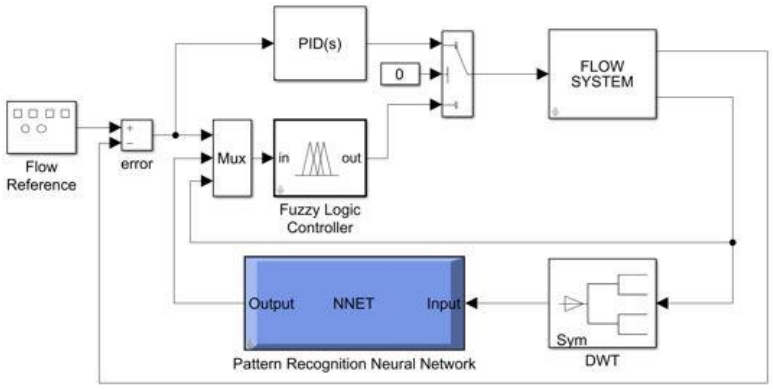

Figure D-0-1: Flow control using information from ANN and fuzzy logic